Consolidation of Rigid Raft by the Program *GEO Tools*

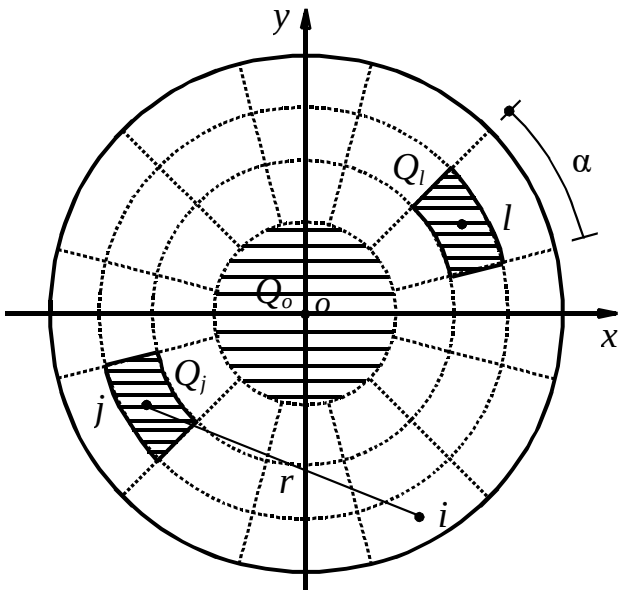

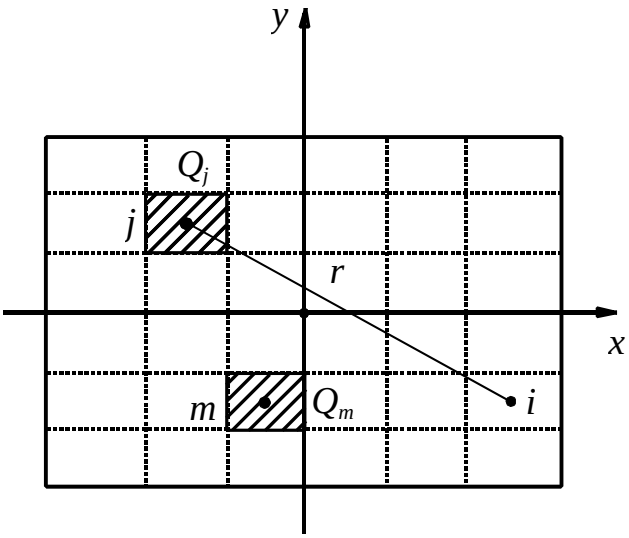

Program authors: *M. El Gendy*
A. El Gendy

GEOTEC Software Inc.
Canada
Tele.:+1(587) 332-3323
geotec@geotecsoftware.com
www.geotecsoftware.com

2022

Content Page

Preface

Various problems in Geotechnical Engineering can be investigated by the program *GEO Tools*. The original version of the program *GEO Tools* in *GEOTEC Office* was developed by Prof. M. Kany, Prof. M. El Gendy and Dr. A. El Gendy. After the death of Prof. Kany, Prof. M. El Gendy and Dr. A. El Gendy further developed the program to meet the needs of practice.

Settlements of rafts may be calculated using either flexibility or stress coefficients-technique. Analyzing rafts on elastic soil layers may be carried out using the first technique, while that on consolidated soil should be carried out by the second one to get realistic results. In this case, compression index C_c of the soil is used to define the consolidation characteristics of the clay deposits. The problem is that there are no enough available formulations of stress coefficients for such type of analysis. In this book, numerical and semi-analytical procedures are developed to determine the magnitude of consolidation settlement under the common regular shapes of rigid rafts on a deeply extended clay layer using stress coefficients-technique.

The book describes the essential equations used in *GEO Tools* to obtain the final consolidation settlement and contact pressure of a rigid raft with some verification examples. The problems of consolidation settlement of rigid raft outlined in this book can be also analyzed by the program *ELPLA* and the same results can be obtained. *GEO Tools* is a simple user interface program and needs little information to define a problem. It is prefer to use it for a simple foundation geometry. Furthermore, *ELPLA* can also read data files of a rigid consolidation problem defined by *GEO Tools*. User can analyze the problem again by *ELPLA*.

Although the numerical procedure outlined here is valid for rigid rafts of any arbitrary shape, but only the two special cases of rigid rafts, rectangular and circular rigid rafts, are taken into consideration.

8 Consolidation of Rigid Raft

8.1 Introduction

In many practice cases, treating the raft as completely rigid is convenient. In this case, due the applied loads the raft will rotate as a rigid body. In a rigid body motion, the points on the rigid body move linearly. An analysis for the contact pressure under a rigid raft on isotopic elastic half-space medium was carried out by many authors. The oldest work for the analysis of foundation rigidity is that of *Borowicka* (1939). He analyzed the problem of distribution of contact stress under uniformly loaded strip and circular rigid foundation on semi-infinite elastic mass. A review about the methods of analysis of rigid rafts may be found in standards such as DIN 4018 or books as example *Selvaduri* (1979). Most of them were focused on the analysis of rafts on isotropic elastic half-space medium according to *Boussinesq's* assumption. The main problem when analyzing raft on clay layer is that the determination of the non-linear increment of the vertical stress on the layer due to the unknown contact pressure at the soil-raft interface. *Griffths* (1984) presented charts for average vertical stress increment beneath a corner of a uniformly loaded rectangular area based on numerical integration of existing solutions for the rectangular problem. The chart is not only limited by the side length of a rectangular load is less than 0.4 of the soil layer thickness but also it cannot be used for computer computation. *El Gendy* (2003) introduced an analysis of rigid circular raft by calculating the stress at mid-depth of soil element. Increment of vertical stress are obtained by numerical integration using trapezoidal rule. The stress due to a ring piece loaded element is determined numerically using *Gaussian's* Quadrature formula. But the value of the depth integration formula must be greater than 0.2 [m] to give good results. Also, this analysis was limited by a certain depth of the clay layer. *El Gendy* (2006) developed stress coefficients for triangular loaded elements and point load acting on the entire clay sub-layer through closed form equations, which may be used for any irregular shape of foundations. As an extension for the previous work, stress coefficients for the special cases of circular, ring piece and rectangular loaded elements acting on the entire clay sub-layer are developed in this book. Using such special types of elements when analyzing rafts of regular shapes, reduces considerably the computation time required for generating stress coefficients comparison with using triangular loaded element. Coefficients developed in this book are used to formulate numerical and semi-analytical procedures to determine the magnitude of consolidation settlement under the common regular shapes of rigid rafts on a deeply extended clay layer. Due to regular shape of foundations, contact pressure distribution at the soil-raft interface on isotopic elastic half-space soil medium can be obtained analytically. This advantage leads to reduce considerably the analysis of regular rafts, where it can be considered that half of the problem is solved. *El Gendy* (2006) had showed that the contact pressure distribution under the raft on deeply extended clay layer is similar to that on isotropic elastic half-space soil medium. Consequently, by using the known contact pressure from closed form solutions of regular foundation shapes, it can be derived a semi-analytical solution for regular rafts on deeply extended clay layer. Also, an analysis of rafts with defining the elastic soil parameter by the coefficient of volume change is presented to show the ability of stress coefficients-technique for analyzing rafts on any soil type.

8.2 Formulation of stress coefficients

8.2.1 Introduction

The stress applied by a foundation to the ground is often assumed to be uniform. The actual distribution of the contact pressure between the foundation and the soil may be far from uniform. This distribution depends mainly on the stiffness of the foundation stiffness of the soil and load distribution on the foundation. In this book, a numerical analysis is developed to consider the actual contact pressure distribution under the rectangular and circular rigid rafts with an eccentric load. The analysis considers the compatibility between the settlement caused by cohesive soil consolidation and the raft displacement. In which, a direct numerical solution without iteration is derived to obtain the nonlinear soil stress under the rigid raft. The present solution is applicable also for the other types of rigid rafts.

The next paragraphs describe a numerical modeling to obtain the nonlinear stress distribution in soil and consequently the consolidation settlement of rigid raft on consolidated clay deposits. The proposed numerical modeling is a direct numerical solution without iteration. Therefore, it can be considered as a rapid method where it reduces the computation time required to analysis large rafts with a fine mesh of elements on consolidated clay deposits.

8.2.2 Defining mesh elements of the raft

In the analysis of either the circular or the rectangular rigid raft, both the raft and the contact area of the supporting medium are divided into elements as shown in Figure 8.1. To avoid losses in contact area when generating the mesh, a circular and ring pieces elements as shown in Figure 8.1 are proposed.

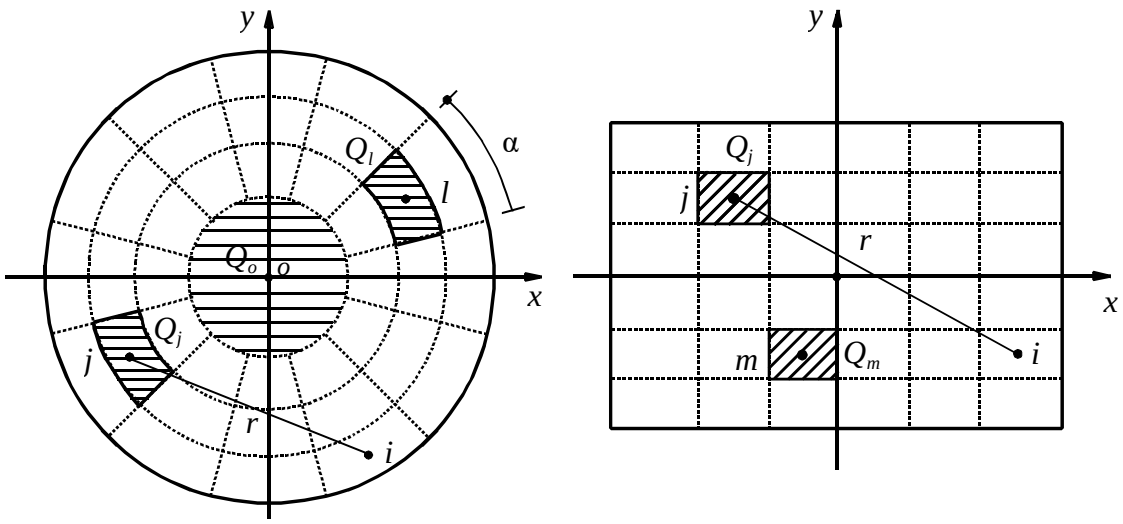

Figure 8.1 Rectangular and circular rafts with element types

The increment of vertical normal stress in a layer is defined as the equivalent uniform vertical stress acting in that layer due to the applied pressure at the surface. This stress is necessary to calculate the consolidation settlement by either the coefficient of volume change or

compression index. Most of derivations of increase of vertical stress are carried out numerically or used equations for point load application. Such stress can be calculated by subdividing the soil in a number of layers, then adding the contribution of each layer. Closed form equations of stress coefficients for the entire layer, leads to less computation effort and short computation time, especially when analyzing large foundation problems.

To study contact pressure effect q_j [kN/m^2] of an element j on other i, the contact pressure may be represented by a contact force Q_j [kN]. Consequently, a stress coefficient for a point load can be used. But applying stress coefficient for a point load directly under the element due to contact force on the element itself, leads to numerical problem due to division by zero. For rafts with rectangular, circular and ring piece elements shown in Figure 8.1, closed form equations of stress coefficients are presented in the next sections.

8.2.2.1 Stress coefficient of a soil layer due to a point load

Figure 8.1 and Figure 8.2 show a point load Q_j [kN] acting on the surface at point j. The increment of vertical stress $\delta\sigma_{i,j}(k)$ [kN/m^2] under the point i in a soil layer k due to a point load on the surface at point j is expressed as:

$$\delta\sigma_{i,j}(k) = \frac{1}{h}\int_{h_1}^{h_2}\sigma_{zi,j}\,dz = f_{i,j}(k)\;Q_j \tag{8.1}$$

where $f_{i,j}(k)$ [1/m^2] is the stress coefficient of a point i due to a load Q_j at point j.

According to *El Gendy* (2006), this coefficient is given by:

$$f_{i,j}(k) = \frac{1}{2\pi h}\left(\frac{r^2}{\left(h_2^2 + r^2\right)^{\frac{3}{2}}} - \frac{3}{\sqrt{h_2^2 + r^2}} - \frac{r^2}{\left(h_1^2 + r^2\right)^{\frac{3}{2}}} + \frac{3}{\sqrt{h_1^2 + r^2}}\right) \tag{8.2}$$

and:

$\sigma_{zi,j}$ stress at depth z under point i due to point load at point j, [kN/m^2].
r radial distance between points i and j, [m].
h thickness of layer k, [m].
h_1 depth of the layer top from the surface, [m].
h_2 depth of the layer bottom from the surface, [m].

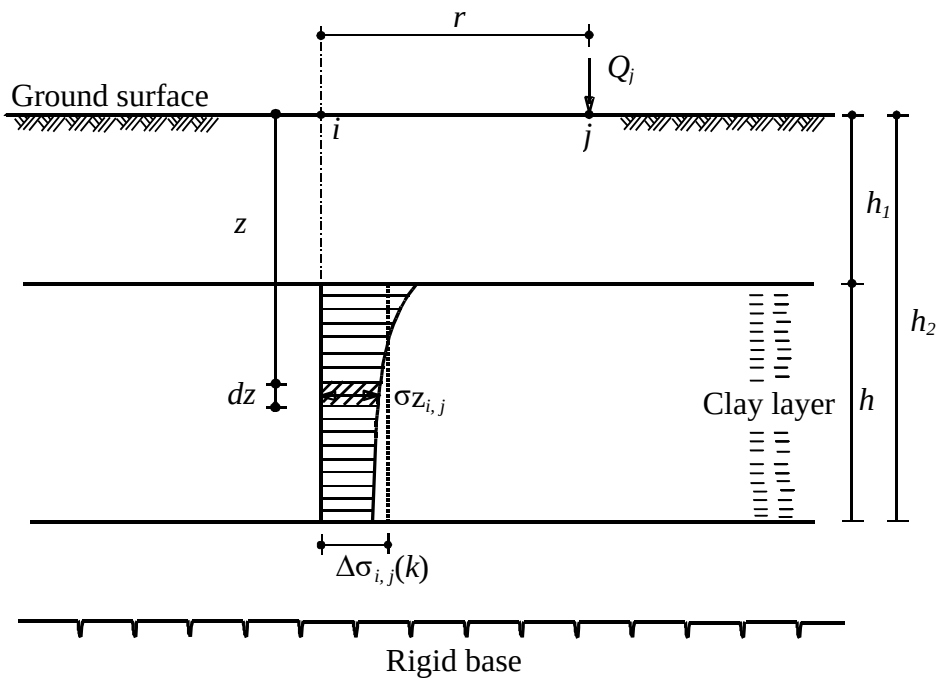

Figure 8.2 Increment of vertical stress in a soil layer due to a point load

8.2.2.2 Stress coefficient of a soil layer due to a rectangular loaded area

To determine the stress coefficient $f_{m,\ m}(k)$ for the rectangular element m in Figure 8.1, consider a quarter of a rectangular loaded area of intensity q_m [kN/m^2] with sides 2a [m] and 2b [m] acting on the surface as shown in Figure 8.3.

For the point load $dQ_m=q_m\ dx\ dy$ on the small element area $dx\ dy$, the stress coefficient $f_{m,\ m}(k)$ at the center of a rectangular loaded area of sides 2a [m] and 2b [m] at the surface can be obtained from:

$$f_{m,\ m}(k) = \frac{1}{a\ b}\int_0^b \int_0^a df_{m,\ m}(k)\ dx\ dy \tag{8.3}$$

or

$$f_{m,m}(k) = \frac{1}{2\,\pi\,h\,a\,b} \int_0^b \int_0^a \left(\frac{x^2 + y^2}{\left(h_2^2 + x^2 + y^2\right)^{\frac{3}{2}}} - \frac{3}{\sqrt{h_2^2 + x^2 + y^2}} \right. \tag{8.4}$$

$$\left. - \frac{x^2 + y^2}{\left(h_1^2 + x^2 + y^2\right)^{\frac{3}{2}}} + \frac{3}{\sqrt{h_1^2 + x^2 + y^2}} \right) dx\,dy$$

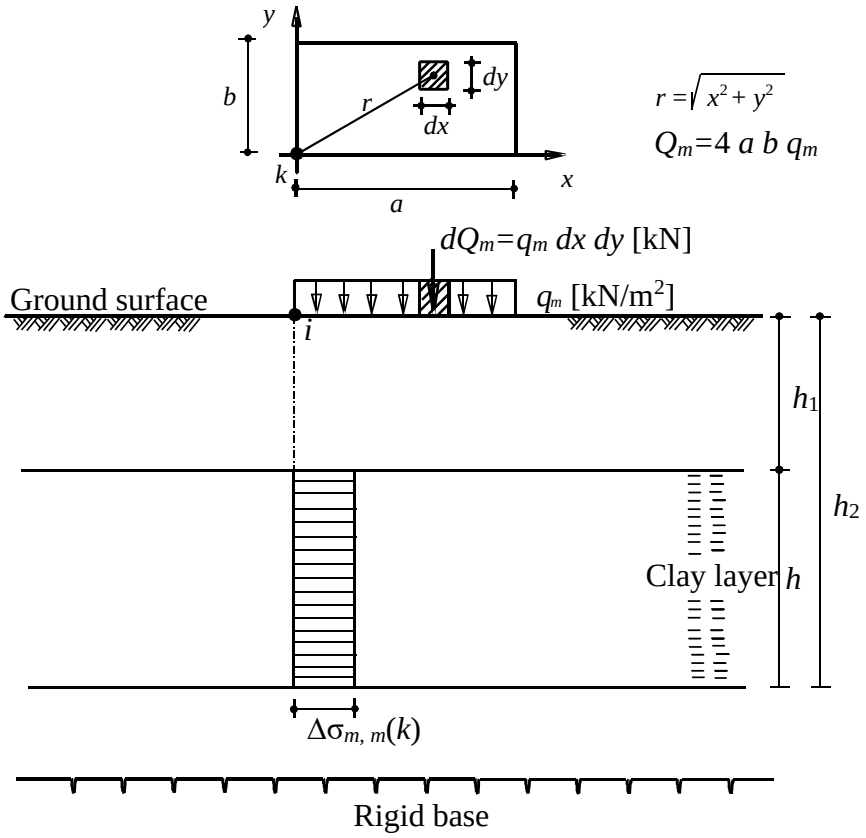

Figure 8.3 Increment of vertical stress in a soil layer due to a rectangular loaded area

Carrying out the integration, leads to:

$$f_{m,m}(k) = \frac{1}{2\,\pi\,h\,a\,b}\left\{\left(b\,\ln\frac{(c_2-a)\,(m+a)}{(c_2+a)\,(m-a)} + a\,\ln\frac{(c_2-b)\,(m+b)}{(c_2+b)\,(m-b)} + h_2\,\tan^{-1}\frac{a\,b}{h_2\,c_2}\right)\right.$$
$$\left. -\left(b\,\ln\frac{(c_1-a)\,(m+a)}{(c_1+a)\,(m-a)} + a\,\ln\frac{(c_1-b)\,(m+b)}{(c_1+b)\,(m-b)} + h_1\,\tan^{-1}\frac{a\,b}{h_1\,c_1}\right)\right\} \qquad (8.5)$$

where $m = \sqrt{a^2 + b^2}$, $c_2 = \sqrt{a^2 + b^2 + h_2^2}$ and $c_1 = \sqrt{a^2 + b^2 + h_1^2}$

8.2.2.3 Stress coefficient of a soil layer due to a circular loaded area

To determine the stress coefficient $f_{o,o}(k)$ for the element o in Figure 8.1, consider a circular loaded area of intensity q_o [kN/m^2] and a radius r_o [m] acting on the surface as shown in Figure 8.4.

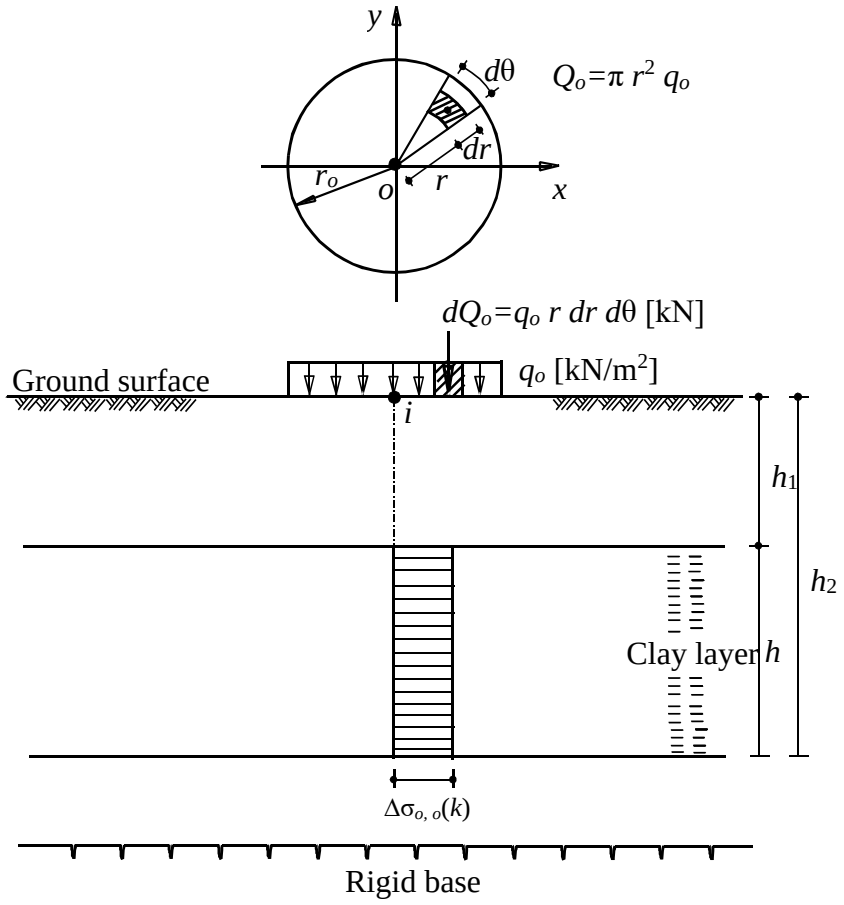

Figure 8.4 Increment of vertical stress in a soil layer due to a circular loaded area

Considering the point load $dQ_o = q_o\ r\ dr\ d\theta$ on the small element area $r\ dr\ d\theta$, the stress coefficient at the center of a circular loaded area at the surface can be obtained from:

$$f_{o,o}(k) = \frac{1}{\pi\, r_o^2} \int_0^{2\pi} \int_0^{r_o} df_{o,o}\ r\ dr\ d\theta$$

$$= \frac{1}{2\, h\, \pi^2\, r_o^2} \int_0^{2\pi} \int_0^{r_o} \left(\frac{r^2}{\left(h_2^2 + r^2\right)^{\frac{3}{2}}} \right. \tag{8.6}$$

$$\left. - \frac{3}{\sqrt{h_2^2 + r^2}} - \frac{r^2}{\left(h_1^2 + r^2\right)^{\frac{3}{2}}} + \frac{3}{\sqrt{h_1^2 + r^2}} \right) r\ dr\ d\theta$$

Carrying out the integration, leads to:

$$f_{o,o}(k) = \frac{1}{h\,\pi\, r_o^2} \left(h - \frac{h_2^2 + 2\, r_o^2}{\sqrt{h_2^2 + r_o^2}} + \frac{h_1^2 + 2\, r_o^2}{\sqrt{h_1^2 + r_o^2}} \right) \tag{8.7}$$

8.2.2.4 Stress coefficient of a soil layer due to a ring piece loaded area

To determine the stress coefficient $f_{l,l}$(k) for the ring piece element l in Figure 8.1, consider a ring piece loaded area of intensity q_l [kN/m^2] acting on the surface with the geometry shown in Figure 8.5. The area of the ring piece A [m] is given by:

$$A = \int_{-\frac{\alpha}{2}}^{\frac{\alpha}{2}} \int_{r_1}^{r_2} r^2\, dr\, d\theta = \frac{\alpha}{2} \left(r_2^2 - r_1^2 \right) \tag{8.8}$$

where:

α Angle of the ring piece, [Rad].
r_1 Short radius of the ring piece, [m].
r_2 Long radius of the ring piece, [m].

The distance c [m] between the center of the element area and the center of the raft is obtained from:

$$c\ A = \int r\ dA = \int_{-\frac{\alpha}{2}}^{\frac{\alpha}{2}} \int_{r_1}^{r_2} r^2\, dr\, d\theta \tag{8.9}$$

Carrying out the integration, leads to:

$$c = \frac{2}{3} \frac{\left(r_2^3 - r_1^3 \right)}{\left(r_2^2 - r_1^2 \right)} \tag{8.10}$$

Considering the point load $dQ_l = q_l \; r \; dr \; d\theta$ on the small element area $r \; dr \; d\theta$, the stress coefficient $f_{l,\,l}(k)$ at the center of a ring piece loaded area at the surface can be obtained from:

$$f_{l,\,l}(k) = \frac{1}{\pi \, h \, \alpha \left(r_2^2 - r_1^2 \right)} \int_{-\frac{\alpha}{2}}^{\frac{\alpha}{2}} \int_{r_1}^{r_2} df_{l,\,l} \; r \; dr \; d\theta$$

$$= \frac{1}{\pi \, h \, \alpha \left(r_2^2 - r_1^2 \right)} \int_{-\frac{\alpha}{2}}^{\frac{\alpha}{2}} \int_{r_1}^{r_2} \left(\frac{r^2 + c^2 - 2 \, c \, r \cos \theta}{\left(h_2^2 + r^2 + c^2 - 2 \, c \, r \cos \theta \right)^{\frac{3}{2}}} \right. \tag{8.11}$$

$$- \frac{3}{\sqrt{h_2^2 + r^2 + c^2 - 2 \, c \, r \cos \theta}} - \frac{r^2 + c^2 - 2 \, c \, r \cos \theta}{\left(h_1^2 + r^2 + c^2 - 2 \, c \, r \cos \theta \right)^{\frac{3}{2}}}$$

$$\left. + \frac{3}{\sqrt{h_1^2 + r^2 + c^2 - 2 \, c \, r \cos \theta}} \right) r \; dr \; d\theta$$

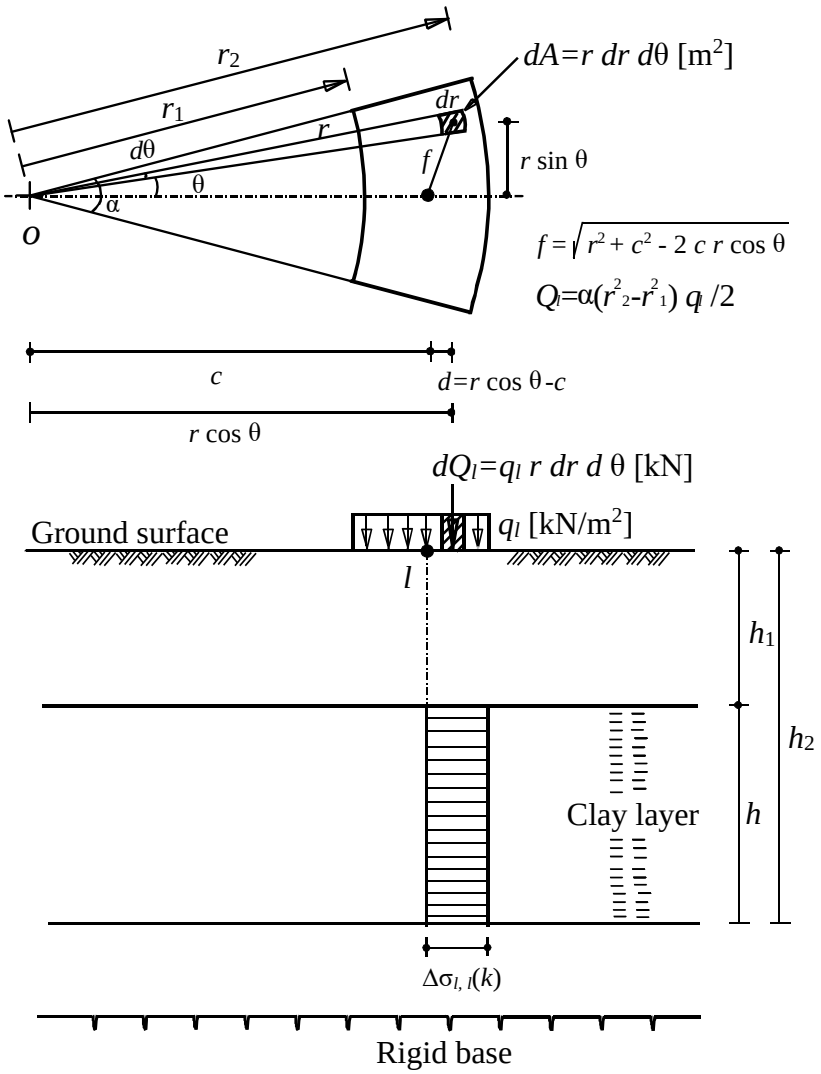

Figure 8.5 Increment of vertical stress in a soil layer due to a ring piece loaded area

Carrying out the integration first for *r* first, leads to:

$$f_{l,l}(k) = \frac{1}{\pi\, h\, \alpha \left(r_2^2 - r_1^2 \right)} \int_{-\frac{\alpha}{2}}^{\frac{\alpha}{2}} \left\{ f_1(\theta) + f_2(\theta) + f_3(\theta) + f_4(\theta) \right\} d\theta$$

$$= \frac{1}{\pi\, h\, \alpha \left(r_2^2 - r_1^2 \right)} \int_{-\frac{\alpha}{2}}^{\frac{\alpha}{2}} f(\theta) d\theta \qquad (8.12)$$

where the functions $f_1(\theta)$ to $f_4(\theta)$ are given by:

$$f_1(\theta) = -2\sqrt{h_2^2 + r_2^2 + c^2 - 2c\,r_2\cos\theta} + 2\sqrt{h_2^2 + r_1^2 + c^2 - 2c\,r_1\cos\theta}$$

$$-2c\cos\theta\ln\frac{r_2 - c\cos\theta + \sqrt{h_2^2 + r_2^2 + c^2 - 2c\,r_2\cos\theta}}{r_1 - c\cos\theta + \sqrt{h_2^2 + r_1^2 + c^2 - 2c\,r_1\cos\theta}} \tag{8.13}$$

$$f_2(\theta) = \frac{h_2^2}{\sqrt{h_2^2 + r_2^2 + c^2 - 2c\,r_2\cos\theta}} - \frac{h_2^2}{\sqrt{h_2^2 + r_1^2 + c^2 - 2c\,r_1\cos\theta}}$$

$$-\frac{h_2^2\,c\cos\theta\,(r_2 - c\cos\theta)}{(h_2^2 + c^2 - c^2\cos\theta)\sqrt{h_2^2 + r_2^2 + c^2 - 2c\,r_2\cos\theta}} \tag{8.14}$$

$$+\frac{h_2^2\,c\cos\theta\,(r_1 - c\cos\theta)}{(h_2^2 + c^2 - c^2\cos\theta)\sqrt{h_2^2 + r_1^2 + c^2 - 2c\,r_1\cos\theta}}$$

$$f_3(\theta) = 2\sqrt{h_1^2 + r_2^2 + c^2 - 2c\,r_2\cos\theta} - 2\sqrt{h_1^2 + r_1^2 + c^2 - 2c\,r_1\cos\theta}$$

$$+2c\cos\theta\ln\frac{r_2 - c\cos\theta + \sqrt{h_1^2 + r_2^2 + c^2 - 2c\,r_2\cos\theta}}{r_1 - c\cos\theta + \sqrt{h_1^2 + r_1^2 + c^2 - 2c\,r_1\cos\theta}} \tag{8.15}$$

$$f_4(\theta) = \frac{-h_1^2}{\sqrt{h_1^2 + r_2^2 + c^2 - 2c\,r_2\cos\theta}} + \frac{h_1^2}{\sqrt{h_1^2 + r_1^2 + c^2 - 2c\,r_1\cos\theta}}$$

$$+\frac{h_1^2\,c\cos\theta\,(r_2 - c\cos\theta)}{(h_1^2 + c^2 - c^2\cos\theta)\sqrt{h_1^2 + r_2^2 + c^2 - 2c\,r_2\cos\theta}} \tag{8.16}$$

$$-\frac{h_1^2\,c\cos\theta\,(r_1 - c\cos\theta)}{(h_1^2 + c^2 - c^2\cos\theta)\sqrt{h_1^2 + r_1^2 + c^2 - 2c\,r_1\cos\theta}}$$

Equation (8.12) as a function in cos θ under the square root is difficult to integrate analytically because it contains incomplete integrals, but if the interval -α/2 to α/2 in the function $f(\theta)$ becomes small, it can prove that:

$$\lim_{\max \Delta\theta \to 0} f(\theta) = f(0) = \text{constant}$$

Therefore, choosing a suitable small angle α for the raft division, gives the value of the integral in Eq. (8.12) as:

$$f_{l,l}(k) = \frac{f(0)}{\pi h \left(r_2^2 - r_1^2 \right)} \tag{8.17}$$

Substituting θ = 0 in Eqs (8.13) to (8.16), gives the stress coefficient at the center of the ring piece loaded area as:

$$f_{l,l}(k) = \frac{1}{\pi h \left(r_2^2 - r_1^2 \right)} \left[- 2 \sqrt{h_2^2 + (r_2 - c)^2} + 2 \sqrt{h_2^2 + (r_1 - c)^2} \right.$$

$$- 2\, c \ln \frac{r_2 - c + \sqrt{h_2^2 + (r_2 - c)^2}}{r_1 - c + \sqrt{h_2^2 + (r_1 - c)^2}} + \frac{h_2^2}{\sqrt{h_2^2 + (r_2 - c)^2}} - \frac{h_2^2}{\sqrt{h_2^2 + (r_1 - c)^2}}$$

$$- \frac{c\,(r_2 - c)}{\sqrt{h_2^2 + (r_2 - c)^2}} + \frac{c\,(r_1 - c)}{\sqrt{h_2^2 + (r_1 - c)^2}} + 2 \sqrt{h_1^2 + (r_2 - c)^2}$$

$$- 2 \sqrt{h_1^2 + (r_1 - c)^2} + 2\, c \ln \frac{r_2 - c + \sqrt{h_1^2 + (r_2 - c)^2}}{r_1 - c + \sqrt{h_1^2 + (r_1 - c)^2}} + \frac{- h_1^2}{\sqrt{h_1^2 + (r_2 - c)^2}}$$

$$\left. + \frac{h_1^2}{\sqrt{h_1^2 + (r_1 - c)^2}} + \frac{c\,(r_2 - c)}{\sqrt{h_1^2 + (r_2 - c)^2}} - \frac{c\,(r_1 - c)}{\sqrt{h_1^2 + (r_1 - c)^2}} \right] \tag{8.18}$$

For more simplification, another alternative equations of stress coefficients can be derived for rectangular, circular and ring piece loaded areas only when $h_1 = 0$ and $r = 0$, Eqns (8.19) to (8.21). This can be done by integrating third and fourth terms in Eq. (8.2) using the same above manner. In other cases when $h_1 \neq 0$ or $r \neq 0$, Eq. (8.2) may be used.

Stress coefficient for a rectangular loaded area when $h_1 = 0$ and $r = 0$ is given by:

$$f_{m,m}(k) = \frac{1}{2\pi\, h_2} \left(\frac{- 3}{h_2} + \frac{2}{a} \ln \frac{(m + a)}{(m - a)} + \frac{2}{b} \ln \frac{(m + b)}{(m - b)} \right) \tag{8.19}$$

Stress coefficient for a circular loaded area when $h_1 = 0$ and $r = 0$ is given by:

$$f_{o,o}(k) = \frac{1}{2\pi\ h_2}\left(\frac{-3}{h_2} + \frac{4}{r_o}\right) \tag{8.20}$$

Stress coefficient for a ring piece loaded area when $h_1 = 0$ and $r = 0$ is given by:

$$f_{l,l}(k) = \frac{1}{2\pi\ h_2}\left(\frac{-3}{h_2} + \frac{4}{r_2 + r_1} + \frac{4\,c}{r_2^2 - r_1^2}\ \ln\ \frac{r_2 - c}{r_1 - c}\right) \tag{8.21}$$

8.3 Numerical analysis of rigid raft when clay is defined by m_v

8.3.1 Formulation of the stress matrix

To formulate the stiffness matrix for analyzing the rigid raft using the soil parameter m_v [m^2/kN] with considering the increment of vertical stress $\Delta\sigma$ [kN/m^2] in the soil layer H [m], consider a set of n elements of the raft. The settlement s_i [m] at a soil element i due to contact loads on n elements (circular raft as an example in Figure 8.6) is given by:

$$s_i = \int_{h_1}^{h_2} m_v(z)\ \sigma_z\ dz \tag{8.22}$$

where:

σ_z	Vertical stress at depth z, [kN/ m^2].
$m_v(z)$	Coefficient of volume change at depth z, [m^2/ kN].

If the coefficient of volume change is assumed to be constant with depth ($m_v(z) = m_v$), then the consolidation settlement will be given by:

$$s_i = m_v\,\Delta\sigma_i\,H \tag{8.23}$$

The increment of vertical stress $\Delta\sigma_i$ [kN/m^2] in a soil layer of thickness H due to n contact forces Q_j [kN] on the surface is given by:

$$\Delta\sigma_i = \sum_{j=1}^{n} f_{i,j}\,Q_j \tag{8.24}$$

where $f_{i,j}(k)$ is the stress coefficient of an element i due to a load Q_j at element j, [1/m^2], Figure 8.6.

Equation (8.24) is rewritten in matrix form as:

$$\{\Delta\sigma\} = [f]\{Q\} \tag{8.25}$$

where:

$\{\Delta\sigma\}$	Vector of increment of vertical stresses.
$[f]$	Matrix of stress coefficients.
$\{Q\}$	Vector of contact forces on element centers.

Inversing the matrix of stress coefficients, gives Eq. (8.25) in the form:

$$\{Q\} = [k]\{\Delta\sigma\} \tag{8.26}$$

where $[k]=[f]^{-1}$.

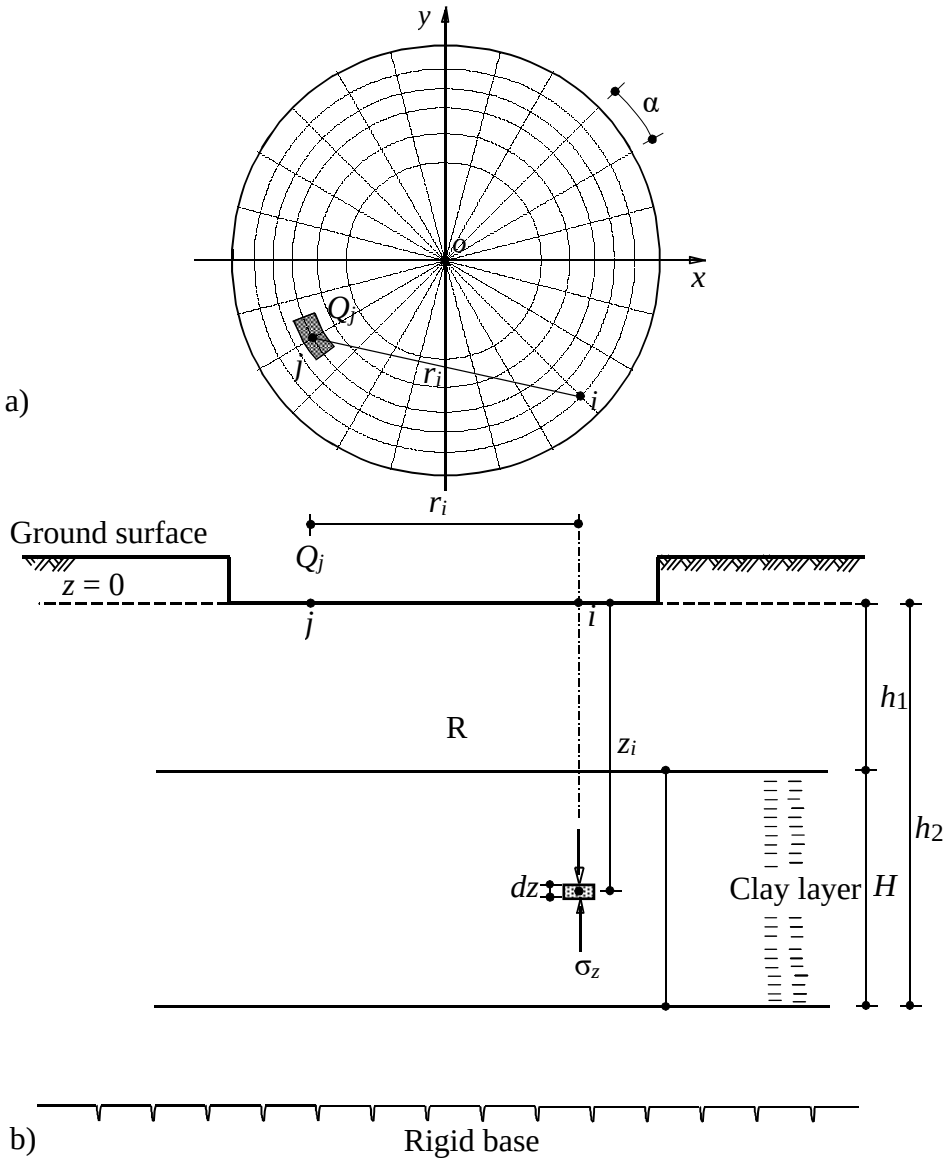

Figure 8.6 Formulation of stress coefficients

a) Raft plan
b) Clay layer

8.3.2 Case of uniform settlement ($e_x = 0$ and $e_y = 0$)

For a raft with a centric load (Figure 8.7), the settlement will be uniform. Therefore, the unknowns of the problem are reduced to n contact forces Q_i and the rigid body translation w_o [m]. The derivation of the uniform settlement for the rigid raft can be carried out by equating the settlement s_i by a uniform translation w_o at all elements on the raft. A uniform translation w_o at all elements on the raft will lead also to a uniform increment of vertical stress on the soil at all elements under the raft.

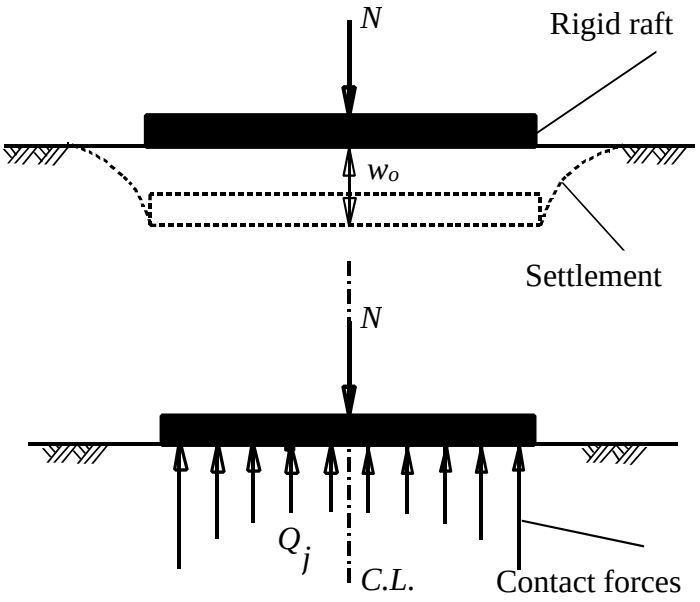

Figure 8.7 Settlement and contact forces under a rigid raft (case of uniform settlement)

In case of a raft with a centric load, Eq. (8.23) may be written as:

$$w_o = m_v \, \Delta\sigma_o \, H \tag{8.27}$$

where $\Delta\sigma_o$ is the uniform increment of vertical stress in the soil at all elements under the raft.

Expanding Eq. (8.26) for all elements and equating all increment of vertical stresses by $\Delta\sigma_o$, yields to the contact forces as a function in terms $k_{i,j}$ of the matrix [k] as follows:

$$\left.\begin{aligned}
Q_1 &= k_{1,1}\,\Delta\sigma_o + k_{1,2}\,\Delta\sigma_o + k_{1,3}\,\Delta\sigma_o + \ldots + k_{1,n}\,\Delta\sigma_o \\
Q_2 &= k_{2,1}\,\Delta\sigma_o + k_{2,2}\,\Delta\sigma_o + k_{2,3}\,\Delta\sigma_o + \ldots + k_{2,n}\,\Delta\sigma_o \\
Q_3 &= k_{3,1}\,\Delta\sigma_o + k_{3,2}\,\Delta\sigma_o + k_{3,3}\,\Delta\sigma_o + \ldots + k_{3,n}\,\Delta\sigma_o \\
&\ldots \\
Q_n &= k_{n,1}\,\Delta\sigma_o + k_{n,2}\,\Delta\sigma_o + k_{n,3}\,\Delta\sigma_o + \ldots + k_{n,n}\,\Delta\sigma_o
\end{aligned}\right\} \tag{8.28}$$

Carrying out the summation of all contact forces in Eq. (8.28), leads to:

$$\sum_{i=1}^{n} Q_i = \Delta\sigma_o \sum_{i=1}^{n} \sum_{j=1}^{n} k_{i,j} \tag{8.29}$$

Replacing the sum of all contact forces in Eq. (8.29) by the resultant force N [kN], gives the uniform increment of vertical stress $\Delta\sigma_o$ by:

$$\Delta\sigma_o = \frac{N}{\sum_{i=1}^{n} \sum_{j=1}^{n} k_{i,j}} \tag{8.30}$$

Substituting Eq. (8.30) in Eq. (8.27), gives the rigid body translation w_o by:

$$w_o = \frac{m_v \, N \, H}{\sum_{i=1}^{n} \sum_{j=1}^{n} k_{i,j}} \tag{8.31}$$

Substituting the uniform increment of vertical stress $\Delta\sigma_o$ in Eq. (8.28), gives the n unknown contact forces Q_k by:

$$Q_k = \frac{N \sum_{j=1}^{n} k_{k,j}}{\sum_{i=1}^{n} \sum_{j=1}^{n} k_{i,j}} \tag{8.32}$$

In Eq. (8.32), the contact force under the rigid raft is found to be independent on the mechanical properties of the clay.

8.3.3 Case of single eccentric load ($e_x \neq 0$)

For a raft with a single eccentric load about y-axis (Figure 8.8), the unknowns of the problem

are n contact forces Q_i, the uniform rigid body translation w_o and the rotation θ_y [Rad] about y-axis. The uniform rigid body translation w_o is obtained by analyzing the same raft without eccentricity. Due to the raft rigidity, the following linear relation expresses the settlement s_i at an element center i that has a distance x_i from the geometry centroid:

$$s_i = w_o + x_i \tan \theta_y \tag{8.33}$$

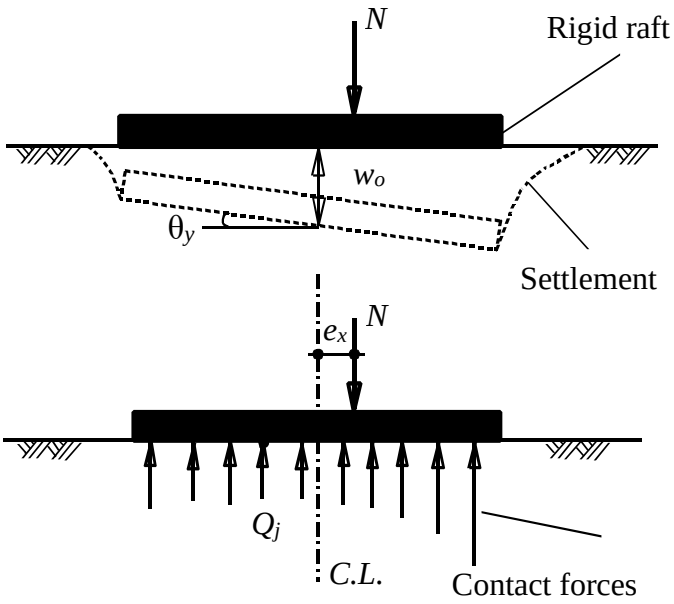

Figure 8.8 Settlement and contact forces under a rigid raft (case of a single eccentric load)

The linear displacement relation, which expresses the raft rigidity due to an eccentric load can be obtained by substituting the value of s_i from Eq. (823) in Eq. (8.33) as follows:

$$m_v \Delta\sigma_i H = w_o + x_i \tan\theta_y \tag{8.34}$$

or

$$\Delta\sigma_i = \frac{w_o}{m_v H} + x_i \frac{\tan\theta_y}{m_v H} \tag{8.35}$$

Substituting Eq. (8.30) and Eq. (8.31) in Eq. (8.35) and rearranging the equation, leads to:

$$\Delta\sigma_i = \Delta\sigma_o + x_i \frac{\tan\theta_y}{m_v H} \tag{8.36}$$

Equation (8.36) may be rewritten in a simple form of linear relation in the stress as:

$$\Delta\sigma_i = \Delta\sigma_o + x_i \beta_y \tag{8.37}$$

where the symbol β_y is expressed as:

$$\beta_y = \frac{\tan\theta_y}{m_v H} \tag{8.38}$$

Similarly to the procedures of derivation w_o, contact forces in Eq. (8.28) becomes:

$$\left.\begin{aligned} Q_1 &= k_{1,1}\,\Delta\sigma_1 + k_{1,2}\,\Delta\sigma_2 + k_{1,3}\,\Delta\sigma_3 + \ldots + k_{1,n}\,\Delta\sigma_n \\ Q_2 &= k_{2,1}\,\Delta\sigma_1 + k_{2,2}\,\Delta\sigma_2 + k_{2,3}\,\Delta\sigma_3 + \ldots + k_{2,n}\,\Delta\sigma_n \\ Q_3 &= k_{3,1}\,\Delta\sigma_1 + k_{3,2}\,\Delta\sigma_2 + k_{3,3}\,\Delta\sigma_3 + \ldots + k_{3,n}\,\Delta\sigma_n \\ &\ldots \\ Q_n &= k_{n,1}\,\Delta\sigma_1 + k_{n,2}\,\Delta\sigma_2 + k_{n,3}\,\Delta\sigma_3 + \ldots + k_{n,n}\,\Delta\sigma_n \end{aligned}\right\} \tag{8.39}$$

Multiplying both sides of a row i in Eq. (8.39) by x_i, gives the following system of linear equations:

$$\left.\begin{aligned} Q_1\ x_1 &= x_1\ k_{1,1}\,\Delta\sigma_1 + x_1\ k_{1,2}\,\Delta\sigma_2 + x_1\ k_{1,3}\,\Delta\sigma_3 + \ldots + x_1\ k_{1,n}\Delta\sigma_n \\ Q_2\ x_2 &= x_2\ k_{2,1}\,\Delta\sigma_1 + x_2\ k_{2,2}\,\Delta\sigma_2 + x_2\ k_{2,3}\,\Delta\sigma_3 + \ldots + x_2\ k_{2,n}\,\Delta\sigma_n \\ Q_3\ x_3 &= x_3\ k_{3,1}\,\Delta\sigma_1 + x_3\ k_{3,2}\,\Delta\sigma_2 + x_3\ k_{3,3}\,\Delta\sigma_3 + \ldots + x_3\ k_{3,n}\,\Delta\sigma_n \\ &\ldots \\ Q_n\ x_n &= x_n\ k_{n,1}\,\Delta\sigma_1 + x_n\ k_{n,2}\,\Delta\sigma_2 + x_n\ k_{n,3}\,\Delta\sigma_3 + \ldots + x_n\ k_{i,n}\,\Delta\sigma_n \end{aligned}\right\} \tag{8.40}$$

Carrying out the summation of all $Q_i\ x_i$, gives the following equation:

$$\sum_{i=1}^{n} Q_i\ x_i = \sum_{i=1}^{n} x_i \sum_{j=1}^{n} k_{i,j}\,\Delta\sigma_j \tag{8.41}$$

Substituting Eq. (8.37) in Eq. (8.41), leads to:

$$\sum_{i=1}^{n} Q_i\ x_i = \sum_{i=1}^{n} x_i \sum_{j=1}^{n} k_{i,j}\left(\Delta\sigma_o + x_j\ \beta_y\right) \tag{8.42}$$

Equating the moment due to resultant N about the y-axis by the sum of moments due to contact forces Q_i about that axis, gives the following equation:

$$N\ e_x = Q_1\ x_1 + Q_2\ x_2 + Q_3\ x_3 + \ldots + Q_n\ x_n = \sum_{i=1}^{n} Q_i\ x_i \tag{8.43}$$

where e_x [m] is the load eccentricity about y-axis.

Substituting Eq (8.42) in Eq (8.43) and rearranging the equation, gives the value of β_y as:

$$\beta_y = \frac{N\ e_x - \Delta\sigma_o \sum_{i=1}^{n} x_i \sum_{j=1}^{n} k_{i,j}}{\sum_{i=1}^{n} x_i \sum_{j=1}^{n} k_{i,j}\ x_j} \tag{8.44}$$

Substituting the value of β_y in Eq. (8.38), gives the rigid rotation θ_y about *y*-axis as:

$$\theta_y = \tan^{-1}\left(\beta_y\ m_v\ H\right) \tag{8.45}$$

Substituting β_y in Eq. (8.37), gives the *n* increment of vertical stresses $\Delta\sigma_i$. Then, substituting $\Delta\sigma_i$ in Eq. (8.39), gives the *n* unknown contact forces Q_i.

8.3.4 General case of double eccentric load ($e_x \neq 0$ and $e_y \neq 0$)

The derivation of the consolidation settlement in the case of an eccentric load in *x*-axis can be carried out in a similar manner to the above procedures, which leads to the following equation in β_x:

$$\beta_x = \frac{N\ e_y - \Delta\sigma_o \sum_{i=1}^{n} y_i \sum_{j=1}^{n} k_{i,j}}{\sum_{i=1}^{n} y_i \sum_{j=1}^{n} k_{i,j}\ y_j} \tag{8.46}$$

The rigid body rotation θ_x [Rad] about *x*-axis is obtained from the symbol β_y as:

$$\theta_x = \tan^{-1}\left(\beta_x\ m_v\ H\right) \tag{8.47}$$

In the general case of an eccentric load in both directions, each case is analyzed separately to find the uniform rigid displacement w_o and rotations θ_y and θ_x about *y*- and *x*-axes, respectively. Then, the consolidation settlement s_i at any point *i* that has coordinates x_i and y_i from the geometry centroid is expressed in general equation as:

$$s_i = w_o + x_i \tan\theta_y + y_i \tan\theta_x \tag{8.48}$$

while the increment of vertical stress in the general case is given by:

$$\Delta\sigma_i = \Delta\sigma_o + x_i \beta_y + y_i \beta_x \tag{8.49}$$

Substituting β_x and β_y in Eq. (8.49), gives the *n* increment of vertical stresses $\Delta\sigma_i$. Then, substituting $\Delta\sigma_i$ in Eq. (8.27), gives the *n* unknown contact forces Q_i.

8.4 Numerical analysis of rigid raft when clay is defined by C_c

8.4.1 Introduction

To simplify the foundation problem, the stress applied by a foundation to the ground is often assumed to be uniform due to a flexible loaded area. The actual distribution of the contact pressure between the foundation and the soil may be far from uniform. This distribution depends mainly on the ratio between the rigidity of the raft and the soil.

Obviously, the nonuniform contact pressure causes some effects on the distribution of the stress in soil and consequently on the soil settlement. It is clear that the behavior of the soil depends essentially on the distribution of contact pressure under the raft. Therefore, a reliable estimate of consolidation for a rigid raft cannot be obtained from flexible analysis. An analysis for the contact pressure under a rigid raft on isotopic elastic half-space medium was carried out by many authors. Several studies have been carried out concerning the analysis of circular elastic or rigid rafts such as *Chakravorty/ Ghosh* (1975), *Krajcinovic* (1976), *Gazetas* (1982), *Kamal* (1983), *Celep* (1988), *Xiao-jing* (1988), *Zaman/ Faruque/ Mahmood* (1990), *Vallabhan* (1991), *Milovic*/ *Djogo* (1991), *Akoz*/ *Kadioglu* (1996), *Melerski* (1997), *Kocatürk*, (1997), *Bose/ Das* (1997). Most dealt with the soil as a Winkler medium or an elastic medium, where the properties of the soil are modeled by either modulus of subgrade reaction or modulus of elasticity. Moreover, most dealt with the interaction between the soil and the circular raft as axisymmetric problem (*Melerski* (1997) and *Bose/ Das* (1997)). The next sections describe a numerical modeling to obtain the nonlinear stress distribution on soil and consequently the consolidation settlement of eccentric loaded rigid raft on consolidated clay deposits. The proposed analysis is a direct numerical solution without iteration.

8.4.2 Formulation of the stress matrix

For normally consolidated clay, the consolidation settlement s_i of a layer H under the point i due to n contact forces at the surface is given by:

$$s_i = \frac{C_c}{1 + e_o} \log \left(\frac{\sigma_o + \Delta\sigma_i}{\sigma_o} \right) H \tag{8.50}$$

where:

C_c Compression index, [-]
e_o Initial void ratio, [-]
σ_o Initial overburden pressure, [kN/m^2]

Changing the common log to the natural log in Eq. (8.50) and rewrite the equation as follows:

$$\Delta\sigma_i = \sigma_o \left(e^{\mu_i} - 1\right) \tag{8.51}$$

where $\mu_i = \dfrac{s_i(1 + e_o)\ln(10)}{C_c H}$

8.4.3 Case of uniform settlement ($e_x = 0$ and $e_y = 0$)

For a raft with centric load, the settlement will be uniform. Therefore, the unknowns of the problem are reduced to n contact forces Q_i and the rigid body translation w_o. The derivation of the uniform settlement for the rigid raft can be carried out by equating the settlement s_i by a uniform translation w_o for all nodes on the raft. Carrying out the summation of all contact forces:

$$\sum_{i=1}^{n} Q_i = \Delta\sigma_o \sum_{i=1}^{n} \sum_{j=1}^{n} k_{i,j} \tag{8.52}$$

where in this case:

$$\Delta\sigma_i = \Delta\sigma_o = \sigma_o \left(e^{\mu_i} - 1\right) \tag{8.53}$$

and

$$\mu_i = \mu_o = \frac{w_o(1 + e_o)\ln(10)}{C_c H} \tag{8.54}$$

Then, the vertical stress $\Delta\sigma_o$, which is constant at all nodes, is obtained from:

$$\Delta\sigma_o = \frac{\sum_{i=1}^{n} Q_i}{\sum_{i=1}^{n} \sum_{j=1}^{n} k_{i,j}} = \frac{N}{\sum_{i=1}^{n} \sum_{j=1}^{n} k_{i,j}} \tag{8.55}$$

where the sum of all contact forces must be equal to the resultant force N. Substituting this value of $\Delta\sigma_o$ into Eq. (8.50) gives the rigid body translation w_o, which equals to the settlement s_i at all nodes:

$$w_o = \frac{C_c}{1 + e_o} \log\left(\frac{\sigma_o + \Delta\sigma_o}{\sigma_o} \right) H \tag{8.56}$$

Substituting the value of $\Delta\sigma_o$ into Eq. (8.39) gives the n unknown contact forces Q_k.

$$Q_k = \frac{N \sum_{j=1}^{n} k_{k,j}}{\sum_{i=1}^{n} \sum_{j=1}^{n} k_{i,j}} \tag{8.57}$$

It can be noticed from Eq. (8.55) that the contact forces under the rigid raft is found to be independent on the mechanical properties of the clay.

8.4.4 Case of eccentric load ($e_x \neq 0$)

Due to the raft rigidity, the following linear relation expresses the settlement s_i at a node i that has a distance x_i from the geometry centroid:

$$s_i = w_o + x_i \tan\theta_y \tag{8.58}$$

In this case the coefficient μ_i is expressed by:

$$\mu_i = \frac{(w_o + x_i \tan\theta_y)(1+e_o)\ln(10)}{C_c H} \tag{8.59}$$

Simplifying Eq. (8.57) to:

$$\mu_i = \mu_o + x_i \alpha_y \tag{8.60}$$

where:

$$\alpha_y = \frac{\tan\theta_y (1+e_o)\ln(10)}{C_c H} \tag{8.61}$$

Substituting Eq. (8.58) into Eq. (8.52) gives:

$$\Delta\sigma_i = \sigma_o \left(e^{(\mu_o + x_i \alpha_y)} - 1\right) \tag{8.62}$$

Substituting Eq (8.42) in Eq (8.59) and rearranging the equation, gives the following equation in n terms and a variable α_y:

$$N e_x = \sum_{i=1}^{n} x_i \sum_{j=1}^{n} k_{i,j} \Delta\sigma_o \left(e^{(\mu_o + x_i \alpha_y)} - 1\right) \tag{8.63}$$

Equation (8.62) is an exponential equation in the unknown α_y. Solving this equation iteratively gives the value of α_y. Then, the rigid rotation about y-axis θ_y is obtained from:

$$\theta_y = \tan^{-1}\left(\frac{\alpha_y C_c H}{(1+e_o)\ln(10)}\right) \tag{8.64}$$

Substituting the value of α_y into Eq. (8.62) gives the n vertical stresses $\Delta\sigma_i$. Then, substituting these values of $\Delta\sigma_i$ into Eq. (8.27) gives the n unknown contact forces Q_i.

8.4.5 General case of eccentric load ($e_x \neq 0$ and $e_y \neq 0$)

Although the analysis of a rigid circular raft needs only to determine single rotation θ_y and a rigid body translation w_o, but it can be derived the general case of eccentric load about both *x*- and *y*-axes for the other types of rafts. Where the derivation of the consolidation settlement in the case of eccentric load in *y*-axis can be carried out in similar manner to the above procedures, which leads to the following equation in α_x:

$$N\ e_y = \sum_{i=1}^{n} y_i \sum_{j=1}^{n} k_{i,j}\, \sigma_o \left(e^{(\mu_o + y_i\, \alpha_y)} - 1\right) \tag{8.65}$$

where:

$$\alpha_x = \frac{\tan\theta_x\,(1+e_o)\ln(10)}{C_c\ H} \tag{8.66}$$

and the rigid rotation about *x*-axis θ_x is obtained from:

$$\theta_x = \tan^{-1}\left(\frac{\alpha_x\ C_c\ H}{(1+e_o)\ \ln(10)}\right) \tag{8.67}$$

Then, the consolidation settlement s_i in the general case of eccentric load at any point *i* that has coordinates x_i and y_i from the geometry centroid is given by:

$$s_i = w_o + x_i \tan\theta_y + y_i \tan\theta_x \tag{8.68}$$

8.5 Semi-analytical analysis of rigid raft

8.5.1 Introduction

Independent on tables and charts semi-analytical procedures using coefficients-technique were developed to calculate the magnitude of consolidation settlement for the two common types of rectangular and circular rafts on a deeply extended clay layer. The semi-analytical procedure gives results identical with those of numerical procedure, which normally requires complicated computations. It can reduce the computation time required to analyzing large raft problems. The procedures is implemented in *Quick-ELPLA*, in which the calculation can be carried out in few steps and short time.

8.5.2 Circular rigid raft

Boussinesq (1885) solved the problem of stress distribution that gives a constant displacement in the half-space medium at all points in the circular region. It is found that the stress is independent on the elastic constants of the half-space medium. *El Gendy* (2006) had also showed that the distribution of contact pressure for rafts on half-space medium of clay layer is quite similar to that on half-space medium of elastic layer. This physical concept is used to determine the consolidation settlement of an extensive, homogeneous deposit of clay. The idea is that the stress which causes a constant elastic displacement in the half-space medium must also cause a constant consolidation settlement in a deeply extended clay layer. This means the formulae used to determine the contact pressure distribution under rigid rafts on elastic medium are also valid for rigid rafts on consolidated medium using the soil properties C_c and e_o. Consequently, the contact pressure becomes known for the problem. In this case the unknown of the problem is considerably reduced to the main displacement w_o and rotation θ_y.

Available formulae used to determine the contact pressure under rigid rafts on the half-space medium may be found in references of *Poulos* et al. (1974), *Lang* et al. (1996) and *Graßhoff* et al. (1997). The contact pressure distribution under a rigid circular raft with $e_x < a/3$, Figure 8.9, is given by:

$$q_i = \frac{N}{2\,\pi\,a}\;\frac{1+3\left(\frac{e_x}{a}\right)\left(\frac{x}{a}\right)}{\sqrt{a^2-r^2}} \tag{8.69}$$

where:

q_i Contact pressure at a point i, [kN/m^2].
a Raft radius, [m].
N Total resultant force, [kN].
e_x Eccentricity of the resultant force in x-direction, [m].
r Radial distance of point i from the center, [m].
θ Angle between r and x-axis, [Rad].

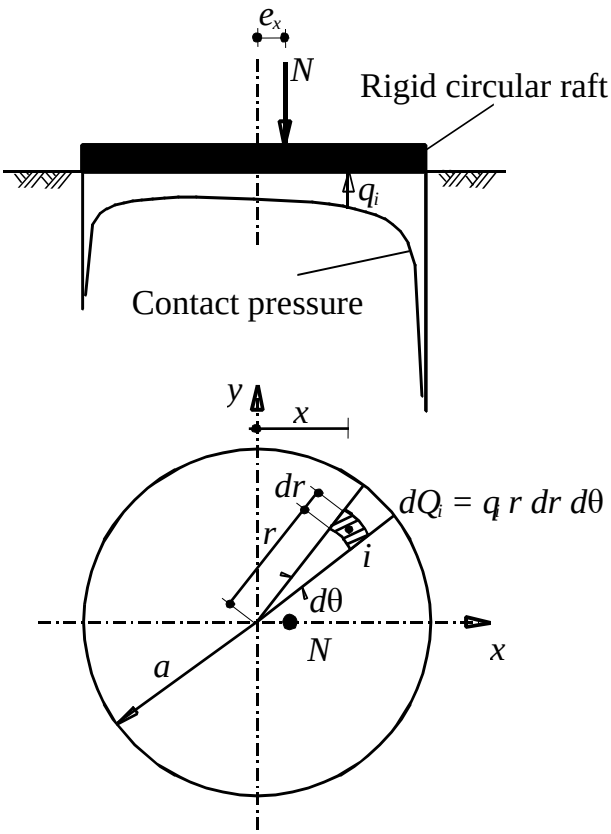

Figure 8.9 Contact pressure on an element *i* under circular raft

8.5.3 Rectangular rigid raft

For a rigid rectangular raft with a centric load, the contact pressure q_i under at a point *i* of coordinates (*x, y*) from the center, Figure 8.10, is given by:

$$q_i = \frac{4\,N}{\pi^2 \sqrt{\left[a^2 - 4\,x^2\right]\left[b^2 - 4\,y^2\right]}} \tag{8.70}$$

where:

q_i	Contact pressure at a point *i*, [kN/m^2].
a	Raft length, [m].
b	Raft width, [m].
N	Total resultant force, [kN].
x, y	Point coordinate in *x*-and *y*-directions.

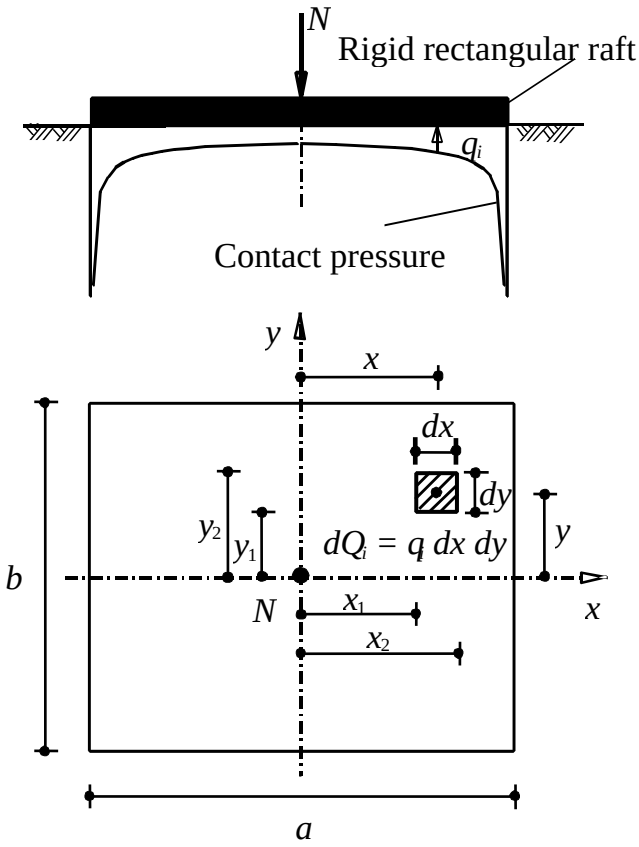

Figure 8.10 Contact pressure on an element *i* under rectangular raft

To formulate the contact force equation for estimating the magnitude of consolidation settlement of deeply extended clay layer, both the raft and the contact area of the supporting medium are divided into elements as carried out before for the numerical procedures. The contact pressure q_i at an element *i* under the raft is replaced by an equivalent contact force Q_i. The contact force Q_i for an element *i* can be obtained by integrating Eqns (8.67) and (8.68) over the element.

For a circular rigid raft, the contact force is given by:

$$Q_i = q_i\, r\, d\theta\, dr = \frac{N}{2\,\pi\, a} \int_{r_1}^{r_2}\int_{\theta_1}^{\theta_2} \left[\frac{1+3\left(\frac{e_x}{a}\right)\left(\frac{r\,\cos\,\theta}{a}\right)}{\sqrt{a^2-r^2}} \right] r\, d\theta\, dr \qquad (8.71)$$

Integrating Eq. (8.69), yields to:

$$Q_i = \frac{N}{2\pi a}\left\{(\theta_2-\theta_1)\left(\sqrt{a^2-r_1^2}-\sqrt{a^2-r_2^2}\right)+\frac{3e_x}{2a^2}(\sin\theta_2-\sin\theta_1)\right.$$

$$\left.\times\left(a^2\sin^{-1}\frac{r_2}{a}+r_2\sqrt{a^2-r_2^2}-a^2\sin^{-1}\frac{r_1}{a}+r_1\sqrt{a^2-r_1^2}\right)\right\} \tag{8.72}$$

while for a rectangular rigid raft, the contact force is given by:

$$Q_i = q_i\,dx\,dy = \frac{4N}{\pi^2}\int_{x_1}^{x_2}\int_{y_1}^{y_2}\frac{dx\,dy}{\sqrt{\left[a^2-4x^2\right]\left[b^2-4y^2\right]}} \tag{8.73}$$

Integrating Eq. (8.71), yields to:

$$Q_i = \frac{N}{\pi^2}\left(\sin^{-1}\frac{2x_2}{a}-\sin^{-1}\frac{2x_1}{a}\right)\left(\sin^{-1}\frac{2y_2}{b}-\sin^{-1}\frac{2y_1}{b}\right) \tag{8.74}$$

Once the contact forces are determined under the raft at different elements, it can determine the increment of vertical stresses in sub-layers shown in Figure 8.11. Referring to the circular raft symmetry about *x*-axis, it is sufficient to determine the settlement at two different points on the axis of symmetry, as example at the center and edge, to find the unknown raft rotation θ_y and then settlements at all elements under the raft. Using the clay properties C_c and e_o, the consolidation settlement s_i at point *i* due to all contact forces at the surface is given by:

$$s_i = \frac{C_c\,h}{1+e_o}\sum_{k=1}^{l}\log\left(\frac{\sigma_o(k)+\Delta\sigma_i(k)}{\sigma_o(k)}\right) \tag{8.75}$$

where:

C_c Compression index, [-].
e_o Initial void ratio, [-].
$\sigma_o(k)$ Initial overburden pressure in sub-layer *k*, [kN/m^2].
$\Delta\sigma_o(k)$ Increment of vertical stress at point *i* in sub-layer *k*, [kN/m^2].
l Number of clay layers.

To consider stress coefficients $f_{i,j}$ for a hundred per cent settlement to occur, the settlement in soil is calculated up to a sub-layer after which the increase in settlement due to the next sub-layer becomes less than 0.001 [cm].

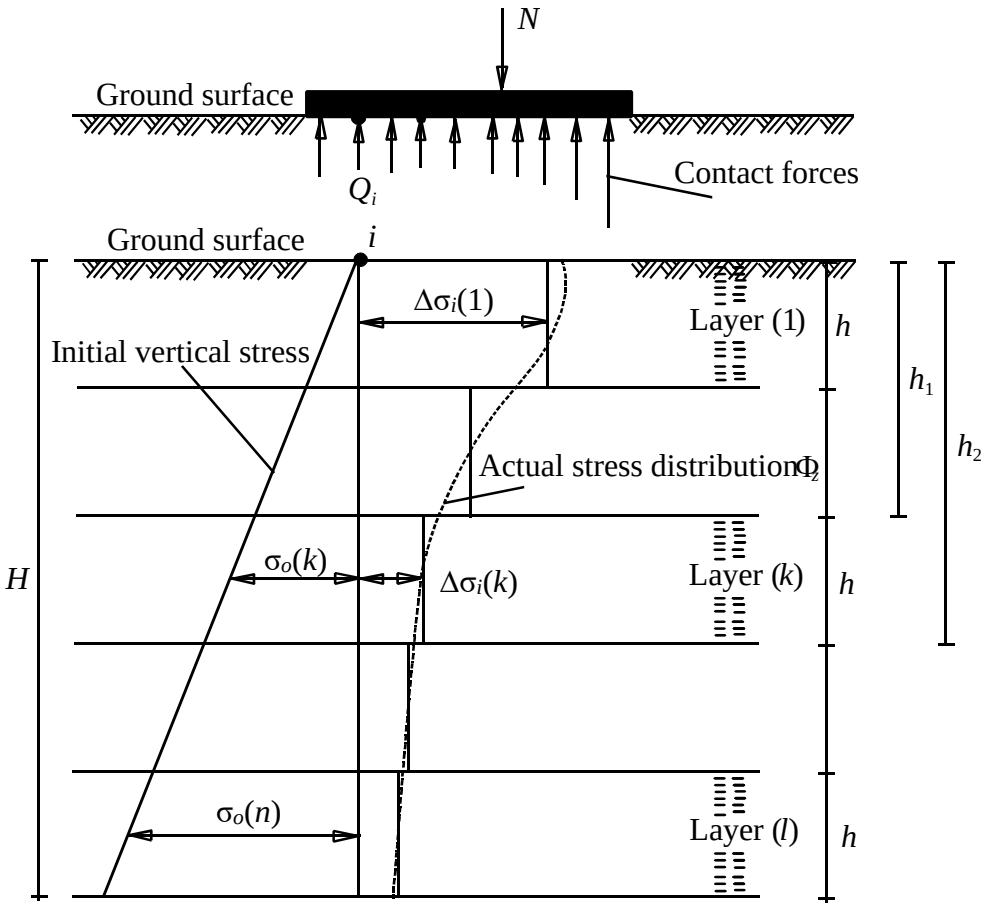

Figure 8.11 Dividing the extended clay soil layer to many sub-layers of thickness *h*

8.6 Soil properties and parameters

8.6.1 *Poisson*'s ratio ν_s

Poisson's ratio ν_s for a soil is defined as the ratio of lateral strain to longitudinal strain. It can be evaluated from the Triaxial test. *Poisson*'s ratio ν_s can be determined from at-rest earth pressure coefficient K_o as follows

$$\nu_s = \frac{K_o}{1 + K_o} \tag{8.76}$$

Some typical values for *Poisson*'s ratio are shown in Table 8.1 according to *Bowles* (1977). *Poisson*'s ratio in general ranges between 0 and 0.5.

Table 8.1 Typical range of values for *Poisson*'s ratio ν_s according to *Bowles* (1977)

Type of soil	*Poisson*'s ratio ν_s [-]
Clay, saturated	0.4 - 0.5
Clay, unsaturated	0.1 - 0.3
Sandy clay	0.2 - 0.3
Silt	0.3 - 0.35
Sand, dense	0.2 - 0.4
Sand, coarse (void ratio = 0.4 - 0.7)	0.15
Sand, fine grained (void ratio = 0.4 - 0.7)	0.25
Rock	0.1 - 0.4

8.6.2 Moduli of compressibility E_s and W_s and unit weight of the soil γ_s

The equations derived in the previous section for calculation of flexibility coefficients require either the moduli of compressibility for loading E_s and reloading W_s or moduli of elasticity for loading E and reloading W for the soil. The yielding of the soil is described by these elastic moduli. The moduli of compressibility E_s and W_s can be determined from the stress-strain curve through a confined compression test (for example Odometer test) as shown in Figure 8.12. In this case, the deformation will occur in the vertical direction only. Therefore, if the moduli of compressibility E_s and W_s are determined from a confined compression test, *Poisson*'s ratio will be taken $\nu_s = 0.0$. If the other moduli of elasticity E and W are used in the equations derived in the previous section, *Poisson*'s ratio will be taken to be $\nu_s \neq 0$. In general, *Poisson*'s ratio ranges in the limits $0 < \nu_s < 0.5$.

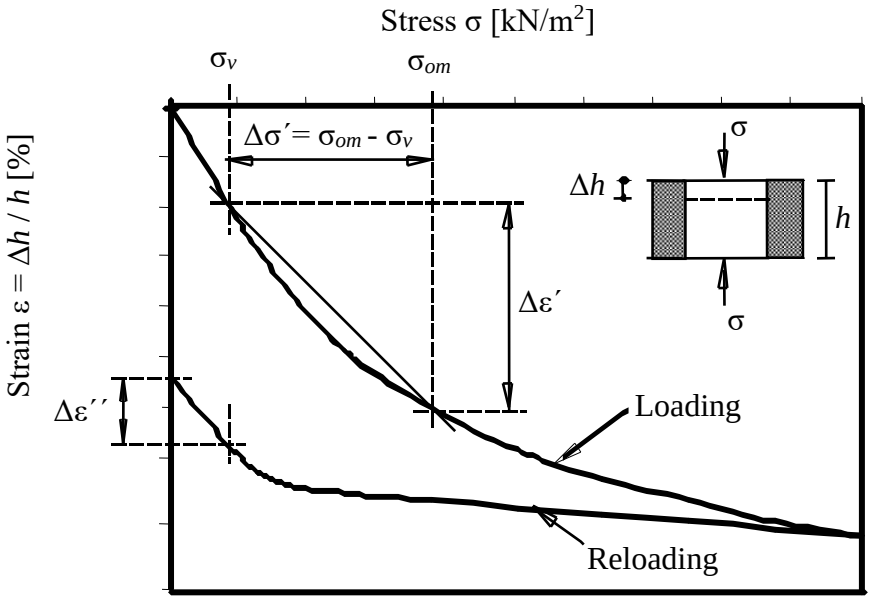

Figure 8.12 Stress-strain diagram from confined compression test (Oedometer test)

The modulus of compressibility E_s [kN/m^2] (or W_s [kN/m^2]) is defined as the ratio of the increase in stress $\Delta\sigma$ to decrease in strain $\Delta\varepsilon$ as (Figure 8.12)

$$\left.\begin{aligned} E_s &= \frac{\Delta\sigma'}{\Delta\varepsilon'} = \frac{\sigma_{om}-\sigma_v}{\Delta\varepsilon'} \\ W_s &= \frac{\Delta\sigma''}{\Delta\varepsilon''} = \frac{\sigma_v}{\Delta\varepsilon''} \end{aligned}\right\} \tag{8.77}$$

where:

$\Delta\sigma'$	Increase in stress from σ_v to σ_{om}	[kN/m^2]
σ_v	Stress equal to overburden pressure	[kN/m^2]
σ_{om}	Stress equal to expected average stress on the soil	[kN/m^2]
$\Delta\varepsilon'$	Decrease in strain due to stress from σ_v to σ_{om}	[-]
$\Delta\sigma''$	Increase in stress due to reloading	[kN/m^2]
$\Delta\varepsilon''$	Decrease in strain due to reloading	[-]

The moduli of compressibility may be expressed in terms of either void ratio or specimen thickness. For an increase in effective stress $\Delta\sigma$ to decrease in void ratio Δe, the moduli of compressibility E_s [kN/m^2] and W_s [kN/m^2] are then expressed as

$$\left.\begin{aligned} E_s &= \frac{1}{m_v'} = \frac{\Delta\sigma'(1+e_o')}{\Delta e'} \\ W_s &= \frac{1}{m_v''} = \frac{\Delta\sigma''(1+e_o'')}{\Delta e''} \end{aligned}\right\} \tag{8.78}$$

where:

m'_v	Coefficient of volume change for loading	[m^2/kN]
m''_v	Coefficient of volume change for reloading	[m^2/kN]
e'_o	Initial void ratio for loading	[-]
e''_o	Initial void ratio for reloading	[-]
$\Delta e'$	Decrease in void ratio due to loading	[-]
$\Delta e''$	Decrease in void ratio due to reloading	[-]

The values of E_s and W_s for a particular soil are not constant but depend on the stress range over which they are calculated. Therefore, for linear analysis it is recommended to determine the modulus of compressibility for loading E_s at the stress range from σ_v to σ_{om}, while that for reloading W_s for a stress increment equal to the overburden pressure σ_v. On the other hand, since the modulus of compressibility increases with the depth of the soil, for more accurate analysis the modulus of compressibility may be taken increasing linearly with depth. Also, according to *Kany* (1976) the moduli of compressibility E_s and W_s may be taken depending on the stress on soil. In these two cases, the moduli of compressibility E_s and W_s can be defined in the analysis for several sub-layers instead of one layer of constants E_s and W_s.

As a rule, before the analysis the soil properties are defined through the tests of soil mechanics, particularly the moduli of compressibility E_s and W_s. For precalculations Table 8.2 for specification of the modulus of compressibility E_s can also be used.

According to *Kany* (1974), the values of W_s range between 3 to 10 times of E_s. From experience, the modulus of compressibility W_s for reloading can be taken 1.5 to 5 times as the modulus of compressibility E_s for loading.

For geologically strongly preloaded soil, the calculation is often carried out only with the modulus of compressibility for reloading W_s. In this case, the same values are defined for E_s and W_s.

Matching with the reality, satisfactory calculations of the settlements are to be expected only if the soil properties are determined exactly from the soil mechanical laboratory, field tests or back calculation of settlement measurements.

Table 8.2 shows mean moduli of compressibility E_s and the unit weight of the soil γ_s for various types of soil according to EAU (1990).

Table 8.2 Mean moduli of compressibility E_s and the unit weight of the soil γ_s for various types of soil

Type of soil	Unit weight γ_s [kN/m^3]		Modulus of compressibility E_s [kN/m^2]
	above water	under water	
Non-cohesive soil			
Sand, loose, round	18	10	20000 - 50000
Sand, loose, angular	18	10	40000 - 80000
Sand, medium dense, round	19	11	50000 - 100000
Sand, medium dense, angular	19	11	80000 - 150000
Gravel without sand	16	10	100000 - 200000
Coarse gravel, sharp edge	18	11	150000 - 300000
Cohesive soil			
Clay, semi-firm	19	9	5000 - 10000
Clay, stiff	18	8	2500 - 5000
Clay, soft	17	7	1000 - 2500
Boulder clay, solid	22	12	30000 - 100000
Loam, semi-firm	21	11	5000 - 20000
Loam, soft	19	9	4000 - 8000
Silt	18	8	3000 - 10000

8.6.3 Moduli of elasticity *E* and *W*

The equations derived in the previous section to determine the flexibility coefficients are used with moduli of elasticity E and W for unconfined lateral strain with *Poisson*'s ratio $\nu_s \neq 0$. It must be pointed out that, when defining *Poisson*'s ratio by $\nu_s = 0$ (limit case), the moduli of compressibility E_s and W_s for confined lateral strain (for example from Odometer test) also can be used.

The modulus of elasticity is often determined from an unconfined Triaxial compression test, Figure 8.13. Plate loading tests may also be used to determine the in situ modulus of elasticity of the soil as elastic and isotropic.

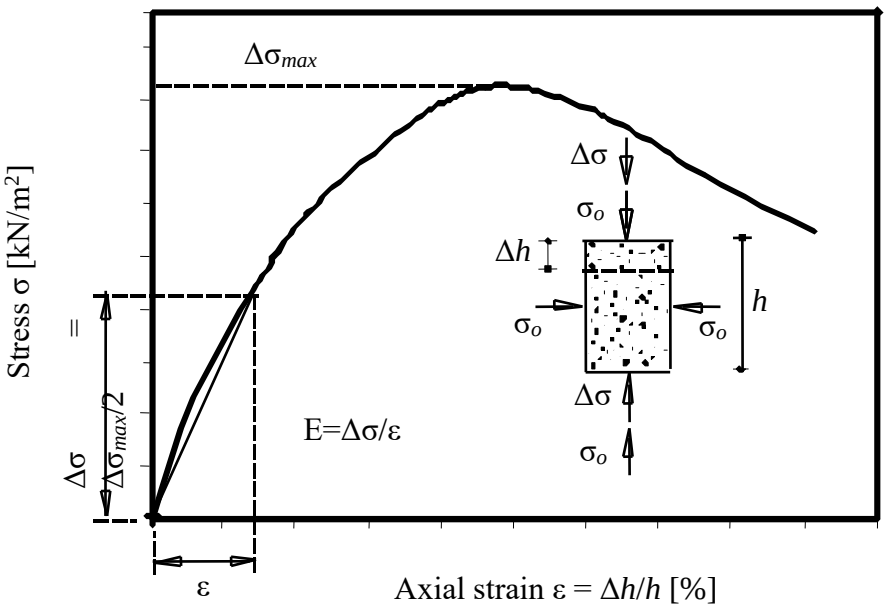

Figure 8.13 Modulus of elasticity *E* from Triaxial test

It is possible to obtain an expression for the moduli of elasticity *E* and *W* in terms of moduli of compressibility E_s, W_s and *Poisson*'s ratio ν_s for the soil as

$$\left.\begin{aligned} E &= E_s \frac{1-\nu_s-2\nu_s^2}{1-\nu_s} \\ W &= W_s \frac{1-\nu_s-2\nu_s^2}{1-\nu_s} \end{aligned}\right\} \tag{8.79}$$

The above equation shows that:

- In the limit case $\nu_s = 0$ (deformation without lateral strain), the values of *E* and E_s (also *W* and W_s) are equal

- In the other limit case $\nu_s = 0.5$ (deformation with constant volume), the moduli of elasticity will be $E = 0 \times E_s$ and $W = 0 \times W_s$. In this case, only the immediate settlement (lateral deformation with constant volume) can be determined.

Table 8.3 shows some typical values of modulus of elasticity according to *Bowles* (1977).

Table 8.3 Typical range of moduli of elasticity *E* for selected soils

Type of soil	Modulus of elasticity E [kN/m^2]
Very soft clay	3000 - 3000
Soft clay	2000 - 4000
Medium clay	4500 - 9000
Hard clay	7000 - 20000
Sandy clay	30000 - 42500
Silt	2000 - 20000
Silty sand	5000 - 20000
Loose sand	10000 - 25000
Dense sand	50000 - 100000
Dense sand and gravel	80000 - 200000
Loose sand and gravel	50000 - 140000
Shale	140000 - 1400000

8.6.4 Compression index C_r und initial void ratio e_o

In case of clayey soil it is recommended to use the settlement parameters C_c, C_r and C_s to represent the elastic properties of the soil in the computation of consolidation settlements. These parameters or indices can be obtained directly from the consolidation test or indirect using some empirical equations such as Equations 8.82 and 8.83.

8.6.5 Compression index C_c from consolidation test

The typical relationship between the void ratio *e* and effective stress σ obtained from the consolidation test is shown in Figure 8.14. The slope of the end part of the *e* versus log σ curve is denoted as the Compression index *Cc* and computed as

$$C_c = \frac{\Delta e}{\log \frac{\sigma_2}{\sigma_1}} \tag{8.80}$$

By analogy, the other indices C_r and C_s can be obtained as shown in Figure 8.14 and Equation 8.81

$$C_r \text{ or } C_c = \frac{\Delta e}{\log \frac{\sigma_2}{\sigma_i}} \tag{8.81}$$

where:

C_r	Recompression index	[-]
C_s	Swell index	[-]
Δe	Change in void ratio between σ_i and σ_2	[-]
σ_i	Any pressure along the appropriate curve	[kN/m^2]

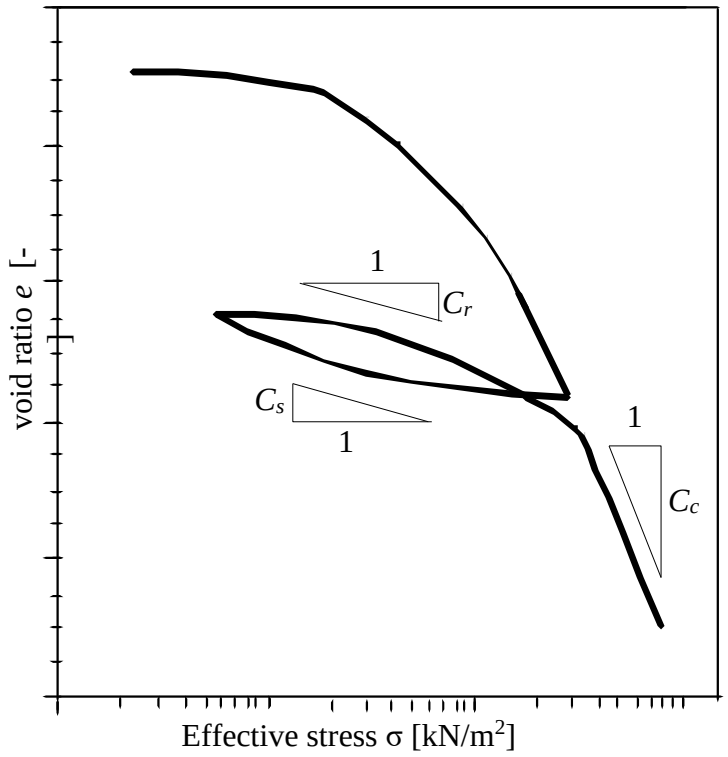

Figure 8.14 Relationship between void ratio and effective stress obtained from consolidation test

8.6.6 Compression index C_c from empirical equations

Because of the number of consolidation tests to obtain the compression indices for a given project is limited, it is often desirable to obtain approximate values by using other soil parameters which are more easily determined. Approximate values may be used for preliminary calculations or to check the laboratory data.

For normally consolidated clays *Terzaghi*/ *Peck* (1967), on the basis of research on undisturbed clays, proposed the following equation to obtain the Compression index C_c [-] from the liquid limit of the soil *LL* [%]

$$C_c = 0.009\,(LL - 10) \tag{8.82}$$

Azzouz (1976) lists several equations to obtain the compression index, one of them is given below to obtain the Compression index C_c [-] from the initial void ratio e_o [-] of the soil

$$C_c = 1.15\,(e_o - 0.35) \tag{8.83}$$

Typical values of compression and swell indices as well as the corresponding void ratio at stress σ_o = 10 [kN/m²] are presented in the following table according to *Gudehus* (1981). The compression index C_c is valid for loading while C_s is valid for both heaving and reloading.

Recompression index is calculated from the plasticity index using the following correlations (*Kullhawy* and *Mayne* (1990):

$$C_r = \frac{PI}{370} \tag{8.84}$$

where *PI* is the plasticity index in percent.

Table 8.4 Compression and swell indices depending on the initial void ratio

Soil type	Compression index C_c [-]	Swell index C_s [-]	Initial void ratio e_o [-]
Gravely sand	0.001	0.0001	0.3
Fine sand, dense	0.005	0.0005	0.5
Fine sand, loose	0.01	0.001	0.7
Coarse silt	0.02	0.002	0.8
Clayey silt	0.03 - 0.6	0.01 - 0.02	0.9 - 1.2
Kaolin-Silt	0.1	0.03	1.5
Silt	0.1 - 0.3	0.03 - 0.1	1.2 - 2.5
Clay	0.5	0.4	5
Peat	1	0.3	10

8.7 Defining the project data

8.7.1 Firm Header

When printing the results, the main data (firm name) are displayed on each page at the top in two lines. Firm name can be defined, modified and saved using the "Firm Header" option from the setting tab (see Figure 8.15).

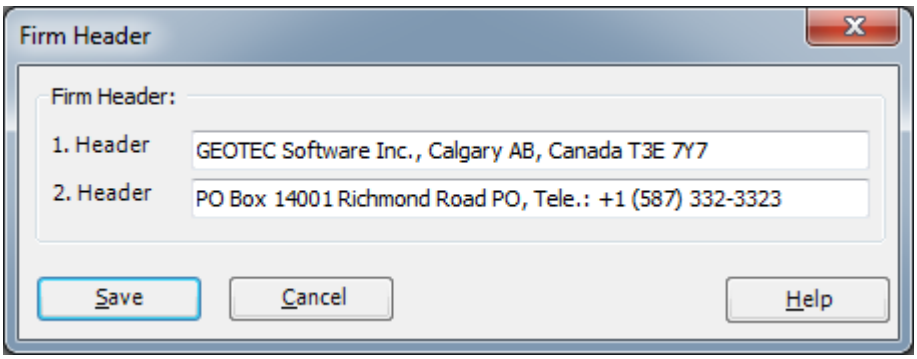

Figure 8.15 Firm Header

8.7.2 Task of the program *GEO Tools* (Analysis Type)

The program *GEO Tools* can be used to analyze various problems in Geotechnical Engineering for shallow foundations and deep foundations, Figure 8.16.

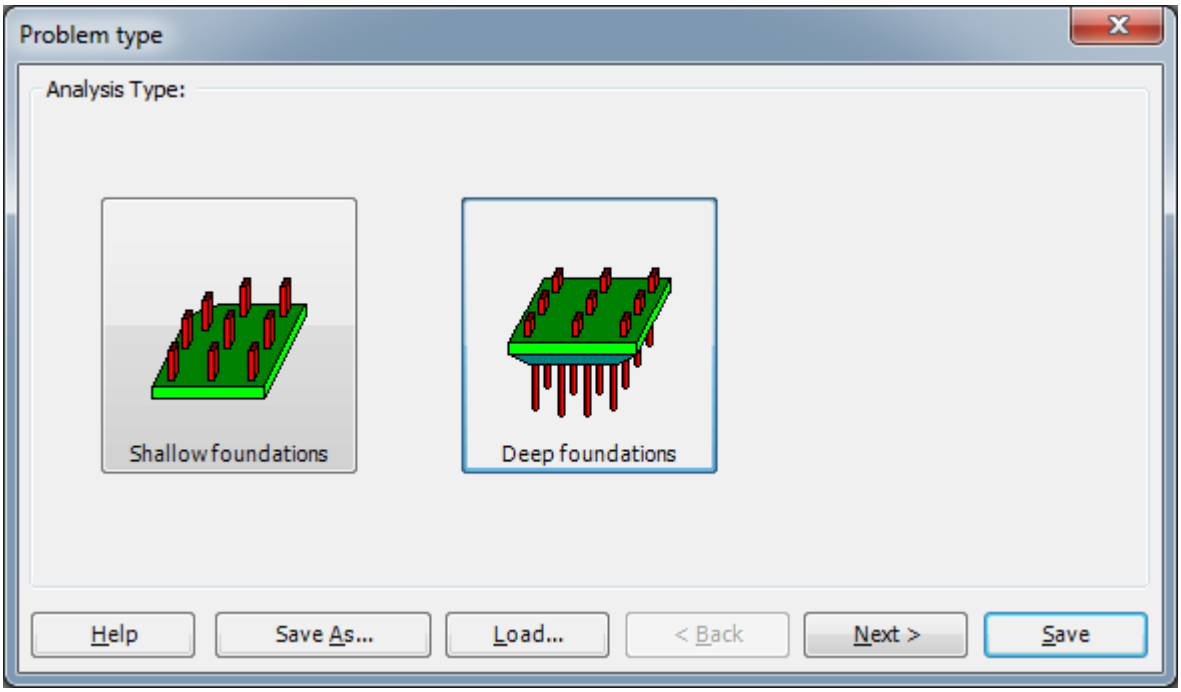

Figure 8.16 Problem type

According to the main menu (Figure 8.17) the following geotechnical problems can be analyzed for shallow foundations:

01-Stresses in soil
02-Strains in soil
03-Displacements in soil
04-Consolidation settlement
05-Degree of consolidation
06-Time-settlement curve
07-Displacements of rigid raft
08-Consolidation of rigid raft
09-Settlements of footing groups

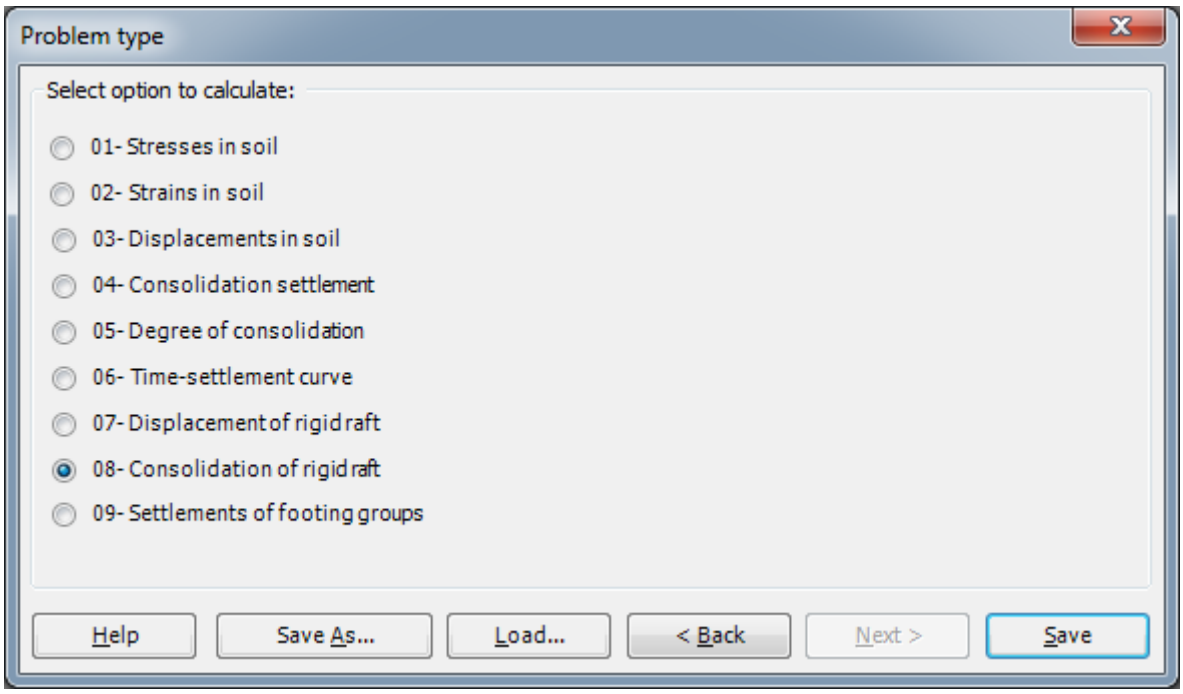

Figure 8.17 Problem type for shallow foundation

In menu of Figure 8.17 select the option:

08-Consolidation of rigid raft

The following paragraph describes how to determine the contact pressure and consolidation settlement for a rigid raft by using the program *GEO Tools*. The input data are the geometry of the rigid raft, load intensity and the properties of the soil.

8.7.3 Project Identification

In the program, it must be distinguished between the following two data groups:

1 System data (For identification of the project that is created and information to the output for the printer).

2 Soil data (Soil properties and so on).

The defining input data for these data groups is carried out as follows:

After clicking on the "Project Identification" option, the following general project data are defined (Figure 8.18):

Title: Title label
Date: Date
Project: Project label

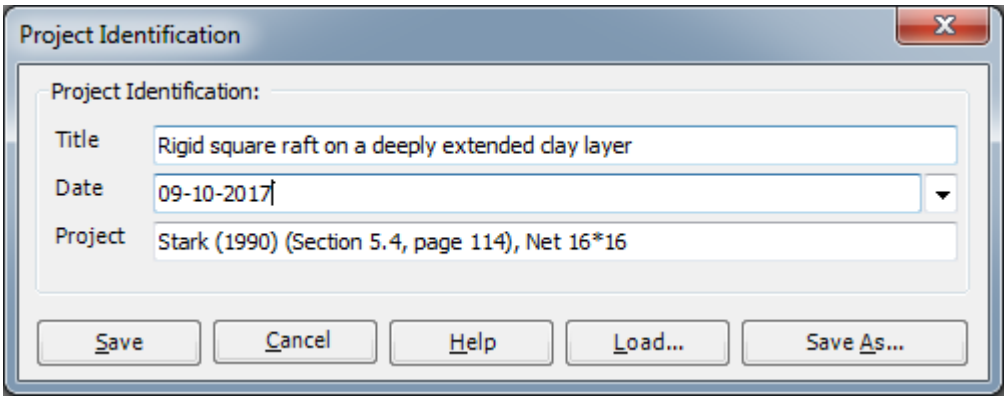

Figure 8.18 Project Identification

8.7.4 Consolidation of rigid raft

After clicking on the "Consolidation of rigid raft" option, the following data of the consolidation of rigid raft are defined (Figure 8.19):

Calculation task:

- Rectangular raft
- Circular raft

und type of the solution:

- Analytical solution
- Numerical solution

Load intensity and geometry:

Q	Point load [kN]
ex	Eccentricity [m]
ey	Eccentricity [m]
a	Length [m]
b	Width [m]

Soil data:

Soil properties are defined by Modulus of Compressibility *Es*

Es	Modulus of Compressibility [kN/m^2]

Layer:

z	Z-Coordinate [m]
h	Layer thickness [m]

Dimensions of the element mesh:

Dx	Element length in x-direction [m]
Dy	Element length in y-direction [m]

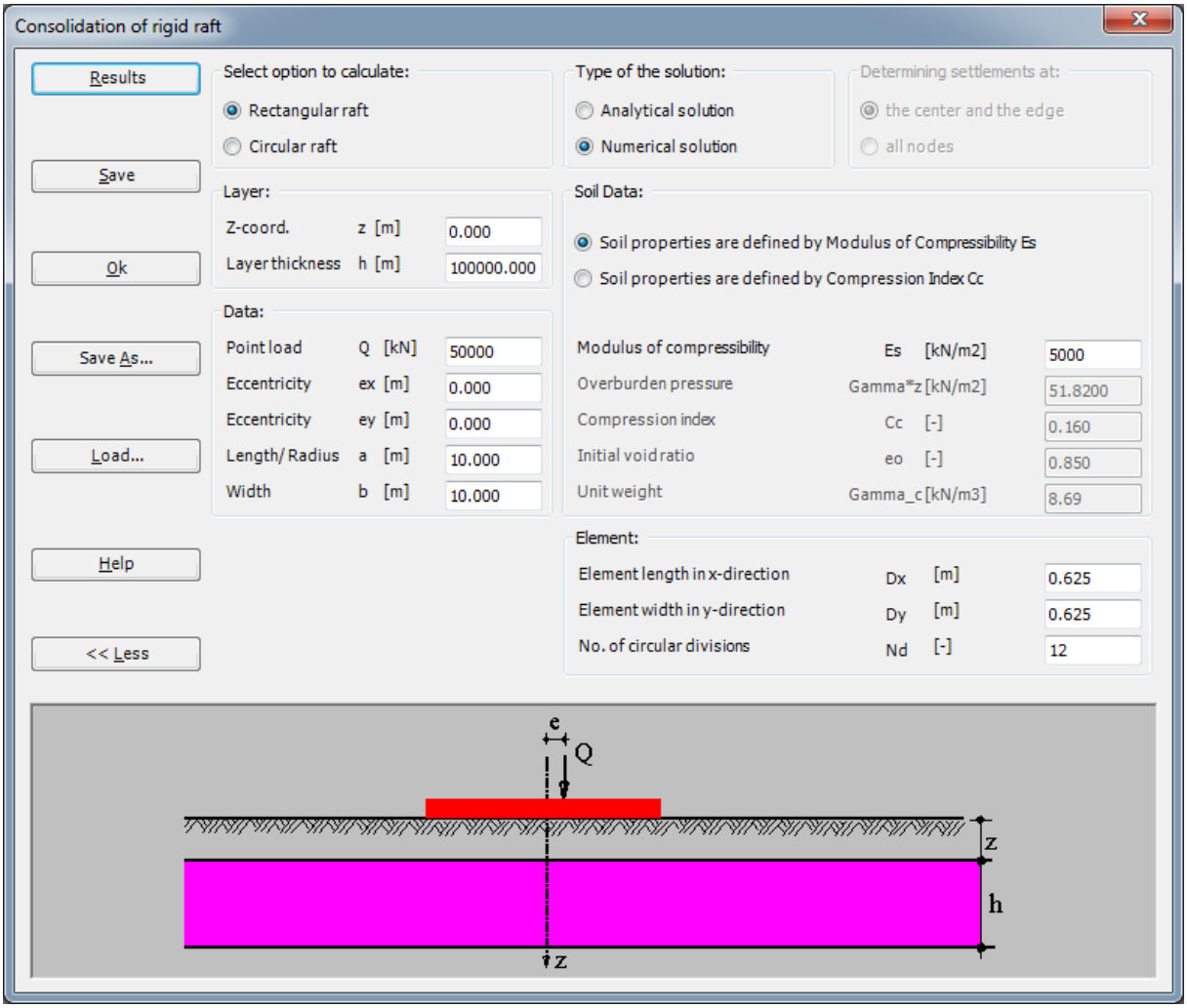

Figure 8.19 Consolidation of rigid raft

8.8 Examples to verify consolidation of rigid raft

8.8.1 Introduction

The application possibilities of the program *GEO Tools* to evaluate the consolidation settlement of rigid rafts on cohesive soil are presented below in some numerical examples. The examples were carried out to verify and test the application of the proposed analytical and numerical procedures outlined in this book.

Although the numerical procedure outlined in this book is valid for rigid rafts of any arbitrary shape, but only the two special cases of rafts, rectangular and circular rafts, are taken into account. This analysis limitation is considered to make a compatibility between both numerical and semi-analytical procedures for the purpose of comparison.

The examples outlined in this section can be also analyzed by the program *ELPLA* and the same results can be obtained. *GEO Tools* is a simple user interface program and needs little information to define a problem. It is prefer to use it for a simple foundation geometry. Furthermore, *ELPLA* can also read data files of a problem of a rigid raft defined by *GEO Tools*. User can analyze the problem again by *ELPLA*.

8.8.2 Example 1: Rigid square raft on a deeply extended clay layer

8.8.2.1 Description of the problem

To verify the mathematical model of *GEO Tools* for rigid square raft, the results of a rigid square raft obtained by other analytical solutions from *Kany* (1974), *Fraser*/ *Wardle* (1976), *Chow* (1987), *Li*/ *Dempsey* (1988) and *Stark* (1990), Section 5.4, page 114, are compared with those obtained by *GEO Tools*.

The vertical displacement *w* [m] of a rigid square raft on Isotropic elastic half-space medium may be evaluated by:

$$w = \frac{P\,B\,(1-\nu_s{}^2)}{E}\,I \tag{8.85}$$

where:
ν_s *Poisson's* ratio of the soil [-]
E *Young's* modulus of the soil [kN/m^2]
B Raft side [m]
I Displacement influence factor [-]
p Load intensity on the raft [kN/m^2]

Eq. (8.85) can be used to verify the rigid rectangular raft by replacing the term $\frac{P\,B\,(1-\nu_s{}^2)}{E}$ by the unit. Equation (8.85) becomes:

$$w = I \tag{8.86}$$

8.8.2.2 Analysis of the raft

A square raft on a deeply extended clay layer defined by coefficient of volume change of the soil m_v, [m^2/kN] is chosen and subdivided to different nets. The nets range from 2 × 2 to 48 × 48 elements. Load on the raft, raft side and the elastic properties of the soil are chosen to make the first term from Eq. (8.77) equal to unit, hence:

Raft side	B	= 10	[m]
Uniform load on the raft	p	= 500	[kN/m^2]
Modulus of compressibility of the soil	E_s (1/ m_v)	= 5000	[kN/m^2]
Poisson's ratio of the soil	ν_s	= 0	[-]

Figure 8.20 shows a quarter of the raft with a net of total 16 × 16 elements. To simulate a deeply extended clay layer, the layer is assumed to have a great depth z=100000 [m].

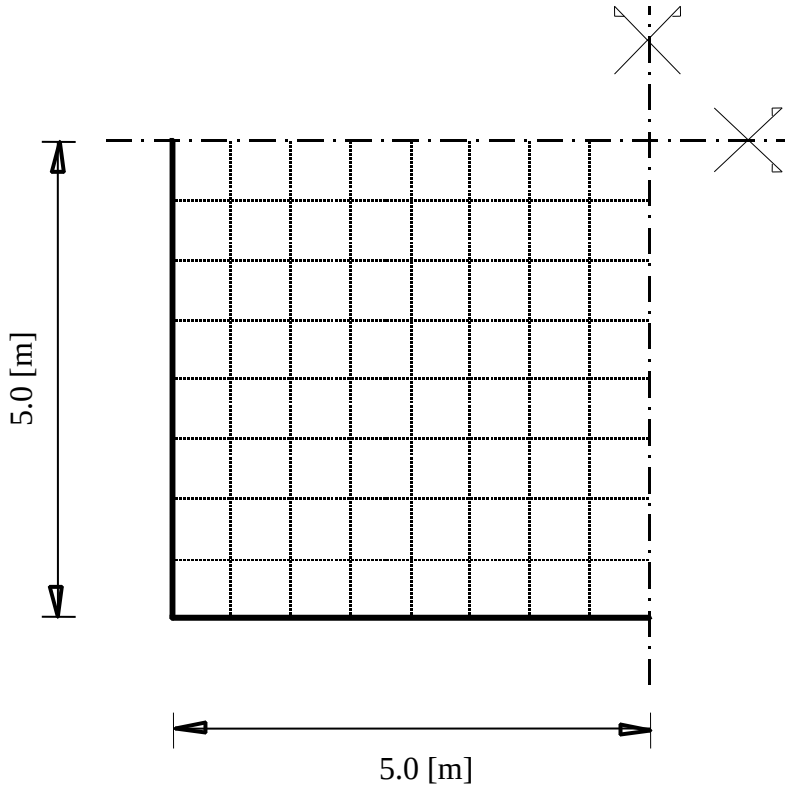

Figure 8.20 Quarter of rigid square raft with dimensions and mesh

8.8.2.3 Results and discussions

Table 8.5 shows the comparison of the displacement influence factor *I* obtained by *GEO Tools* with those obtained by other published solutions from *Fraser*/ *Wardle* (1976), *Chow* (1987), *Li*/ *Dempsey* (1988) and *Stark* (1990) for a net of 16 × 16 elements. In addition, the displacement influence factor *I* is obtained by using *Kany's* charts (1974) through the conventional solution of a rigid raft and also by *ELPLA*. The slight difference between *I* obtained by *GEO Tools* and that by *ELPLA* is related to *ELPLA* calculates the contact pressure and settlements at nodes, while *GEO Tools* calculates them at element centers.

Table 8.5 Comparison of displacement influence factor *I* obtained by *GEO Tools* with those obtained by other authors for a net of 16 × 16 elements

	Displacement influence factor *I* [-]					
Kany (1974)	*Fraser*/ *Wardle* (1976)	*Chow* (1987)	*Li*/ *Dempsey* (1988)	*Stark* (1990)	*ELPLA*	*GEO Tools*
0.85	0.835	0.8675	0.8678	0.8581	0.8497	0.8278

Table 8.6 shows the convergence of solution for the displacement influence factor *I* obtained by *GEO Tools* and *ELPLA* with those obtained by *Stark* (1990) for different nets. Under the assumption of *Li*/ *Dempsey* (1988), the convergence of the solution occurs when the displacement influence factor $I = 0.867783$ while using *Kany's* charts (1974) gives $I = 0.85$ for the ratio $z/B = 100$. *Fraser*/ *Wardle* (1976) give $I = 0.87$ based on an extrapolation technique, *Gorbunov-Possadov*/ *Serebrjanyi* (1961) give $I = 0.88$ and *Absi* (1970) gives $I = 0.87$. In general, the displacement influence factor *I* in this example ranges between $I = 0.85$ and $I = 0.88$. Table 8.6 shows that a net of 16 × 16 elements gives a reasonable result for a rigid square raft in this example by *GEO Tools*.

Table 8.6 Convergence of solution for displacement influence factor *I* obtained by *GEO Tools* with those obtained by *Stark* (1990) for different nets

Net		Displacement influence factor *I* [-]	
	Stark (1990)	*ELPLA*	*GEO Tools*
2 × 2	0.8501	0.7851	0.6317
4 × 4	0.8477	0.8143	0.7308
6 × 6	0.8498	0.8281	0.7708
8 × 8	0.8525	0.8360	0.7926
12 × 12	0.8559	0.8449	0.8157
16 × 16	0.8581	0.8497	0.8278
20 × 20	0.8597	0.8528	0.8353
24 × 24	0.8601	0.8550	0.8404
32 × 32	0.8626	0.8578	0.8470
48 × 48	0.8647	0.8609	0.8539

8.8.2.4 Semi-analytical analysis of rigid raft

In *GEO Tools*, it can be determined the rigid consolidation using semi-analytical solution, where the settlements are determined only at the center and the edge of the raft due to known contact pressure.

Table 8.7 shows the comparison of the displacement influence factor *I* obtained by semi-analytical solution with those obtained by numerical solution for different nets. From the table, it can be concluded that, the size of net elements has a little influence on the results by semi-analytical analysis of rigid raft.

Table 8.7 Influence factor *I* obtained by *GEO Tools* using analytical solution, where the settlements are determined at the center and the edge

Net	Displacement influence factor *I* [-]	
	Analytical solution	Numerical solution
2 × 2	0.7324	0.6317
4 × 4	0.7889	0.7308
6 × 6	0.8015	0.7708
8 × 8	0.8069	0.7926
12 × 12	0.8116	0.8157
16 × 16	0.8136	0.8278
20 × 20	0.8148	0.8353
24 × 24	0.8154	0.8404
32 × 32	0.8164	0.8470
48 × 48	0.8173	0.8539

8.8.2.5 Rigid consolidation by GEO Tools

The input data and results of *GEO Tools* for a net of 16 × 16 elements are presented on the next pages. By comparison, one can see a good agreement with those obtained by other published solutions.

```
************************************************************
                        GEO Tools
                         Version 10
     Program authors Prof. M. El Gendy/ Dr. A. El Gendy
************************************************************
Title: Rigid square raft on a deeply extended clay layer
Date: 09-10-2017
Project: Stark (1990) (Section 5.4, page 114), Net 16*16
File: Ex1-Raft16
------------------------------------------------------------
Consolidation of rigid raft
Type of the solution Numerical solution
------------------------------------------------------------
Data:
Point load                              Q  [kN]    = 50000
Eccentricity                            ex [m]     = 0.000
Eccentricity                            ey [m]     = 0.000
Length                                  a  [m]     = 10.000
Width                                   b  [m]     = 10.000
Z-coord.                                z  [m]     = 0.000
Layer thickness                         h  [m]     = 100000.000
Element length in x-direction           Dx [m]     = 0.625
Element width in y-direction            Dy [m]     = 0.625

Soil Data:
Modulus of compressibility              Es [kN/m2] = 5000

Result:
Table T1
----------
Contact pressure/ Contact force/ Consolidation settlement:
------------------------------------------------------------
No.     Coord.      Contact     Contact force     Settlement
                    pressure
  I          x             q                 f              s
[-]        [m]      [kN/m2]              [kN]            [m]
------------------------------------------------------------
  1      0.000    1604.0260          313.2863         0.8278
  2      0.625     369.6449          144.3925         0.8278
  3      1.250     302.7613          118.2661         0.8278
  4      1.875     266.9413          104.2739         0.8278
  5      2.500     246.6993           96.3669         0.8278
  6      3.125     234.3688           91.5503         0.8278
  7      3.750     226.8967           88.6315         0.8278
  8      4.375     222.8492           87.0505         0.8278
  9      5.000     221.5694           86.5506         0.8278
 10      5.625     222.8540           87.0523         0.8278
 11      6.250     226.8960           88.6312         0.8278
 12      6.875     234.3686           91.5502         0.8278
 13      7.500     246.6987           96.3667         0.8278
 14      8.125     266.9430          104.2746         0.8278
 15      8.750     302.7573          118.2646         0.8278
 16      9.375     369.6457          144.3929         0.8278
 17     10.000    1604.0360          313.2882         0.8278
------------------------------------------------------------
```

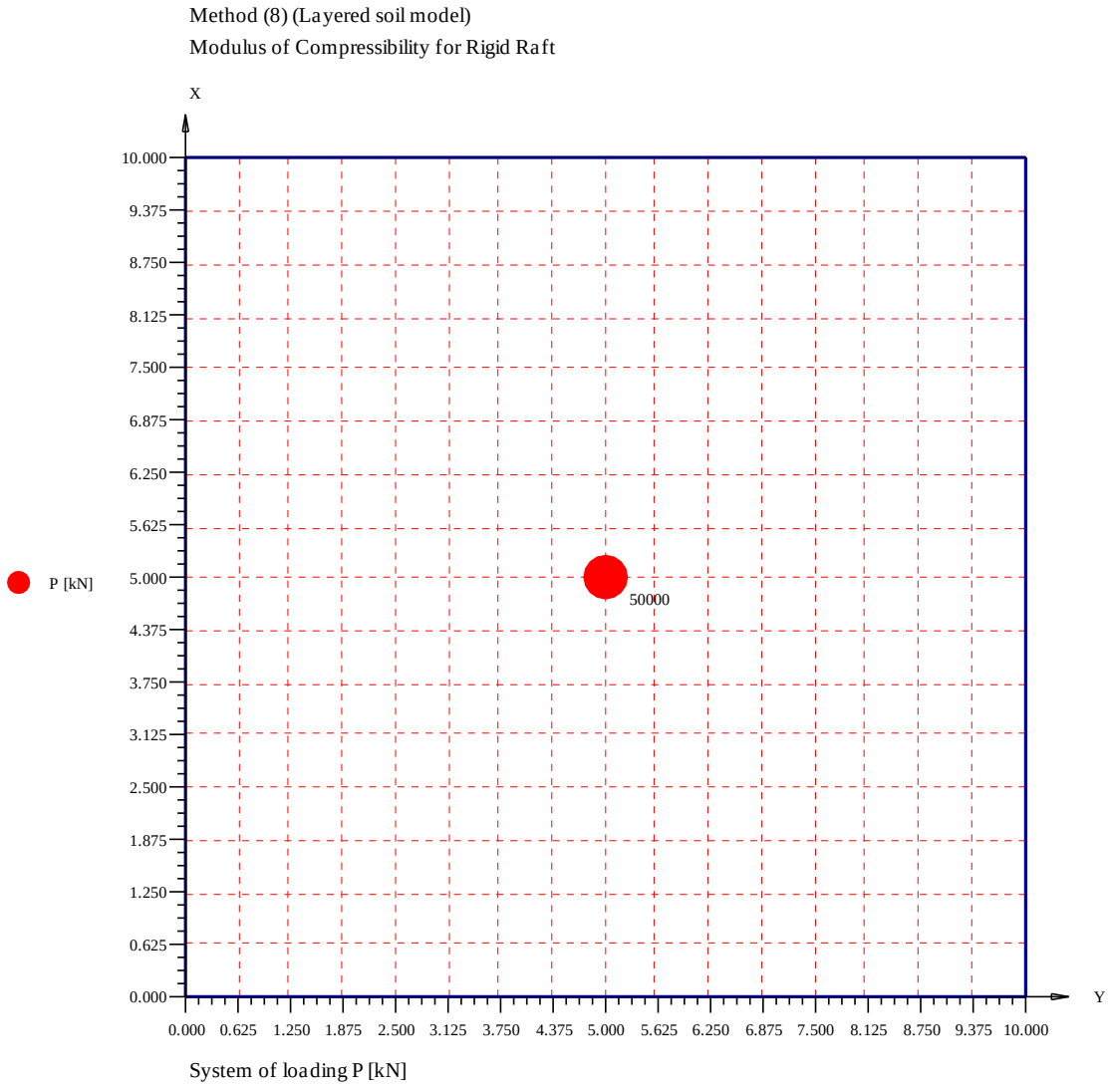

GEOTEC Software Inc., Calgary AB, Canada T3E 7Y7	
PO Box 14001 Richmond Road PO, Tele.: +1 (587) 332-3323	
Scale: 64	**Project: Stark (1990) (Section 5.4, page 114), Net 16*16**
File: Ex1-Raft16	**Date: 09-10-2017**
Page No.:	**Title: Rigid square raft on a deeply extended clay layer**

Method (8) (Layered soil model)
Modulus of Compressibility for Rigid Raft

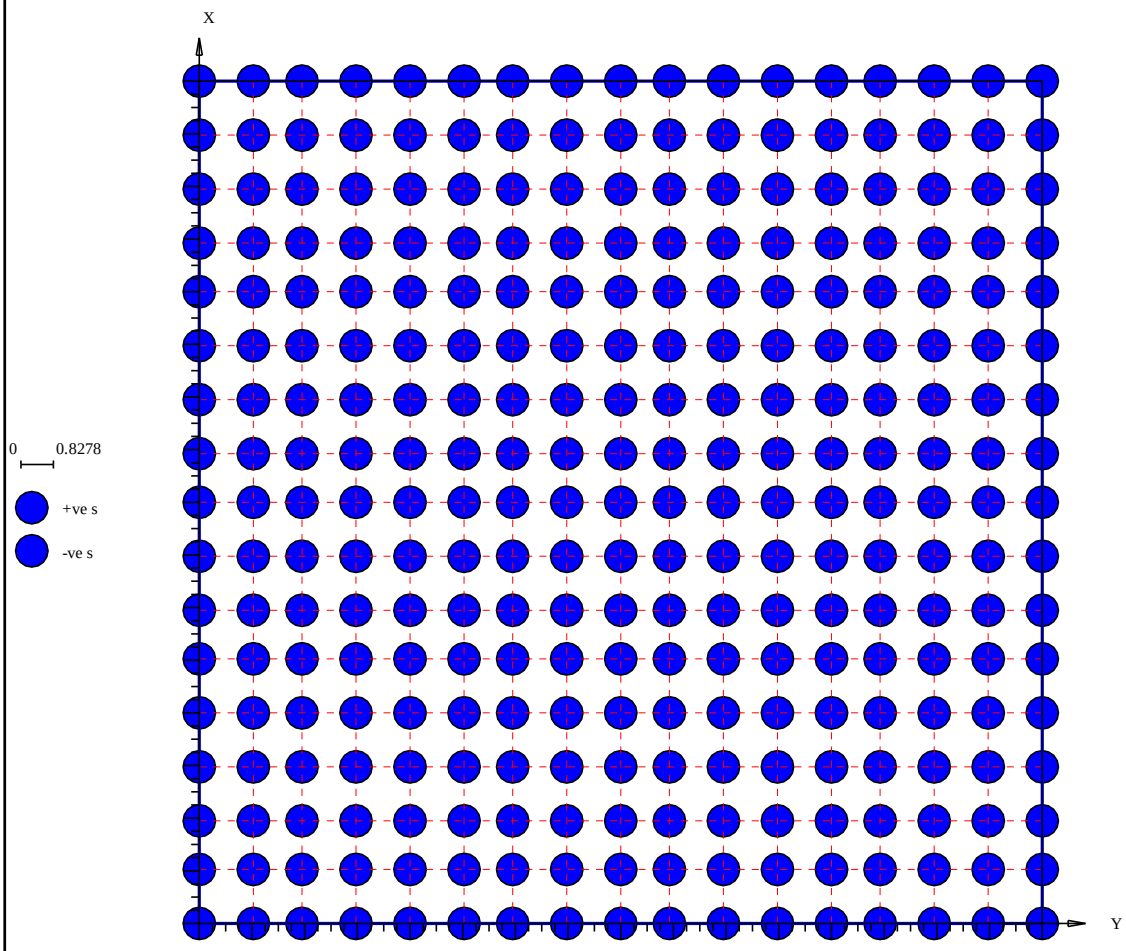

Settlements s [m]
Max. s = 0.8278 at node 1, Min. s = 0.8278 at node 289

GEOTEC Software Inc., Calgary AB, Canada T3E 7Y7
PO Box 14001 Richmond Road PO, Tele.: +1 (587) 332-3323

Scale: 64	**Project: Stark (1990) (Section 5.4, page 114), Net 16*16**
File: Ex1-Raft16	**Date: 09-10-2017**
Page No.:	**Title: Rigid square raft on a deeply extended clay layer**

Method (8) (Layered soil model)

Modulus of Compressibility for Rigid Raft

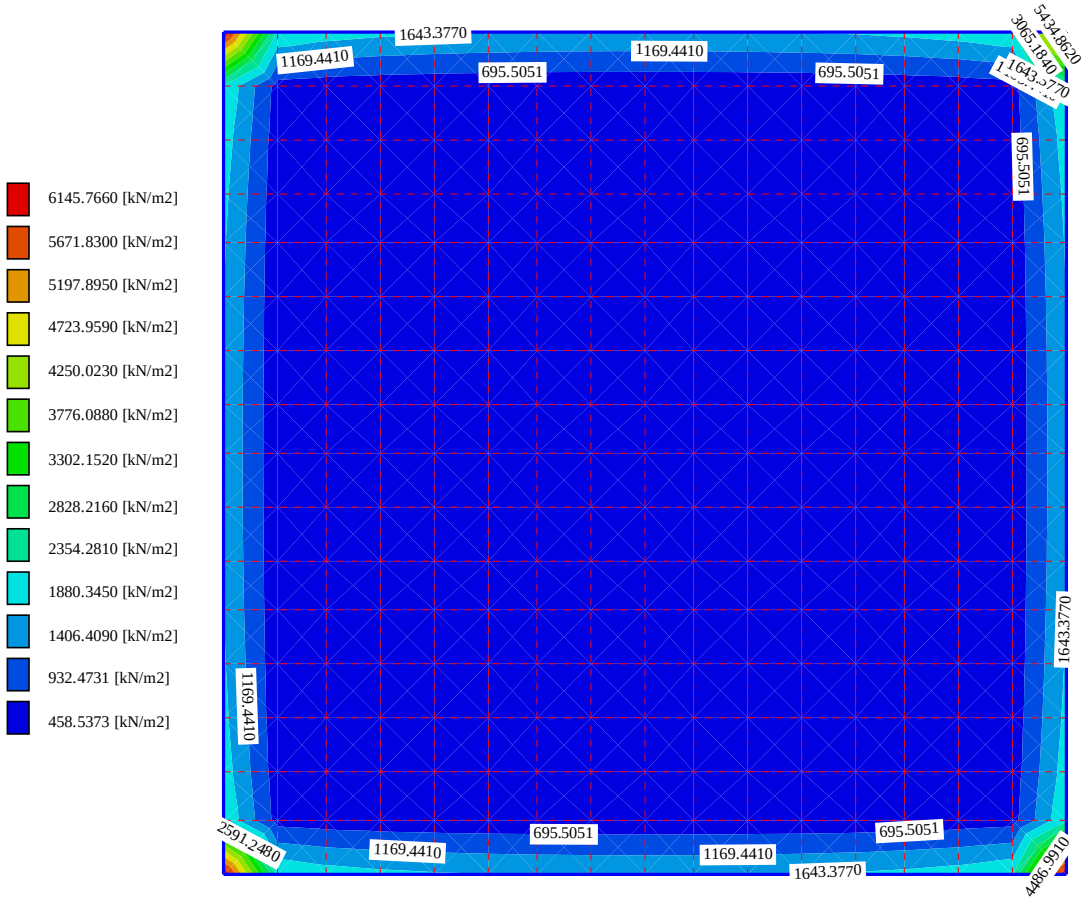

Contact pressure q [kN/m2]

Max. q = 6382.7340 at node 289, Min. q = 221.5694 at node 145

GEOTEC Software Inc., Calgary AB, Canada T3E 7Y7	
PO Box 14001 Richmond Road PO, Tele.: +1 (587) 332-3323	
Scale: 64	**Project: Stark (1990) (Section 5.4, page 114), Net 16*16**
File: Ex1-Raft16	**Date: 09-10-2017**
Page No.:	**Title: Rigid square raft on a deeply extended clay layer**

Method (8) (Layered soil model)
Modulus of Compressibility for Rigid Raft

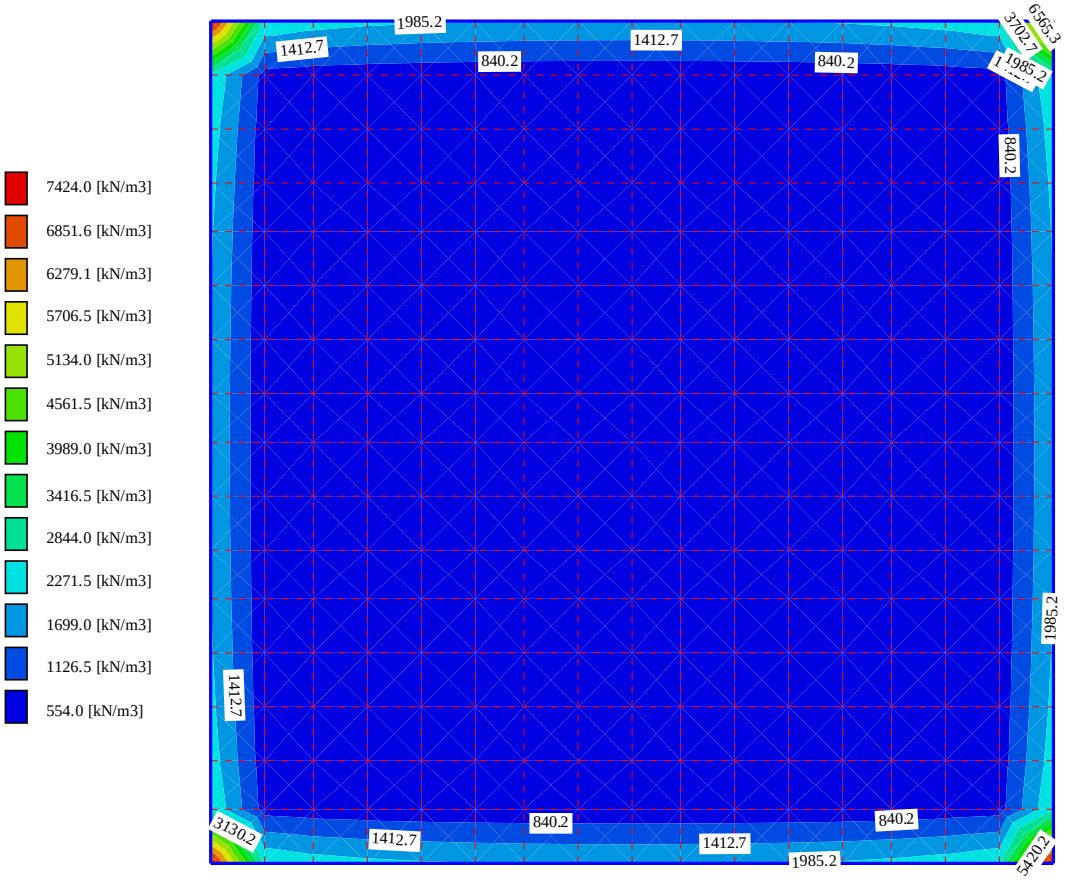

Moduli of subgrade reactions ks [kN/m3]
Max. ks = 7710.3 at node 289, Min. ks = 267.7 at node 145

GEOTEC Software Inc., Calgary AB, Canada T3E 7Y7	
PO Box 14001 Richmond Road PO, Tele.: +1 (587) 332-3323	
Scale: 64	**Project: Stark (1990) (Section 5.4, page 114), Net 16*16**
File: Ex1-Raft16	**Date: 09-10-2017**
Page No.:	**Title: Rigid square raft on a deeply extended clay layer**

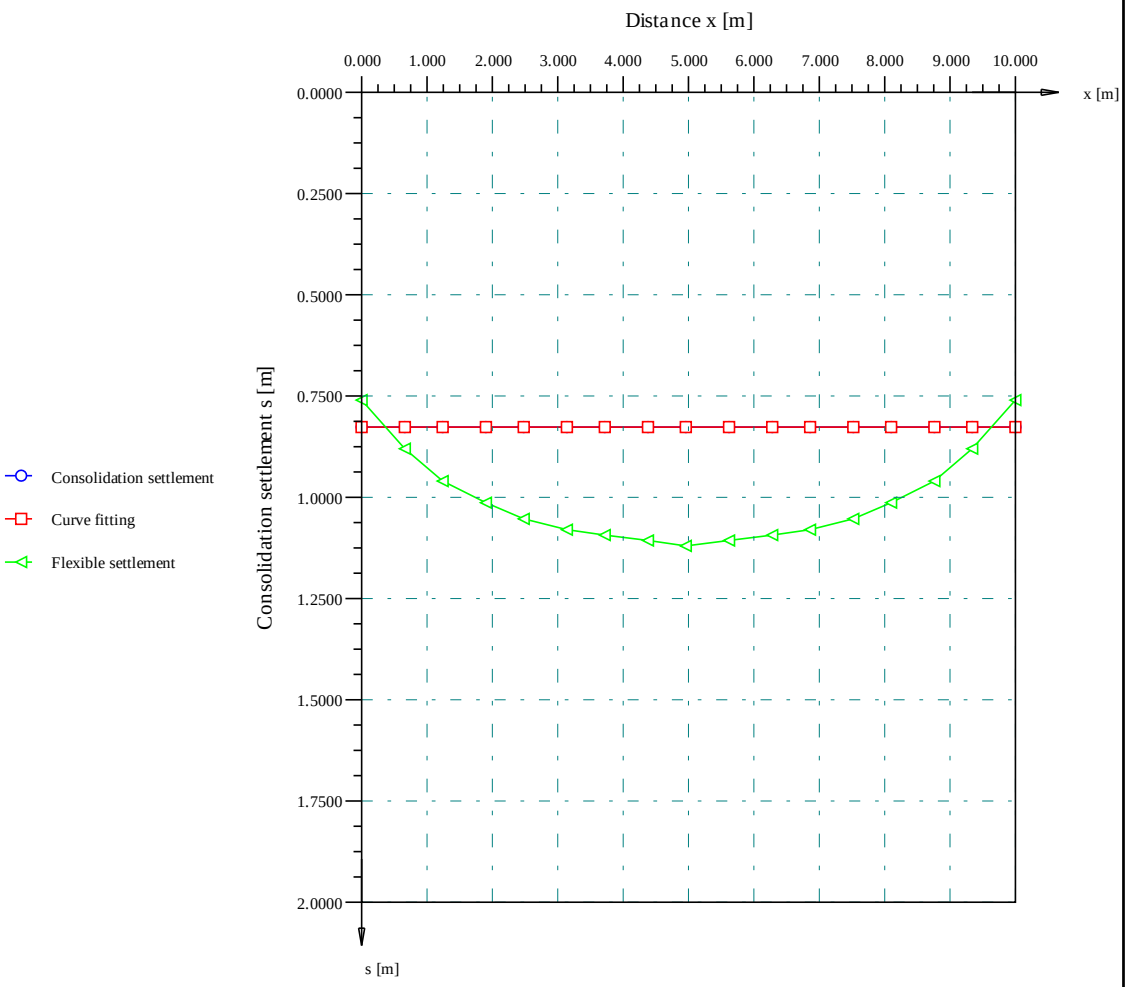

Consolidation settlement

GEOTEC Software Inc., Calgary AB, Canada T3E 7Y7	
PO Box 14001 Richmond Road PO, Tele.: +1 (587) 332-3323	
Scale: 83	**Project: Stark (1990) (Section 5.4, page 114), Net 16*16**
File: Ex1-Raft16	**Date: 09-10-2017**
Page No.:	**Title: Rigid square raft on a deeply extended clay layer**

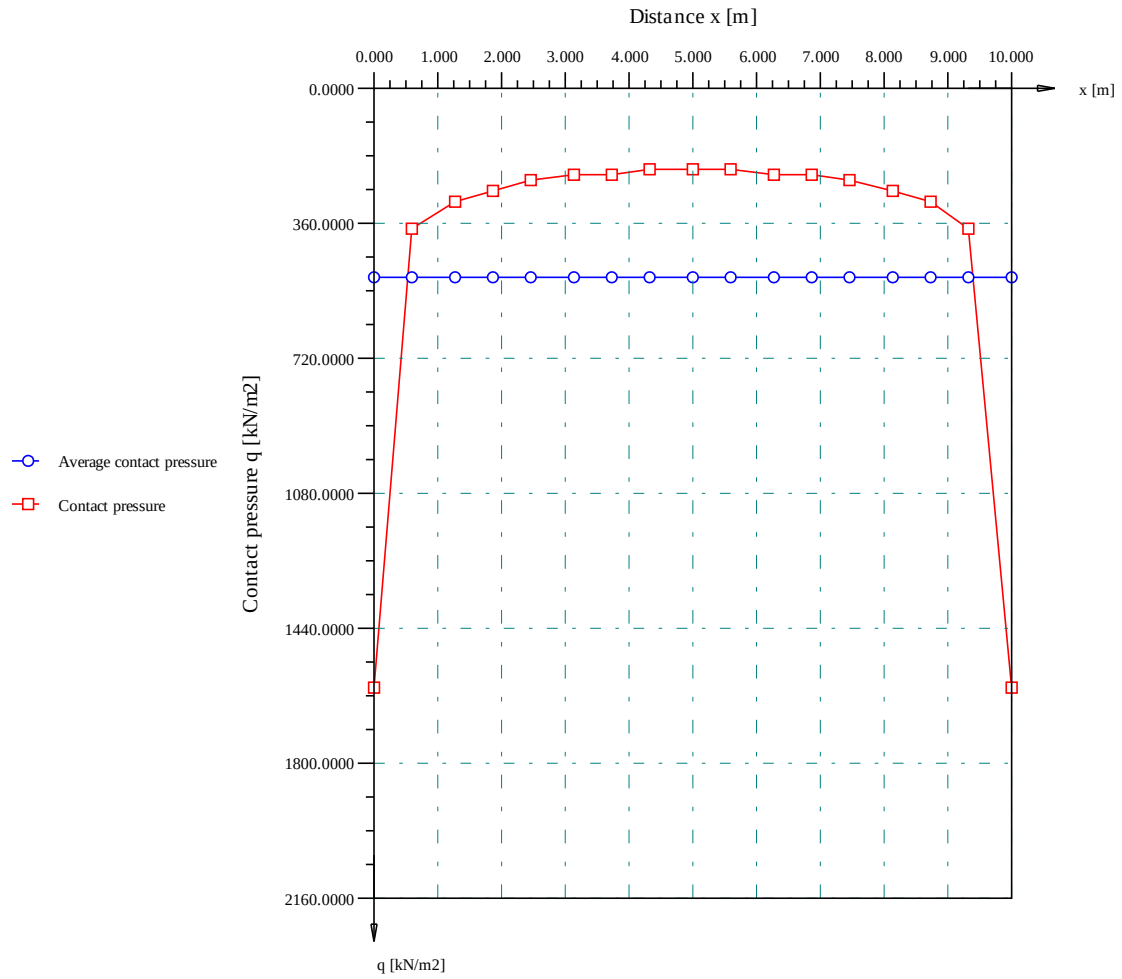

Contact pressure of a rigid raft

GEOTEC Software Inc., Calgary AB, Canada T3E 7Y7	
PO Box 14001 Richmond Road PO, Tele.: +1 (587) 332-3323	
Scale: 85	**Project: Stark (1990) (Section 5.4, page 114), Net 16*16**
File: Ex1-Raft16	**Date: 09-10-2017**
Page No.:	**Title: Rigid square raft on a deeply extended clay layer**

8.8.3 Example 2: Rigid circular raft on a deeply extended clay layer

8.8.3.1 Description of the problem

To verify the mathematical model of *GEO Tools* for rigid circular raft, results of a rigid circular raft obtained by other analytical solutions from *Borowicka* (1939) and *Stark* (1990), Section 5.2, page 106, are compared with those obtained by *GEO Tools*.

According to *Borowicka* (1939), the vertical displacement *w* [m] of a rigid circular raft on Isotropic elastic half-space medium may be evaluated by:

$$w = \frac{P\, r\, \pi\, (1-\nu_s{}^2)}{2E} \tag{8.87}$$

where:
ν_s *Poisson's* ratio of the soil [-]
E *Young's* modulus of the soil [kN/m^2]
r Raft radius [m]
p Load intensity on the raft [kN/m^2]

While the contact pressure distribution *q* [kN/m^2] under the raft at a distance *e* [m] from the center may be evaluated by:

$$q = \frac{P\, r}{2\sqrt{r^2 - e^2}} \tag{8.88}$$

Eq. (8.76) can be used to verify the rigid rectangular raft on a deeply extended clay layer by replacing the term $\frac{(1-\nu_s{}^2)}{E}$ by the coefficient of volume change of the soil $m_{v,}$ [m^2/kN]. Equation (8.78) becomes:

$$w = \frac{P\, r\, \pi\, m_v}{2} \tag{8.89}$$

8.8.3.2 Analysis of the raft

A circular raft on a deeply extended clay layer defined by coefficient of volume change of the soil $m_{v,}$ [m^2/kN] is chosen. To simulate a deeply extended clay layer, the layer is assumed to have a great depth *z*=100000 [m]. Figure 8.20 shows a quarter of the raft with mesh.

Load on the raft, raft radius and the elastic properties of the soil are chosen as follows:

Raft radius	*r*	= 5	[m]
Uniform load on the raft	*p*	= 100	[kN/m^2]
Modulus of compressibility of the soil	E_s (1/ m_v)	= 6400	[kN/m^2]

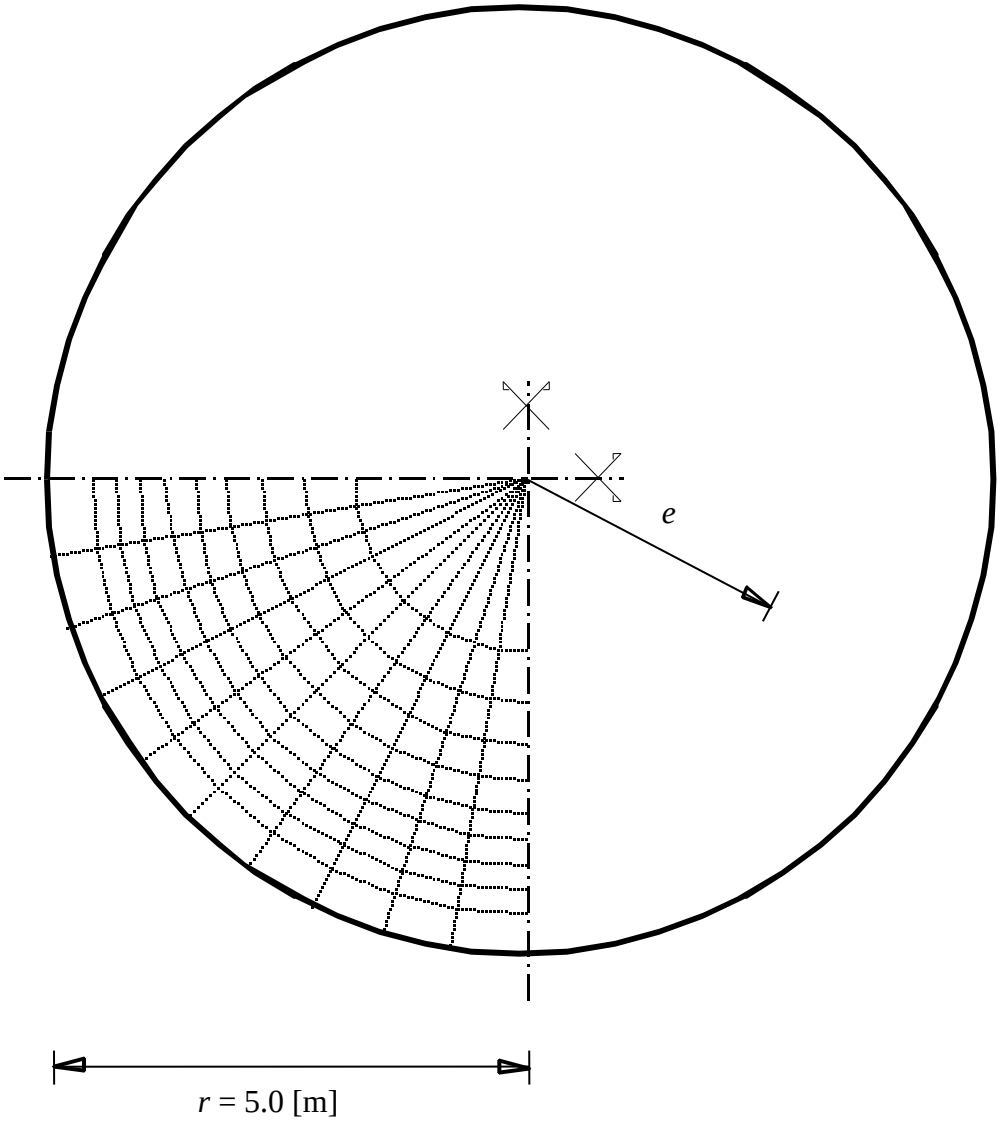

Figure 8.21 Quarter of rigid circular raft with dimensions and mesh

8.8.3.3 Results

Figure 8.22 shows the comparison of the contact pressure ratio *q/p* [-] at the middle section of the raft obtained by *GEO Tools* with those obtained by *Borowicka* (1939) and *Stark* (1990). Besides, Table 8.8 shows the comparison of the central displacement *w* obtained by *GEO Tools* with those obtained by *Borowicka* (1939) and *Stark* (1990) and also by *ELPLA*. The slight difference between *I* obtained by *GEO Tools* and that by *ELPLA* is related to *ELPLA* calculates the contact pressure and settlements at nodes, while *GEO Tools* calculates them at element centers.

Table 8.8 Comparison of the central displacement *w* obtained by *GEO Tools* with those obtained by *Borowicka* (1939) and *Stark* (1990)

	Borowicka (1939)	*Stark* (1990)	*ELPLA*	*GEO Tools*
Central displacement *w* [cm]	12.272	12.195	12.164	12.322

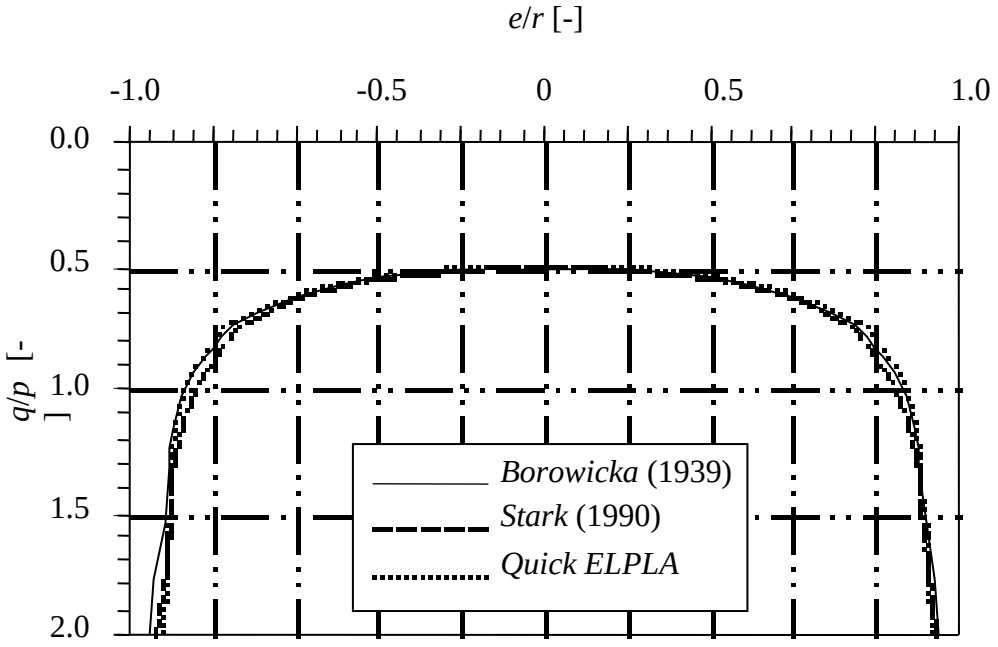

Figure 8.22 Contact pressure ratio *q/p* [-] under the middle of the circular rigid raft

It is obviously from Table 8.8 and Figure 8.22 that results of the circular rigid raft obtained by *GEO Tools* are nearly equal to those obtained by *Borowicka* (1939) and *Stark* (1990).

8.8.3.4 Rigid consolidation by GEO Tools

The input data and results of *GEO Tools* are presented on the next pages. By comparison, one can see a good agreement with those obtained by other published solutions.

```
************************************************************
                        GEO Tools
                         Version 10
     Program authors Prof. M. El Gendy/ Dr. A. El Gendy
************************************************************
Title: Rigid circular raft on a deeply extended clay layer
Date: 09-10-2017
Project: Borowicka (1939) and Stark (1990) (Section 5.2, page 106)
File: Ex2-Rig

------------------------------------------------------------
Consolidation of rigid raft
Type of the solution Numerical solution
------------------------------------------------------------

Data:
Point load                        Q  [kN]     = 7854
Eccentricity                      ex [m]      = 0
Eccentricity                      ey [m]      = 0
Radius                            a  [m]      = 5
Z-coord.                          z  [m]      = 0
Layer thickness                   h  [m]      = 100000
No. of circular divisions         Nd [-]      = 20

Soil Data:
Modulus of compressibility        Es [kN/m2] = 6400.0000

Result:
```

Table T1

Contact pressure/ Contact force/ Consolidation settlement:

No.	Coord.	Contact pressure	Contact force	Settlement
I	x	q	f	s
[-]	[m]	[kN/m2]	[kN]	[cm]
1	-5	351.5	62.7	12.32
2	-5	89.1	15.9	12.32
3	-4	118.3	21.1	12.32
4	-4	90.0	16.1	12.32
5	-4	81.4	14.5	12.32
6	-4	73.3	13.1	12.32
7	-3	67.3	12.0	12.32
8	-3	62.5	11.1	12.32
9	-2	58.7	10.5	12.32
10	-2	58.5	10.4	12.32
11	0	49.4	352.4	12.32
12	2	58.5	10.4	12.32
13	2	58.7	10.5	12.32
14	3	62.5	11.1	12.32
15	3	67.3	12.0	12.32
16	4	73.3	13.1	12.32
17	4	81.4	14.5	12.32
18	4	90.0	16.1	12.32
19	4	118.3	21.1	12.32
20	5	89.1	15.9	12.32
21	5	351.5	62.7	12.32

Method (8) (Layered soil model)
Modulus of Compressibility for Rigid Raft

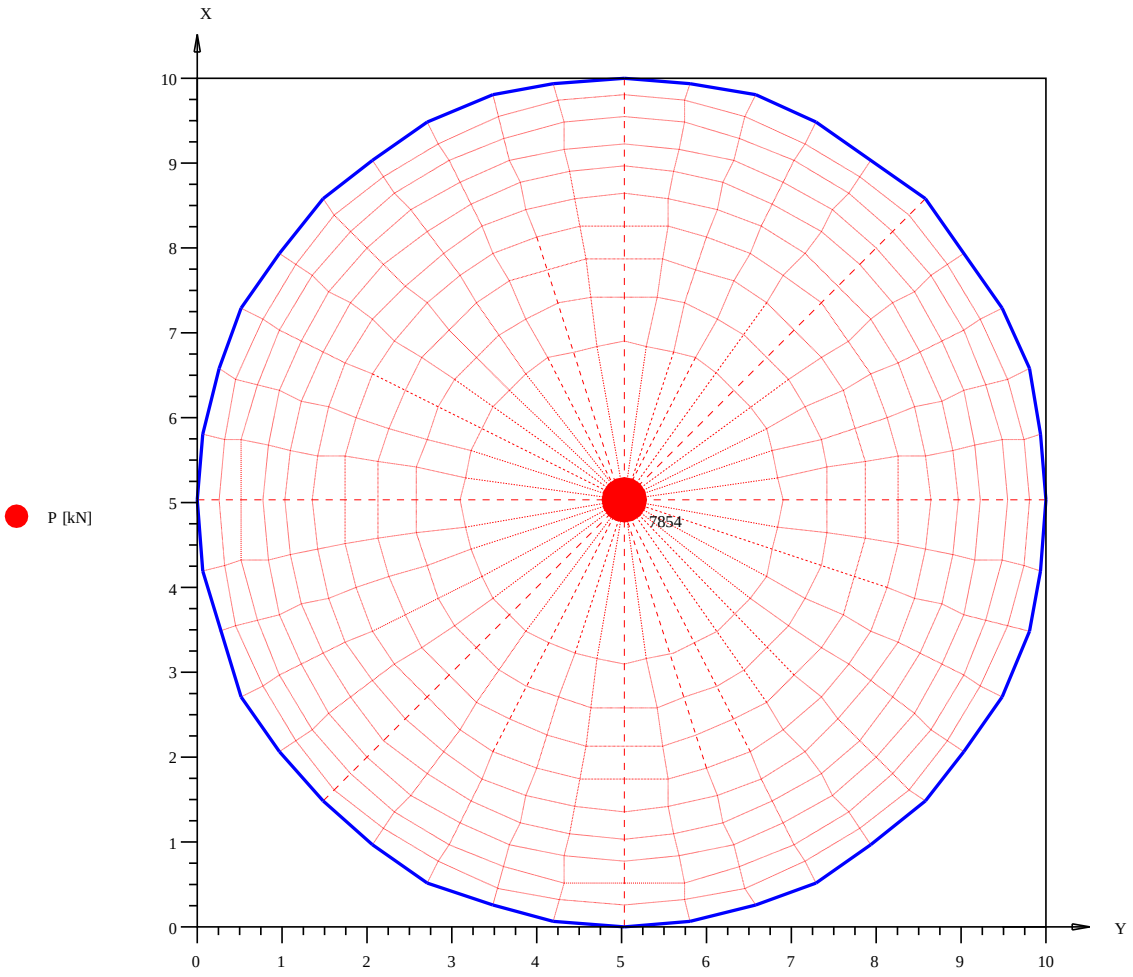

System of loading P [kN]

GEOTEC Software Inc., Calgary AB, Canada T3E 7Y7
PO Box 14001 Richmond Road PO, Tele.: +1 (587) 332-3323

Scale: 63	**Project: Borowicka (1939) and Stark (1990) (Section 5.2, page 106)**
File: Ex2-Rig	**Date: 09-10-2017**
Page No.:	**Title: Rigid circular raft on a deeply extended clay layer**

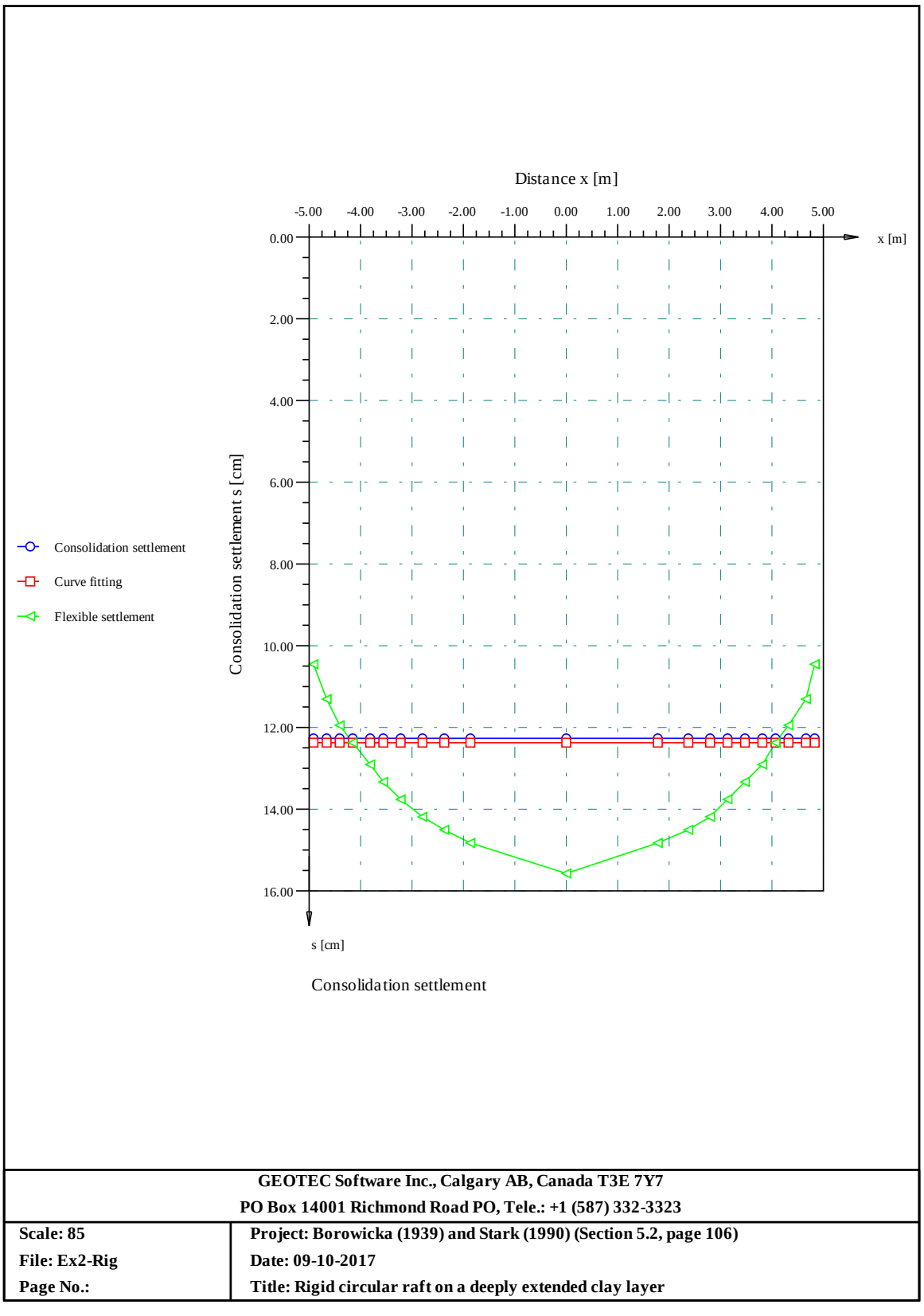

GEOTEC Software Inc., Calgary AB, Canada T3E 7Y7	
PO Box 14001 Richmond Road PO, Tele.: +1 (587) 332-3323	
Scale: 85	**Project: Borowicka (1939) and Stark (1990) (Section 5.2, page 106)**
File: Ex2-Rig	**Date: 09-10-2017**
Page No.:	**Title: Rigid circular raft on a deeply extended clay layer**

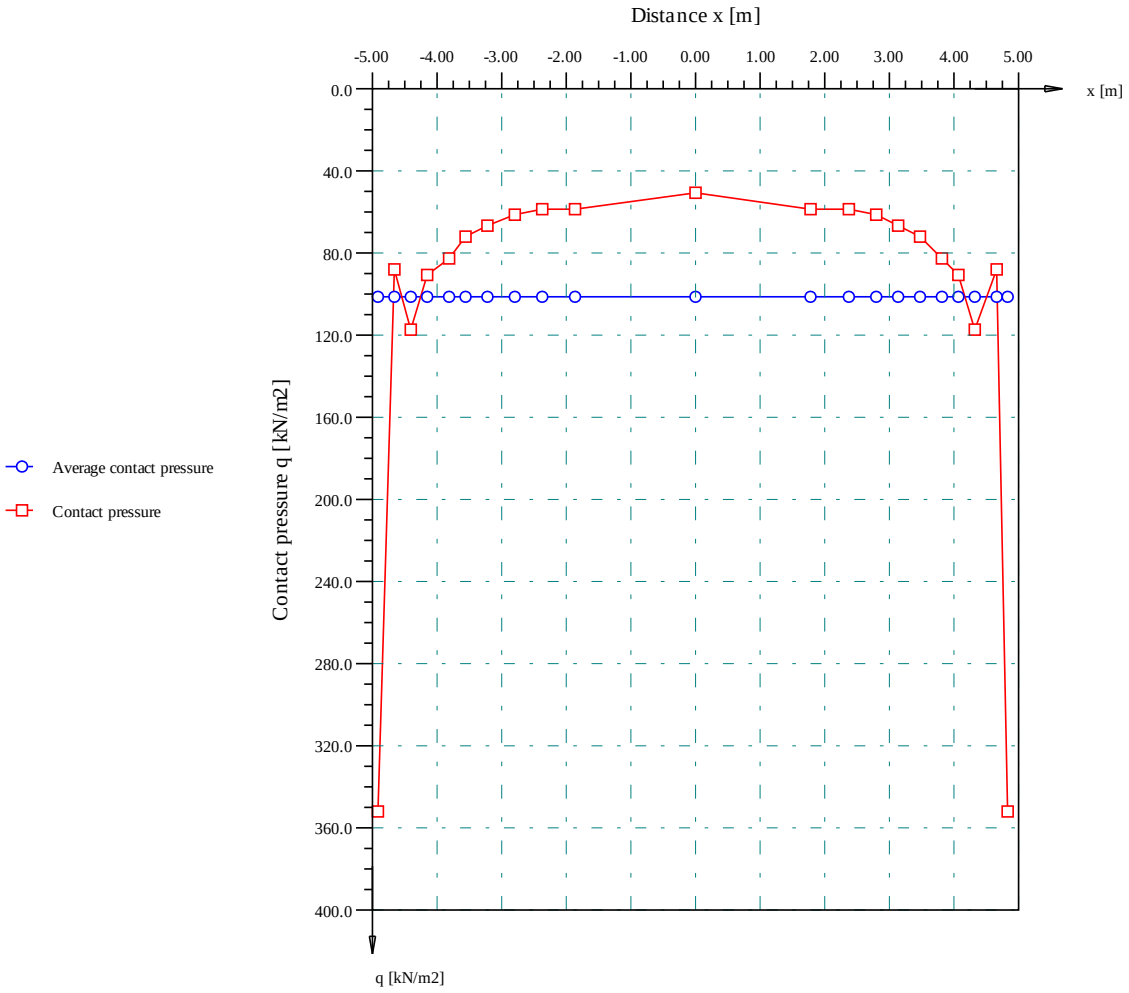

Contact pressure of a rigid raft

GEOTEC Software Inc., Calgary AB, Canada T3E 7Y7	
PO Box 14001 Richmond Road PO, Tele.: +1 (587) 332-3323	
Scale: 85	**Project: Borowicka (1939) and Stark (1990) (Section 5.2, page 106)**
File: Ex2-Rig	**Date: 09-10-2017**
Page No.:	**Title: Rigid circular raft on a deeply extended clay layer**

Method (8) (Layered soil model)
Modulus of Compressibility for Rigid Raft

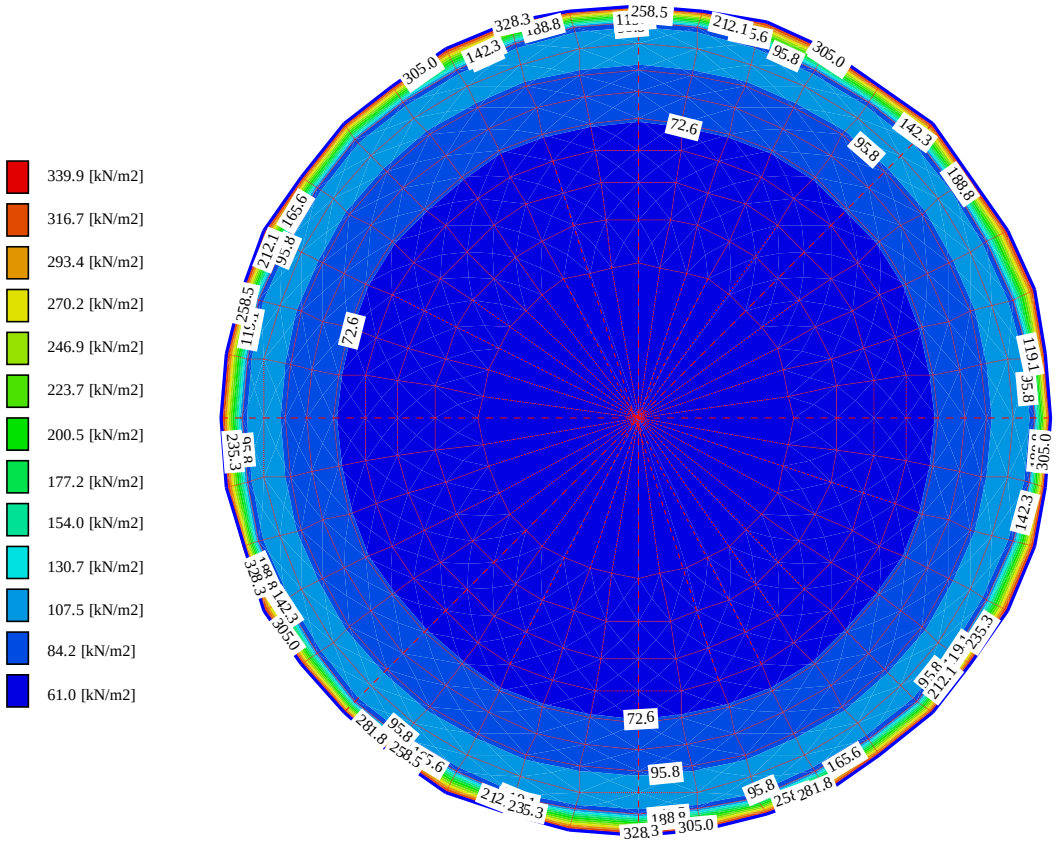

Contact pressure q [kN/m2]
Max. q = 351.5 at node 91, Min. q = 49.4 at node 1

GEOTEC Software Inc., Calgary AB, Canada T3E 7Y7	
PO Box 14001 Richmond Road PO, Tele.: +1 (587) 332-3323	
Scale: 63	**Project: Borowicka (1939) and Stark (1990) (Section 5.2, page 106)**
File: Ex2-Rig	**Date: 09-10-2017**
Page No.:	**Title: Rigid circular raft on a deeply extended clay layer**

Method (8) (Layered soil model)
Modulus of Compressibility for Rigid Raft

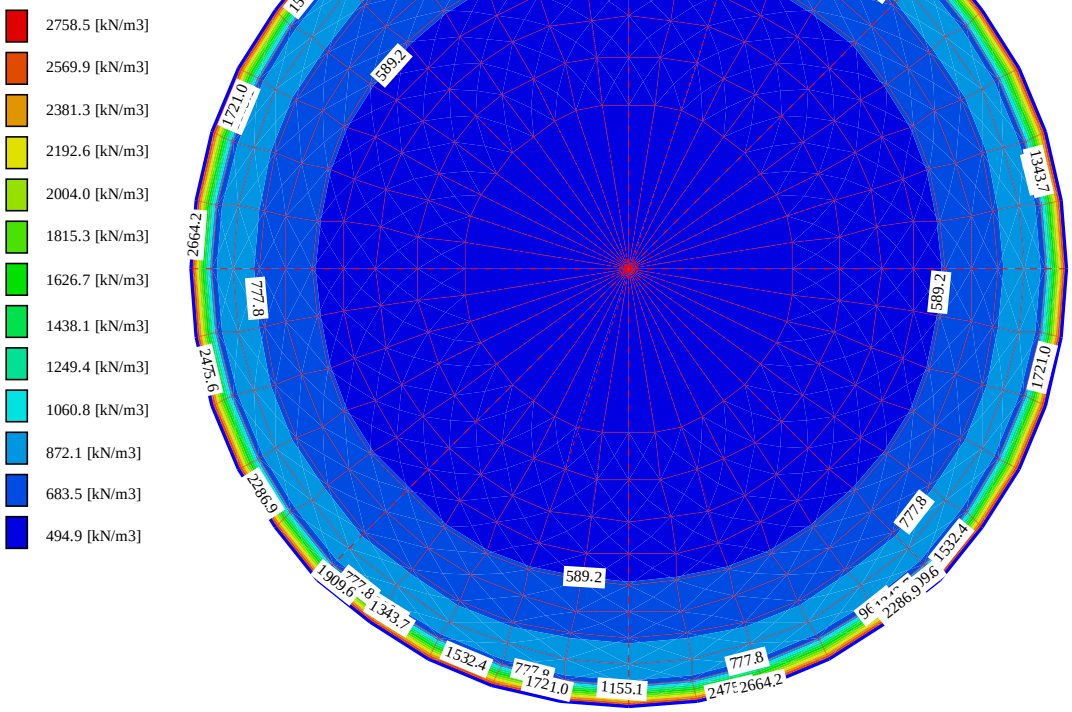

Moduli of subgrade reactions ks [kN/m3]
Max. ks = 2852.8 at node 91, Min. ks = 400.5 at node 1

GEOTEC Software Inc., Calgary AB, Canada T3E 7Y7	
PO Box 14001 Richmond Road PO, Tele.: +1 (587) 332-3323	
Scale: 59	**Project: Borowicka (1939) and Stark (1990) (Section 5.2, page 106)**
File: Ex2-Rig	**Date: 09-10-2017**
Page No.:	**Title: Rigid circular raft on a deeply extended clay layer**

Method (8) (Layered soil model)

Modulus of Compressibility for Rigid Raft

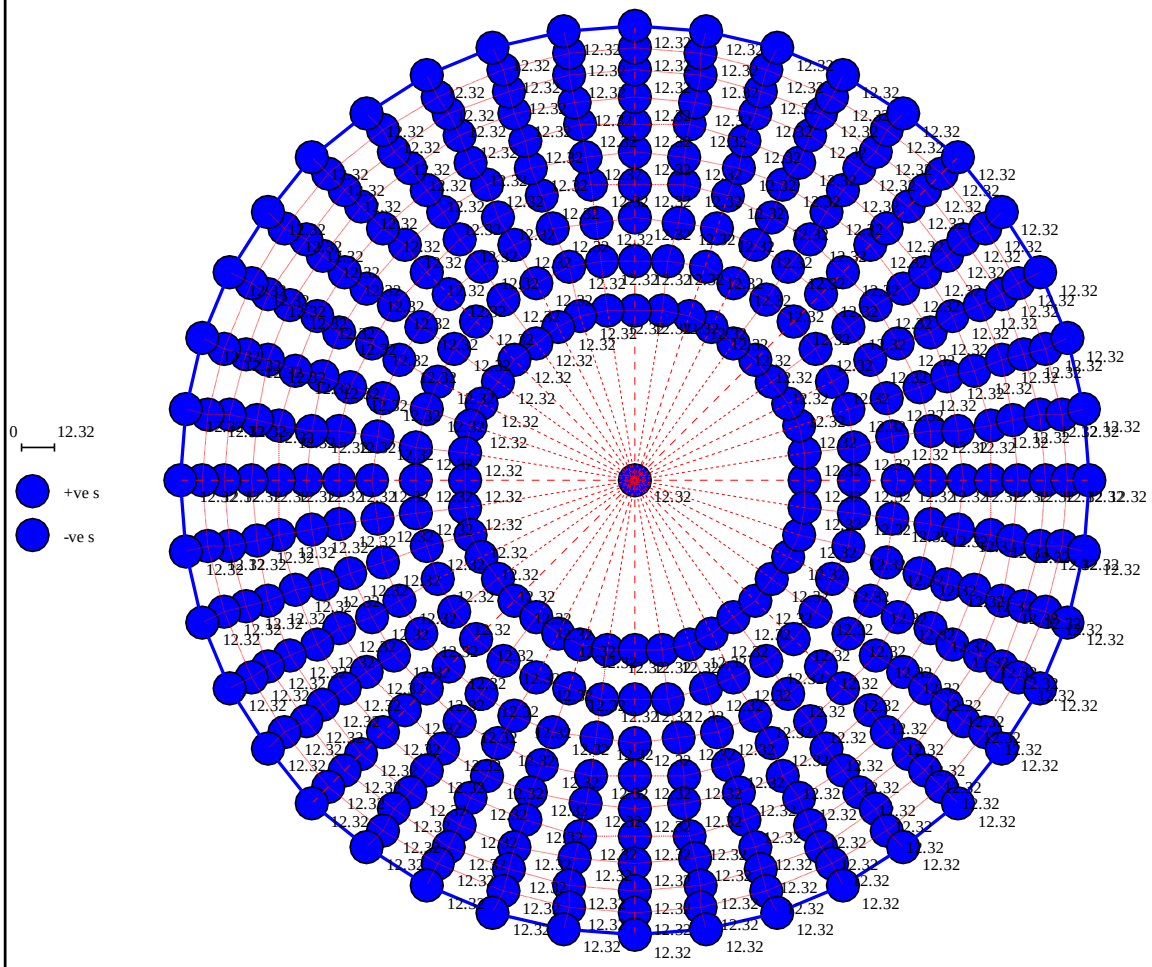

Settlements s [cm]

Max. s = 12.32 at node 1, Min. s = 12.32 at node 1

GEOTEC Software Inc., Calgary AB, Canada T3E 7Y7	
PO Box 14001 Richmond Road PO, Tele.: +1 (587) 332-3323	
Scale: 59	**Project: Borowicka (1939) and Stark (1990) (Section 5.2, page 106)**
File: Ex2-Rig	**Date: 09-10-2017**
Page No.:	**Title: Rigid circular raft on a deeply extended clay layer**

8.8.4 Example 3: Rigid circular raft on a deeply extended clay layer

8.8.4.1 Description of the problem

To verify the proposed procedures of a rigid raft on consolidated clay deposits, first both semi-analytical and numerical procedure are checked. Then, the results of a rigid raft obtained by semi-analytical solutions are compared with those obtained by the numerical solution. A circular raft of a radius a = 5.0 [m] on a deeply extended clay layer is chosen and subdivided into 576 elements as shown in Figure 10. The raft is subjected to an average uniform load of p = 100 [kN/m^2]. To check the accuracy of the proposed procedures, the raft analysis is carried out for two different cases:

1. Case of a centric load
2. Case of an eccentric load with extreme eccentricity $e_x = a/3$

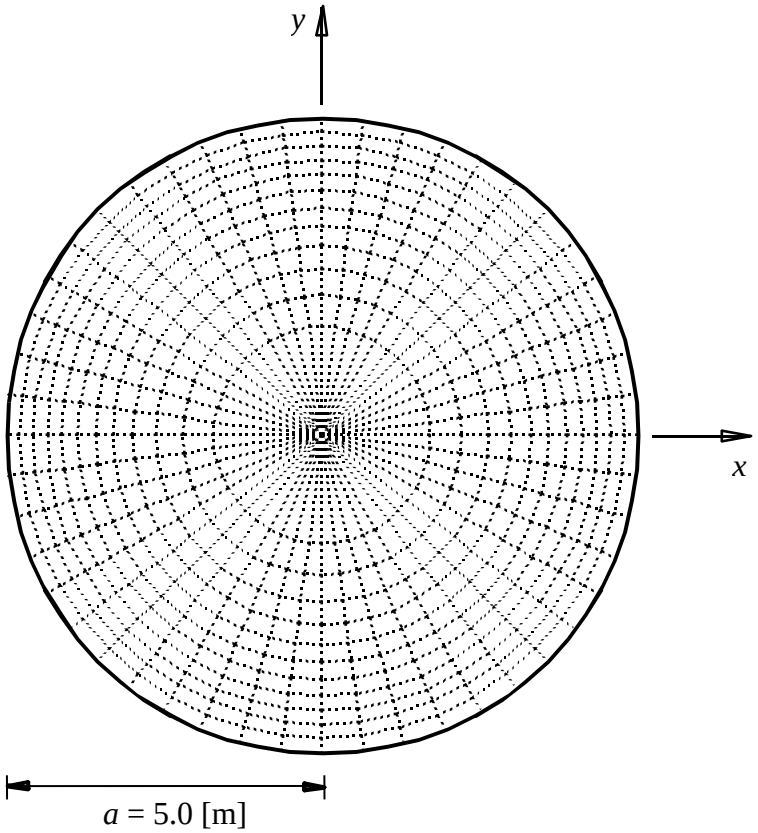

Figure 8.23 Rigid circular raft with dimension and mesh

8.8.4.2 Clay properties

Both of the two parameters, coefficient of volume change m_v and compression index C_c are used to define the consolidation characteristics of the clay deposits. For the comparison purpose, the clay properties are chosen such that either of the two parameters gives nearly the

same average consolidation settlement.

The clay has the following properties:

Coefficient of volume change	m_v	= 0.0002	[m^2/kN]
Term of compression index and initial void ratio	$C_c/(e_o+1)$	= 0.0378	[-]
Compression index and initial void ratio	C_c	= 0.07	[-]
Initial void ratio	e_o	= 0.85	[-]
Dry unit weight of the clay	γ	= 18.5	[kN/m^3]
Submerged unit weight of the clay	γ'	= 8.69	[kN/m^3]

8.8.4.3 Analysis of the raft

The analytical contact pressure distribution under the rigid circular raft is derived with the assumption of a semi-infinite soil layer. Therefore, the settlement is calculated up to a depth z after which the increase in settlement due to the next soil strip becomes less than 0.001 [cm]. In this example, the clay layer is considered as semi-infinite soil layer when the clay has a thickness of z = 150 [m]. The whole clay layer is divided into sub-layers each of thickness h = 5.0 [m]. For the numerical procedure in case of defining the clay layer by C_c, *GEO Tools* is used, where the system of linear equations is solved using iteration. The accuracy of ε = 0.000624 [m] is reached after 5 cycles in the case of a centric load, while in the case of an eccentric load the accuracy of ε = 0.000978 [m] is reached after 11 cycles. The definition of the characteristic point according to *Graßhoff* (1955) can be used to verify both of the semi-analytical and numerical solutions. The characteristic point is defined as that point of a surface area loaded by a uniformly distributed pressure, where the settlement s_o due to that pressure is identical with the displacement w_o of a rigid raft of the same shape and loading. For a circular raft, the characteristic point lies at distance a_c =0.845 a from the center. Therefore, the analysis is carried out also for a flexible raft, where the contact stress is equal to the applied stress on the soil.

8.8.4.4 Results and discussions

Figure 8.24 shows the consolidation settlement at the middle of the raft in case of a centric load, while Figure 8.25 shows that in case of an eccentric load with extreme eccentricity e_x = a/3. Table 8.9 compares the consolidation settlements at the characteristic point for the rigid raft with those for the flexible raft. It can be shown from these figures that although the settlement for the analytical solution is determined under all points on the raft, but the settlement is distributed linearly under the raft with maximum difference 2 [%] in case of a centric load and 5 [%] in case of an eccentric load in respect to fitting curves. Also, both of the semi-analytical and numerical settlements are in a good agreement especially in case of a centric load. It can be clearly observed from Figure 8.24 and also from Table 8.9 that the settlements at characteristic points for a flexible raft are nearly identical to those for a rigid raft for both numerical and semi-analytical procedures with the two soil parameters m_v and C_c.

Table 8.9 Consolidation settlements *s* [cm] at the characteristic point

Item	Clay is defined by m_v			Clay is defined by C_c		
	semi-analytical	Numerical	Flexible	semi-analytical	Numerical	Flexible
Settlement	15.00	14.89	15.09	15.18	15.19	15.30
Diff. [%]	0.60	1.30	-	0.78	0.72	-

Figure 8.26 shows the comparison of the contact pressure ratio *q/p* [-] at the at the middle of the raft in case of a centric load while Figure 8.27 shows that of an eccentric load. It can be found from these figures that the results of the circular rigid raft obtained by the numerical procedure are nearly equal to those obtained by semi-analytical procedure for all locations except near the raft edge.

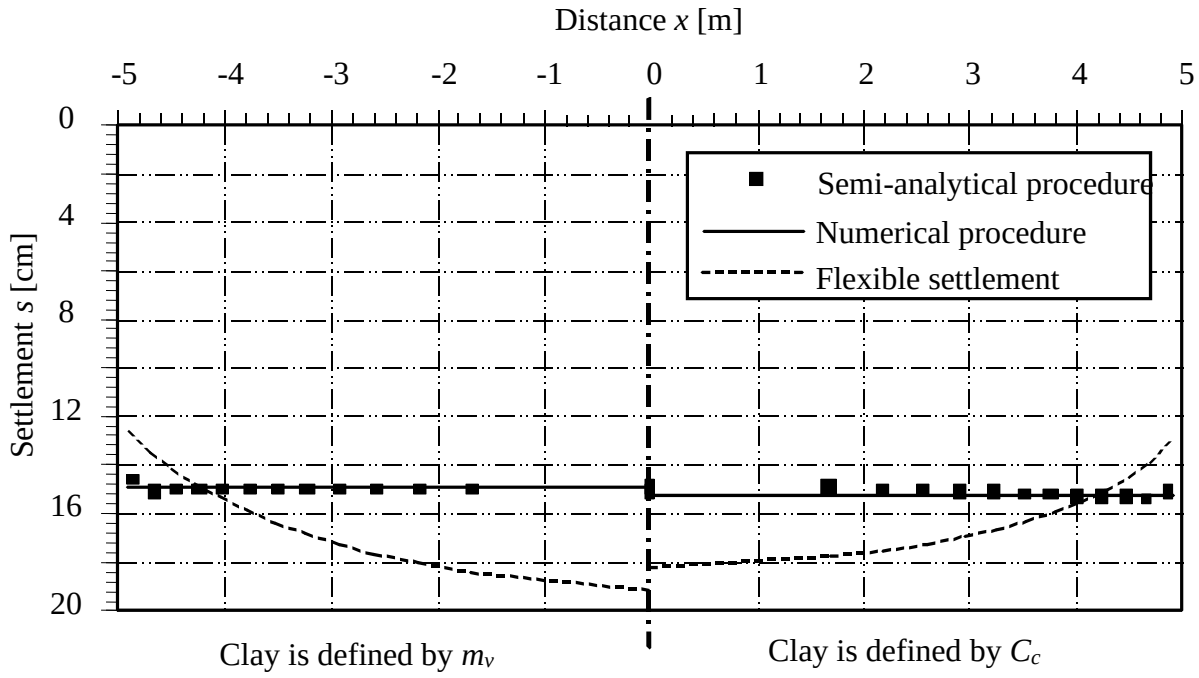

Figure 8.24 Consolidation settlement *s* [cm] at the middle of the raft (case of a centric load)

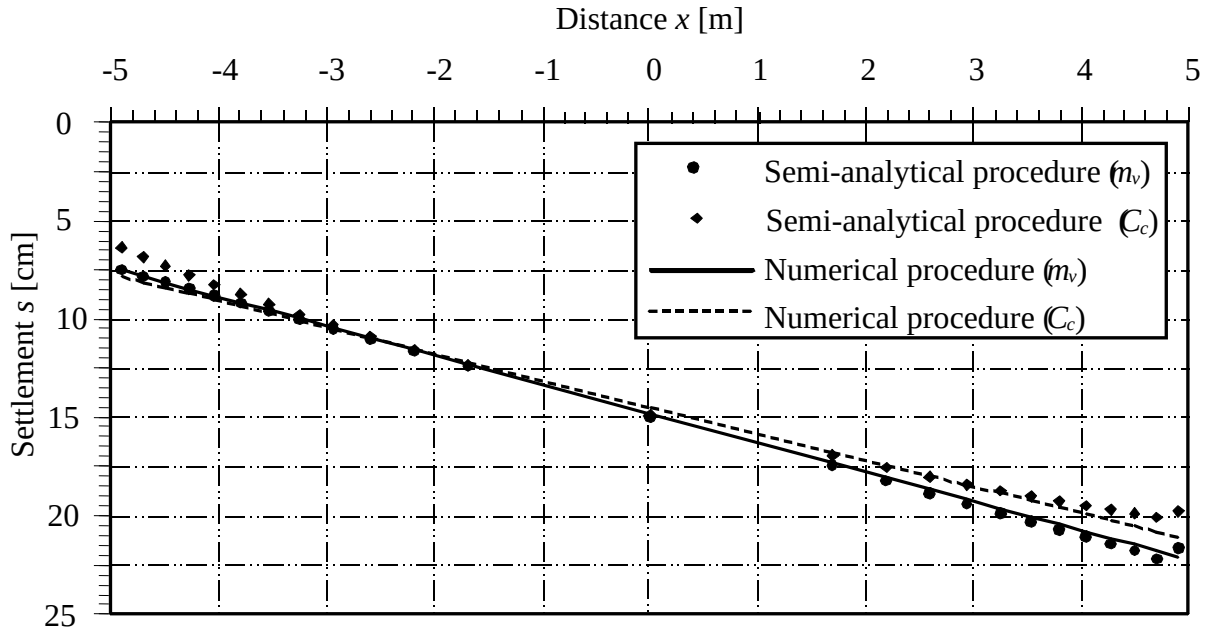

Figure 8.25 Consolidation settlement *s* [cm] at the middle of the raft (case of an eccentric load)

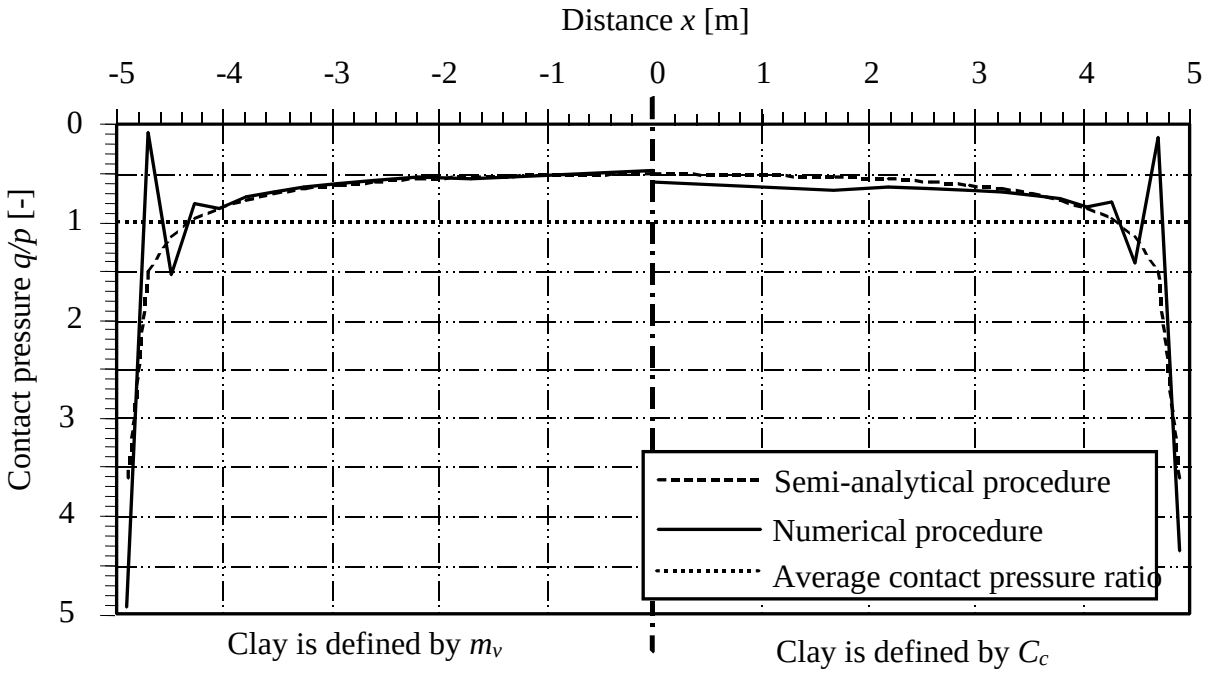

Figure 8.26 Contact pressure ratio *q/p* [-] at the middle of the raft (case of a centric load)

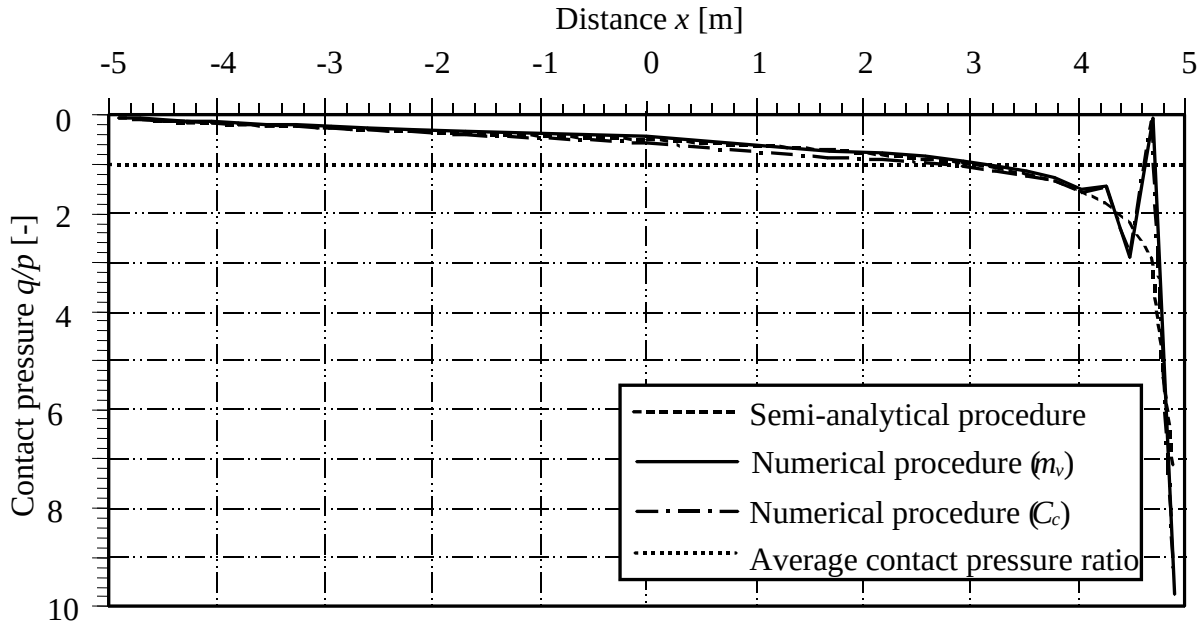

Figure 8.27 Contact pressure ratio *q/p* [-] at the middle of the raft (case of an eccentric load)

8.8.4.5 Rigid consolidation by GEO Tools

The input data and results of *GEO Tools* are presented on the next pages. By comparison, one can see a good agreement in results for semi-analytical solution with numerical solution for the two cases; a centric load and an eccentric load with extreme eccentricity ex = a/3.

```
************************************************************
                        GEO Tools
                         Version 10
     Program authors Prof. M. El Gendy/ Dr. A. El Gendy
************************************************************
Title: Comparison between settlements obtained by analytical and numerical
Date: 10-10-2017
Project: User's Manual
File: Ex3-Ana

------------------------------------------------------------
Consolidation of rigid raft
Type of the solution Analytical solution
Determining settlements at the center and the edge
------------------------------------------------------------

Data:
Point load                      Q       [kN]     = 7854
Eccentricity                    ex      [m]      = 1.60
Eccentricity                    ey      [m]      = 0.00
Radius                          a       [m]      = 5.00
No. of circular divisions       Nd      [-]      = 24

Soil Data:
Compression index               Cc      [-]      = 0.070
Initial void ratio              eo      [-]      = 0.850
Unit weight                     Gamma_c [kN/m3]  = 8.69
Overburden pressure             Gamma*z [kN/m2]  = 0.0

Result:
```

Table T1

Contact pressure/ Contact force/ Consolidation settlement:

No.	Coord.	Contact pressure	Contact force	Settlement
I	x	q	f	s
[-]	[m]	[kN/m2]	[kN]	[cm]
1	-4.90	19.2	2.4	10.99
2	-4.70	14.4	1.8	11.22
3	-4.49	15.7	2.0	11.47
4	-4.27	17.3	2.2	11.72
5	-4.04	19.1	2.4	11.99
6	-3.80	20.9	2.6	12.27
7	-3.53	22.8	2.9	12.57
8	-3.25	24.8	3.1	12.90
9	-2.94	26.9	3.4	13.26
10	-2.59	29.4	3.7	13.66
11	-2.19	32.3	4.1	14.13
12	-1.69	35.9	4.5	14.71
13	0.00	51.0	308.1	16.66
14	1.69	70.4	8.9	18.61
15	2.19	79.0	9.9	19.19
16	2.59	87.6	11.0	19.66
17	2.94	96.8	12.2	20.06
18	3.25	107.0	13.5	20.42
19	3.53	118.8	14.9	20.75
20	3.80	133.0	16.7	21.05
21	4.04	151.2	19.0	21.33
22	4.27	175.9	22.1	21.60
23	4.49	213.5	26.9	21.85
24	4.70	284.3	35.8	22.10
25	4.90	702.0	88.4	22.33

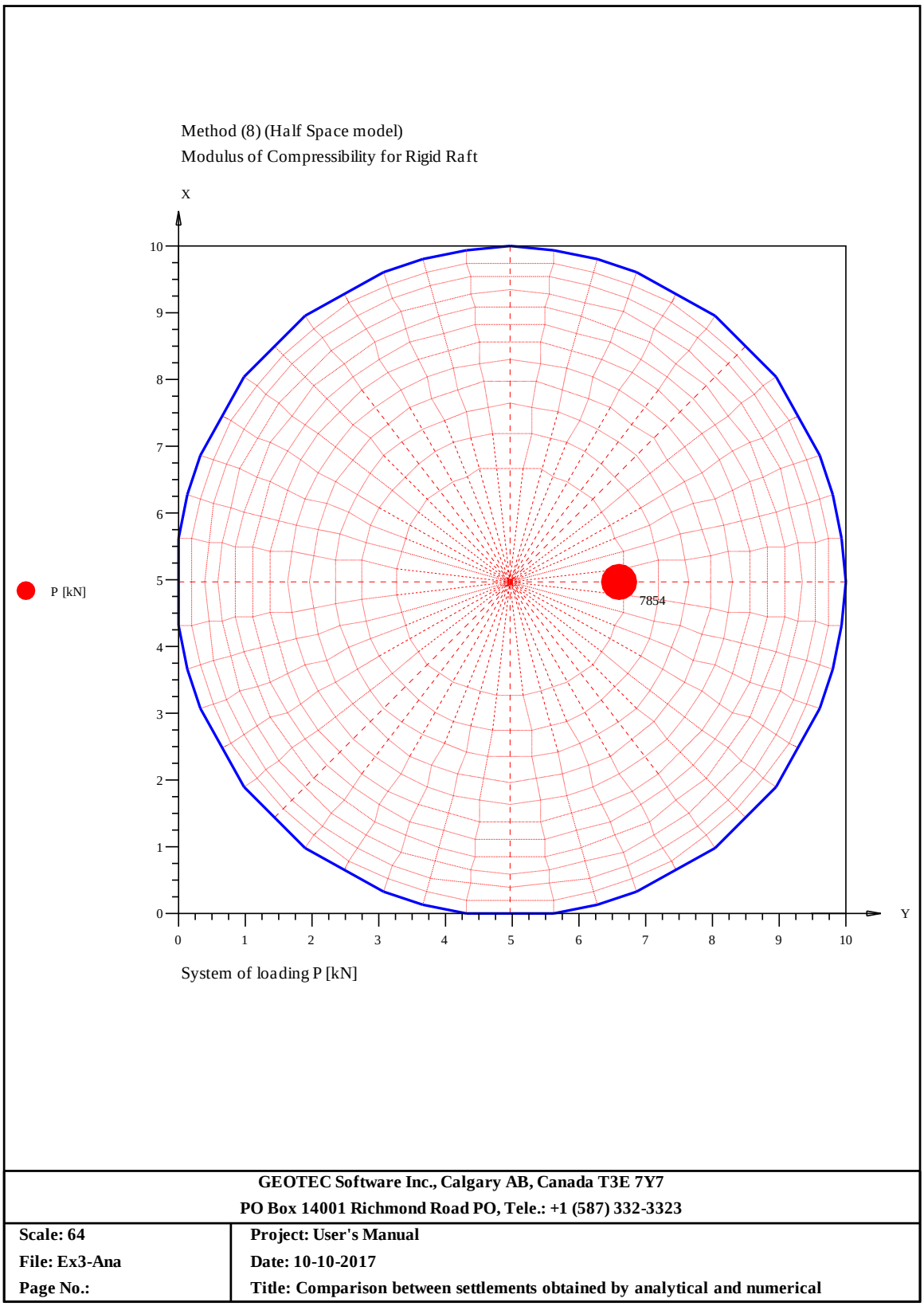

GEOTEC Software Inc., Calgary AB, Canada T3E 7Y7	
PO Box 14001 Richmond Road PO, Tele.: +1 (587) 332-3323	
Scale: 64	**Project: User's Manual**
File: Ex3-Ana	**Date: 10-10-2017**
Page No.:	**Title: Comparison between settlements obtained by analytical and numerical**

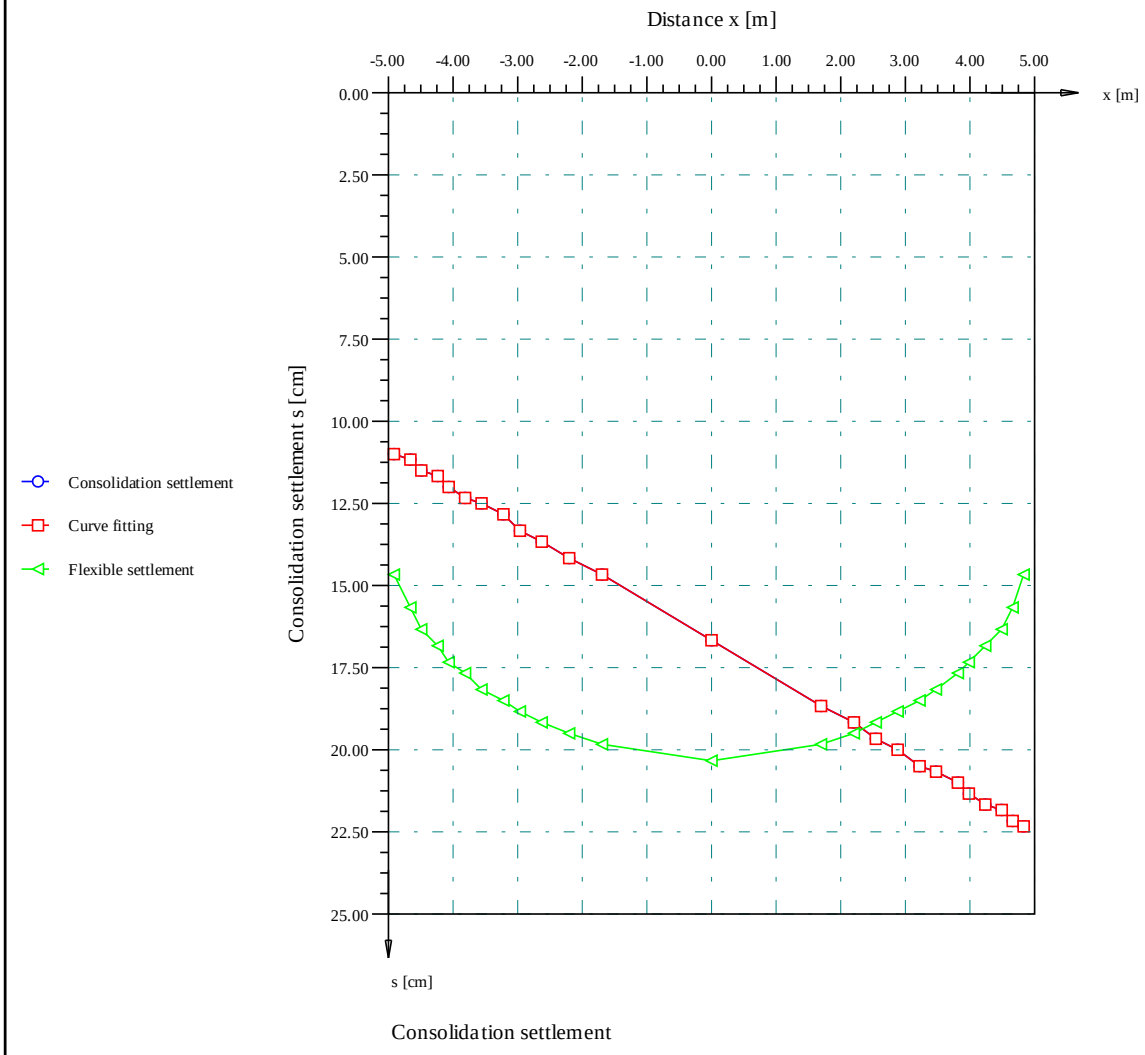

GEOTEC Software Inc., Calgary AB, Canada T3E 7Y7	
PO Box 14001 Richmond Road PO, Tele.: +1 (587) 332-3323	
Scale: 85	**Project: User's Manual**
File: Ex3-Ana	**Date: 10-10-2017**
Page No.:	**Title: Comparison between settlements obtained by analytical and numerical**

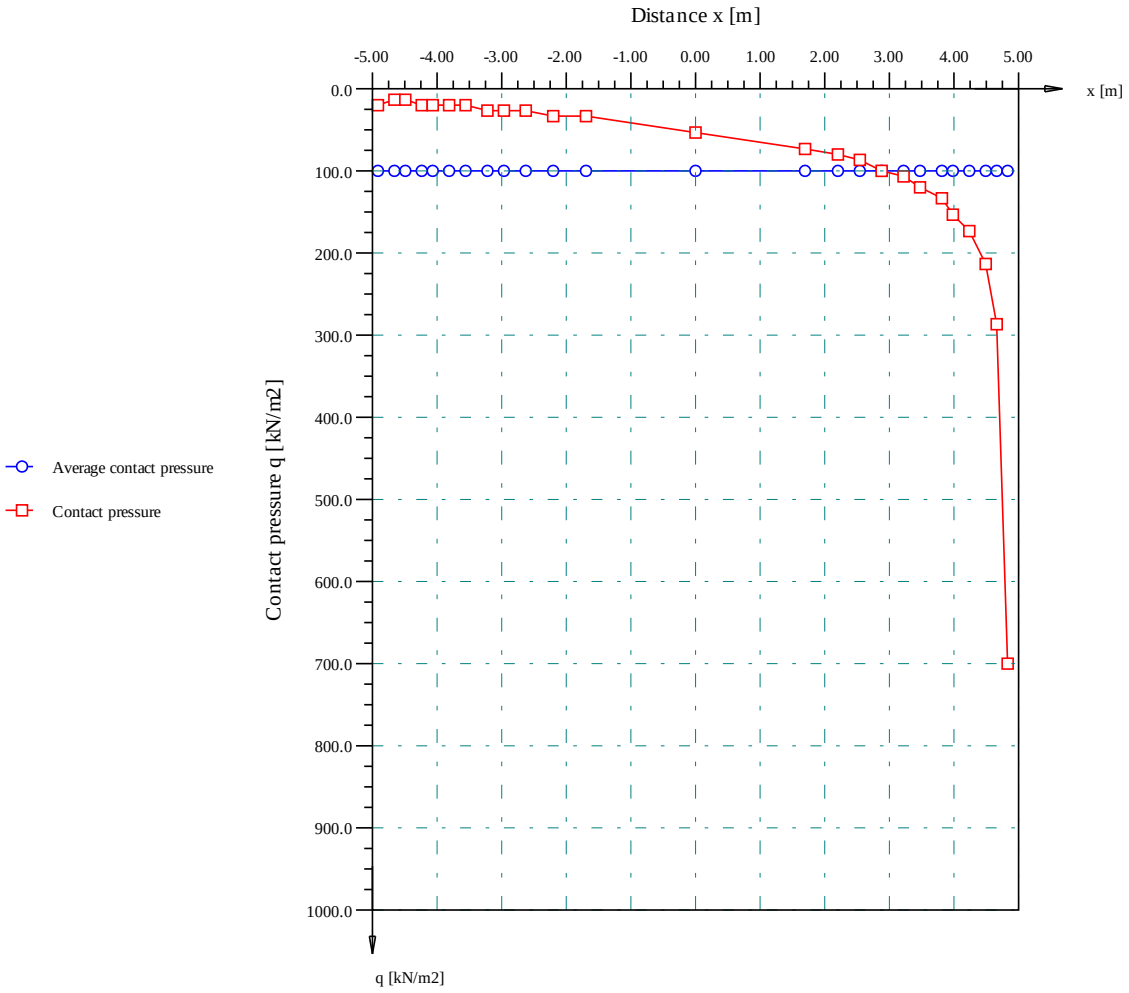

Contact pressure of a rigid raft

GEOTEC Software Inc., Calgary AB, Canada T3E 7Y7	
PO Box 14001 Richmond Road PO, Tele.: +1 (587) 332-3323	
Scale: 85	**Project: User's Manual**
File: Ex3-Ana	**Date: 10-10-2017**
Page No.:	**Title: Comparison between settlements obtained by analytical and numerical**

Method (8) (Half Space model)
Modulus of Compressibility for Rigid Raft

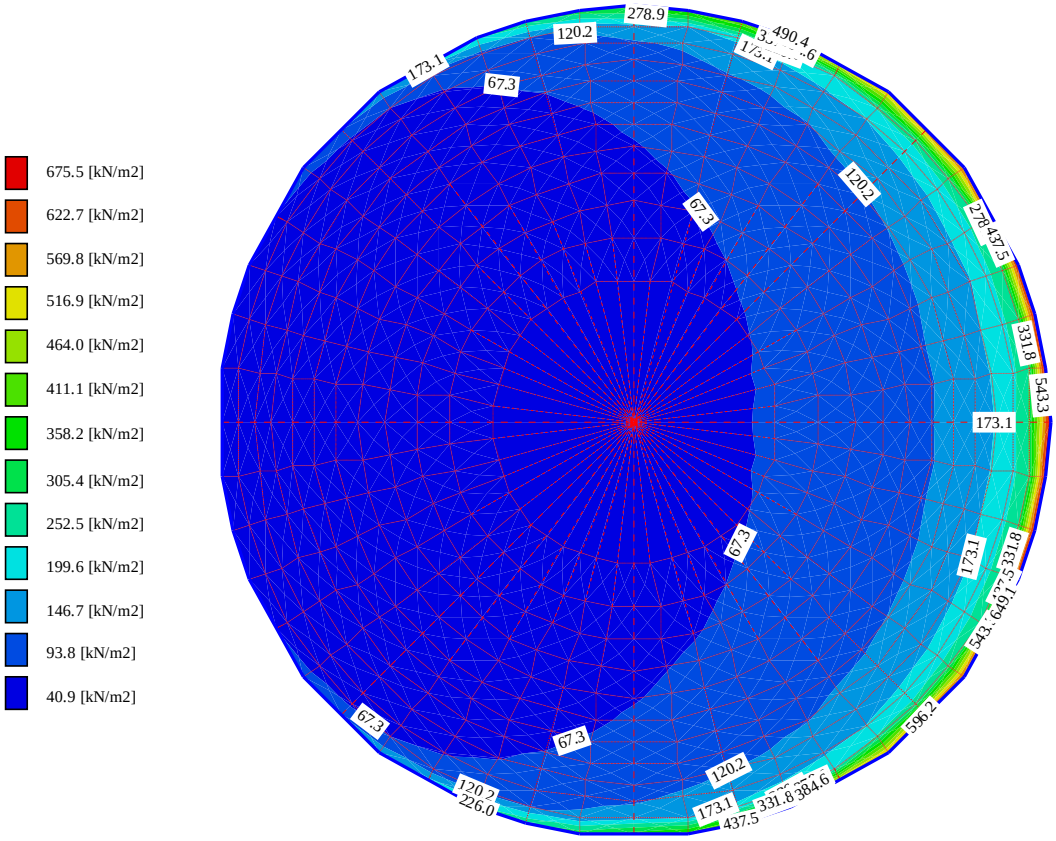

Contact pressure q [kN/m2]
Max. q = 702.0 at node 13, Min. q = 14.4 at node 300

GEOTEC Software Inc., Calgary AB, Canada T3E 7Y7	
PO Box 14001 Richmond Road PO, Tele.: +1 (587) 332-3323	
Scale: 64	**Project: User's Manual**
File: Ex3-Ana	**Date: 10-10-2017**
Page No.:	**Title: Comparison between settlements obtained by analytical and numerical**

Method (8) (Half Space model)
Modulus of Compressibility for Rigid Raft

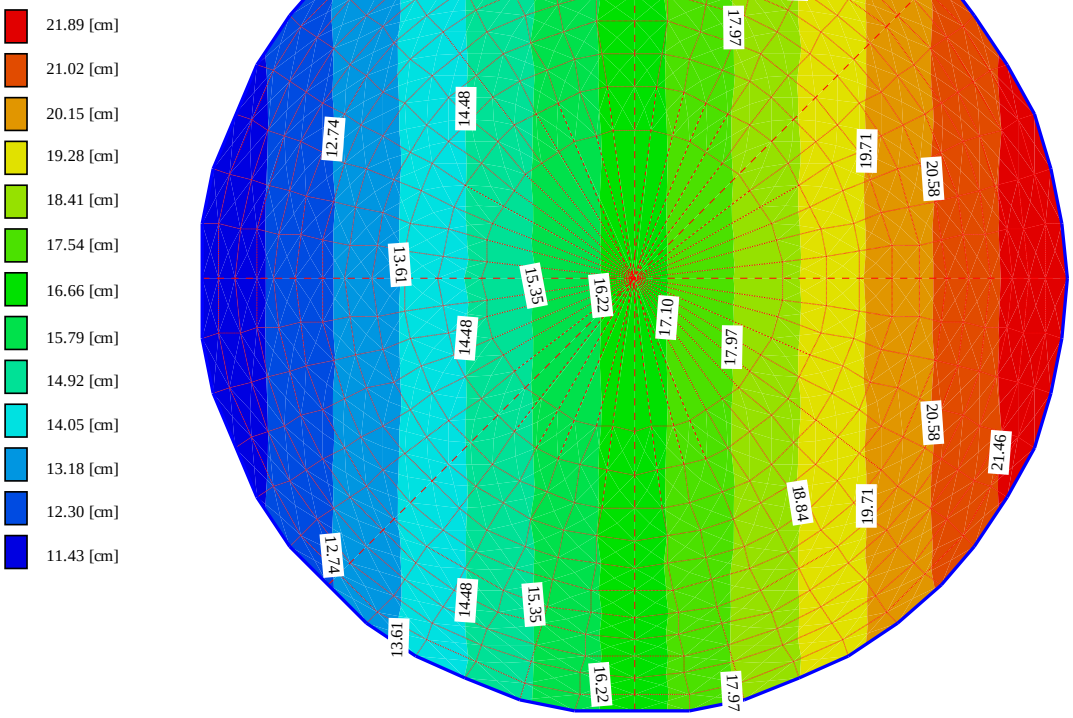

Settlements s [cm]
Max. s = 22.33 at node 13, Min. s = 10.99 at node 301

GEOTEC Software Inc., Calgary AB, Canada T3E 7Y7	
PO Box 14001 Richmond Road PO, Tele.: +1 (587) 332-3323	
Scale: 62	**Project: User's Manual**
File: Ex3-Ana	**Date: 10-10-2017**
Page No.:	**Title: Comparison between settlements obtained by analytical and numerical**

Method (8) (Half Space model)
Modulus of Compressibility for Rigid Raft

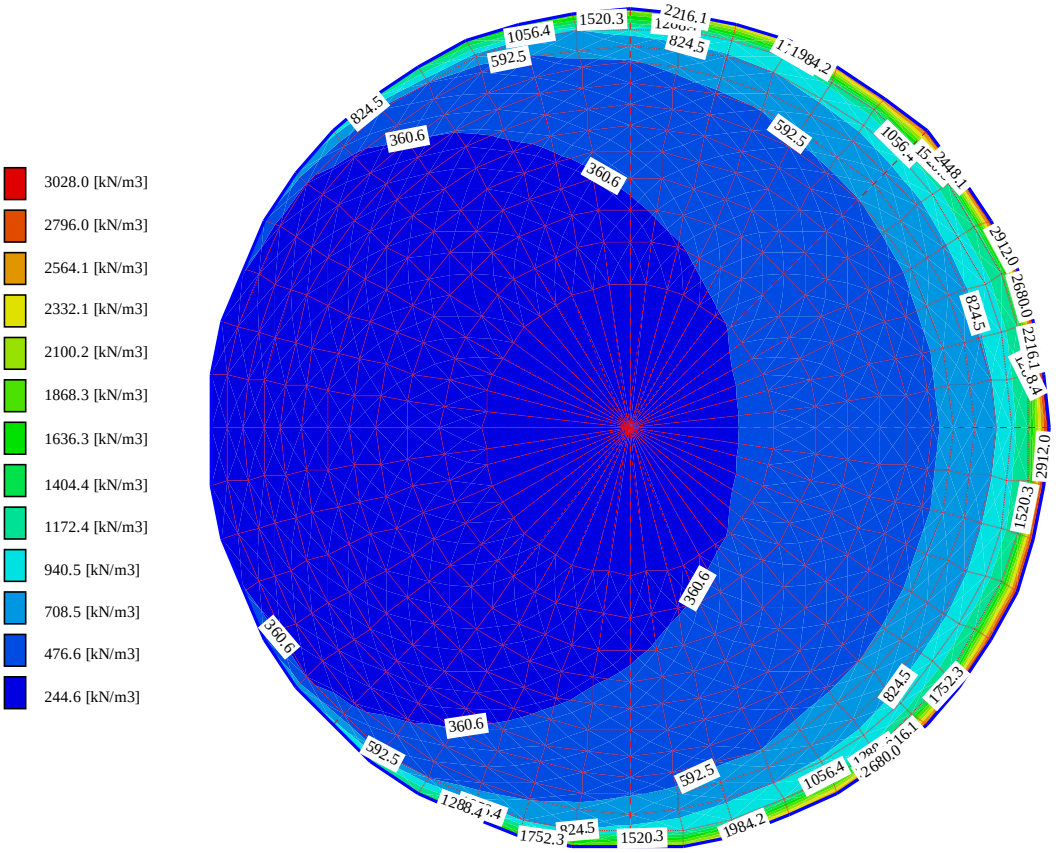

Moduli of subgrade reactions ks [kN/m3]
Max. ks = 3143.9 at node 13, Min. ks = 128.6 at node 300

GEOTEC Software Inc., Calgary AB, Canada T3E 7Y7	
PO Box 14001 Richmond Road PO, Tele.: +1 (587) 332-3323	
Scale: 62	**Project: User's Manual**
File: Ex3-Ana	**Date: 10-10-2017**
Page No.:	**Title: Comparison between settlements obtained by analytical and numerical**

```
************************************************************
                        GEO Tools
                         Version 10
     Program authors Prof. M. El Gendy/ Dr. A. El Gendy
************************************************************
Title: Comparison between settlements obtained by analytical and numerical
analyses
Date: 10-10-2017
Project: User's Manual
File: Ex3-Num

------------------------------------------------------------
Consolidation of rigid raft
Type of the solution Numerical solution
------------------------------------------------------------

Data:
Point load                      Q       [kN]     = 7854
Eccentricity                    ex      [m]      = 1.60
Eccentricity                    ey      [m]      = 0.00
Radius                          a       [m]      = 5.00
Z-coord.                        z       [m]      = 0.00
Layer thickness                 h       [m]      = 150.00
No. of circular divisions       Nd      [-]      = 24

Soil Data:
Compression index               Cc      [-]      = 0.070
Initial void ratio              eo      [-]      = 0.850
Unit weight                     Gamma_c [kN/m3]  = 8.69
Overburden pressure             Gamma*z [kN/m2]  = 0.0

Result:
```

Table T1

Contact pressure/ Contact force/ Consolidation settlement:

No.	Coord.	Contact pressure	Contact force	Settlement
I	x	q	f	s
[-]	[m]	[kN/m2]	[kN]	[cm]
1	-4.90	71.8	9.0	9.45
2	-4.70	22.5	2.8	9.73
3	-4.49	30.0	3.8	10.03
4	-4.27	26.0	3.3	10.34
5	-4.04	26.0	3.3	10.67
6	-3.80	26.1	3.3	11.02
7	-3.53	26.7	3.4	11.39
8	-3.25	27.7	3.5	11.79
9	-2.94	29.0	3.7	12.23
10	-2.59	30.8	3.9	12.73
11	-2.19	33.2	4.2	13.30
12	-1.69	37.1	4.7	14.00
13	0.00	49.8	301.0	16.40
14	1.69	78.8	9.9	18.79
15	2.19	84.9	10.7	19.50
16	2.59	94.0	11.8	20.07
17	2.94	104.0	13.1	20.57
18	3.25	115.4	14.5	21.01
19	3.53	128.5	16.2	21.41
20	3.80	144.2	18.1	21.78
21	4.04	165.0	20.8	22.13
22	4.27	186.3	23.4	22.46
23	4.49	254.8	32.1	22.77
24	4.70	190.8	24.0	23.06
25	4.90	792.1	99.7	23.35

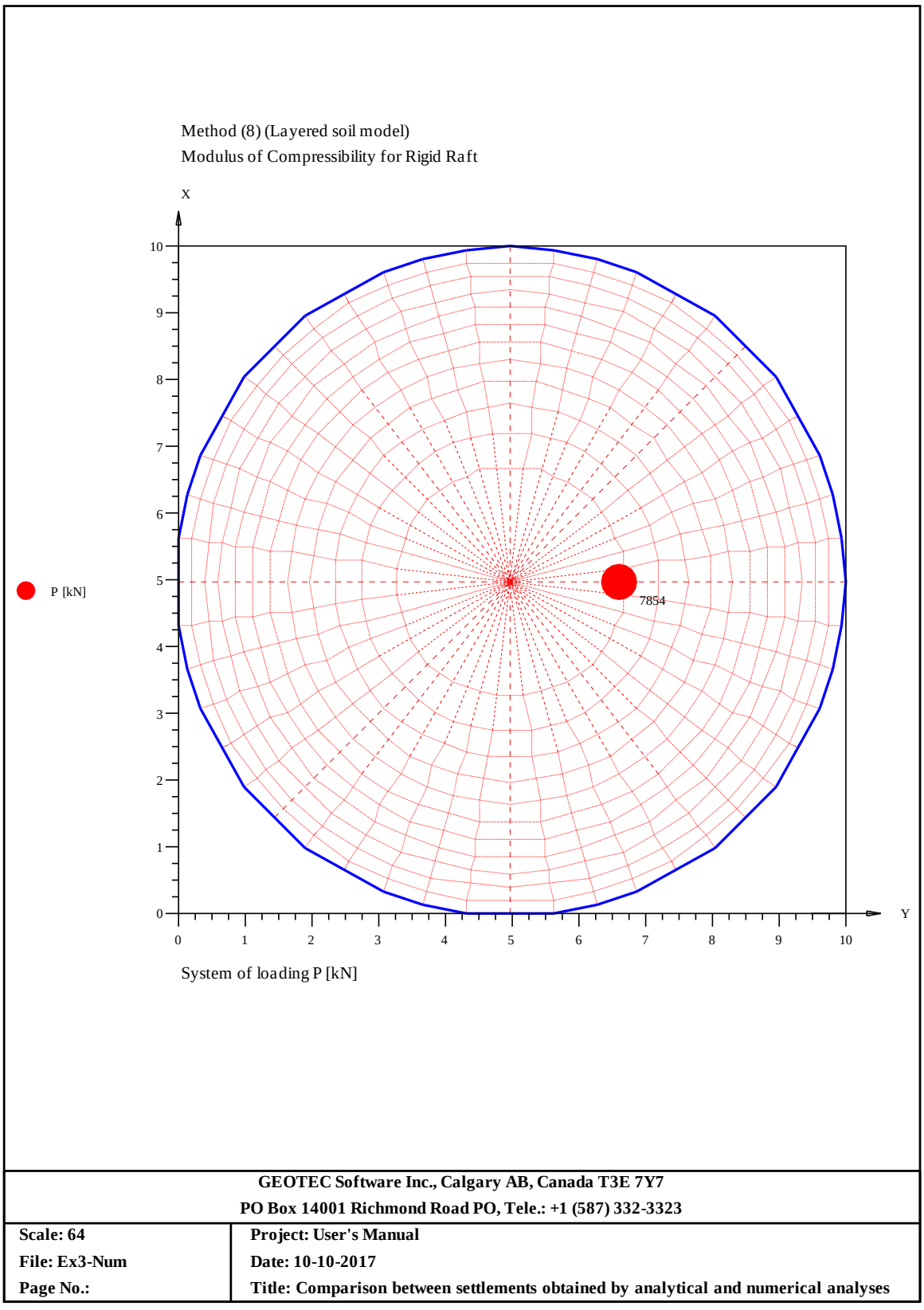

GEOTEC Software Inc., Calgary AB, Canada T3E 7Y7	
PO Box 14001 Richmond Road PO, Tele.: +1 (587) 332-3323	
Scale: 64	**Project: User's Manual**
File: Ex3-Num	**Date: 10-10-2017**
Page No.:	**Title: Comparison between settlements obtained by analytical and numerical analyses**

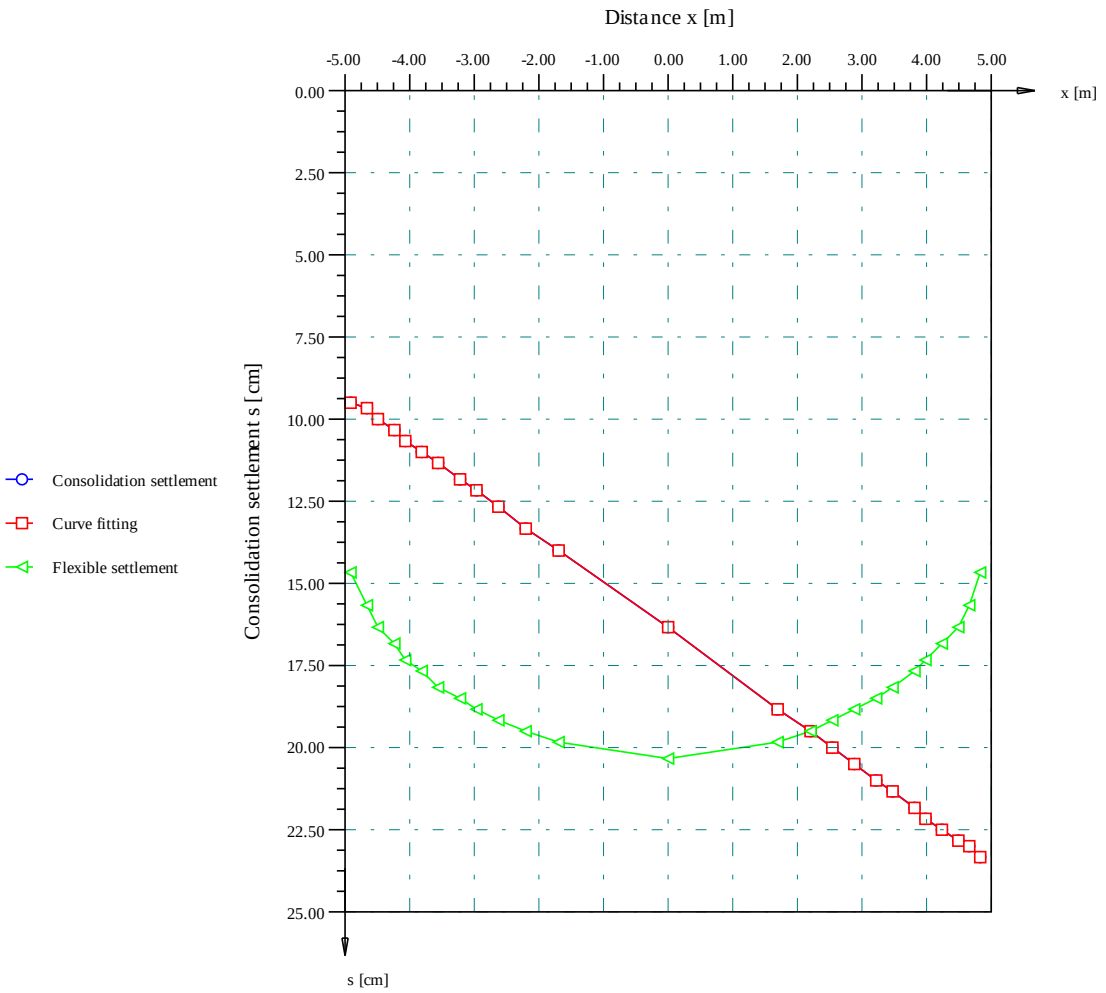

Consolidation settlement

GEOTEC Software Inc., Calgary AB, Canada T3E 7Y7	
PO Box 14001 Richmond Road PO, Tele.: +1 (587) 332-3323	
Scale: 85	**Project: User's Manual**
File: Ex3-Num	**Date: 10-10-2017**
Page No.:	**Title: Comparison between settlements obtained by analytical and numerical analyses**

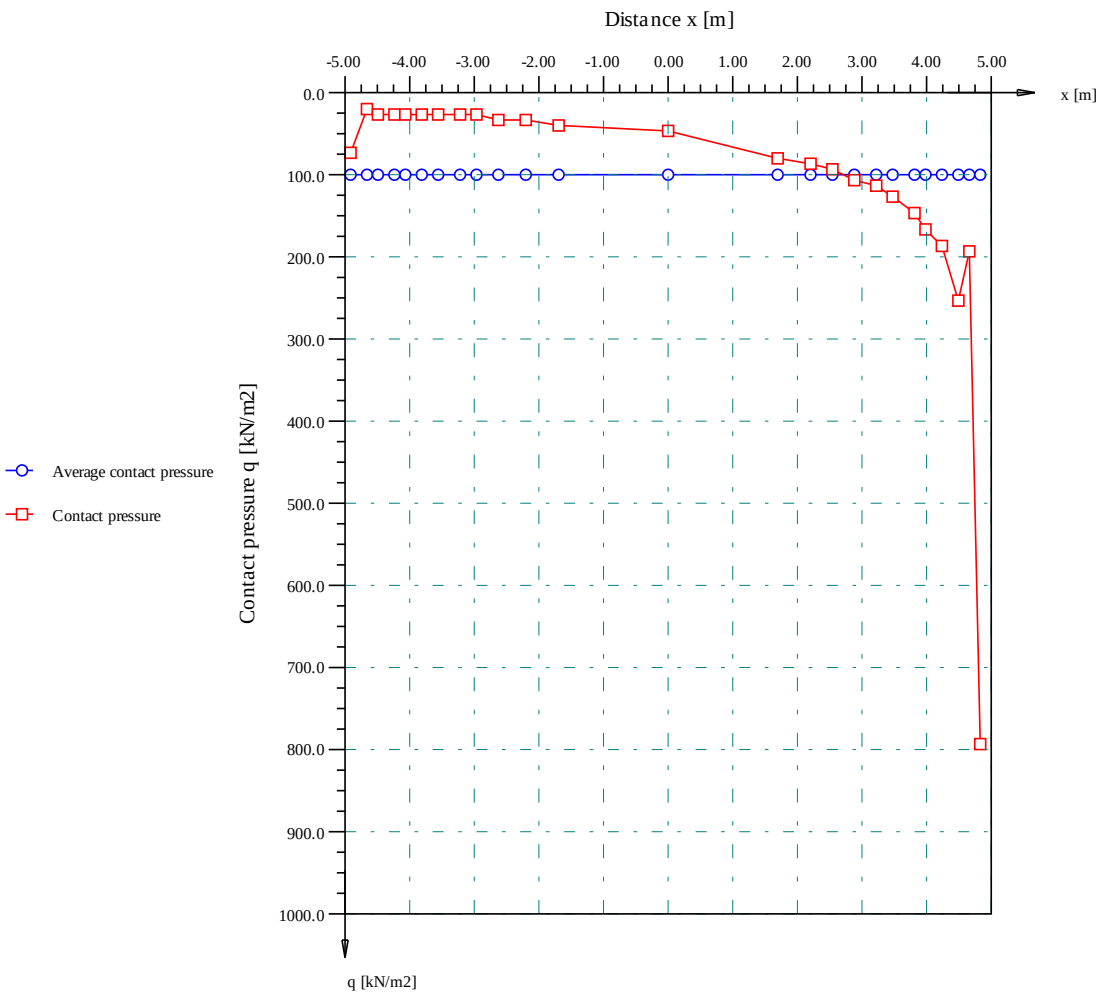

Contact pressure of a rigid raft

GEOTEC Software Inc., Calgary AB, Canada T3E 7Y7	
PO Box 14001 Richmond Road PO, Tele.: +1 (587) 332-3323	
Scale: 85	**Project: User's Manual**
File: Ex3-Num	**Date: 10-10-2017**
Page No.:	**Title: Comparison between settlements obtained by analytical and numerical analyses**

Method (8) (Layered soil model)
Modulus of Compressibility for Rigid Raft

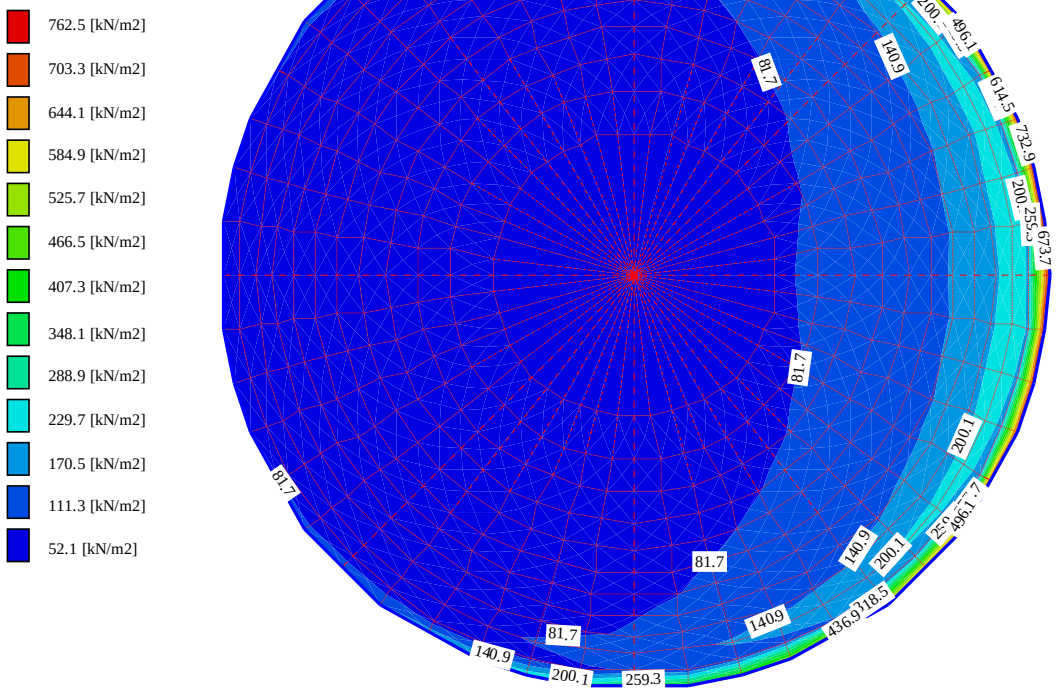

Contact pressure q [kN/m2]
Max. q = 792.1 at node 13, Min. q = 22.5 at node 300

GEOTEC Software Inc., Calgary AB, Canada T3E 7Y7	
PO Box 14001 Richmond Road PO, Tele.: +1 (587) 332-3323	
Scale: 64	**Project: User's Manual**
File: Ex3-Num	**Date: 10-10-2017**
Page No.:	**Title: Comparison between settlements obtained by analytical and numerical analyses**

Method (8) (Layered soil model)

Modulus of Compressibility for Rigid Raft

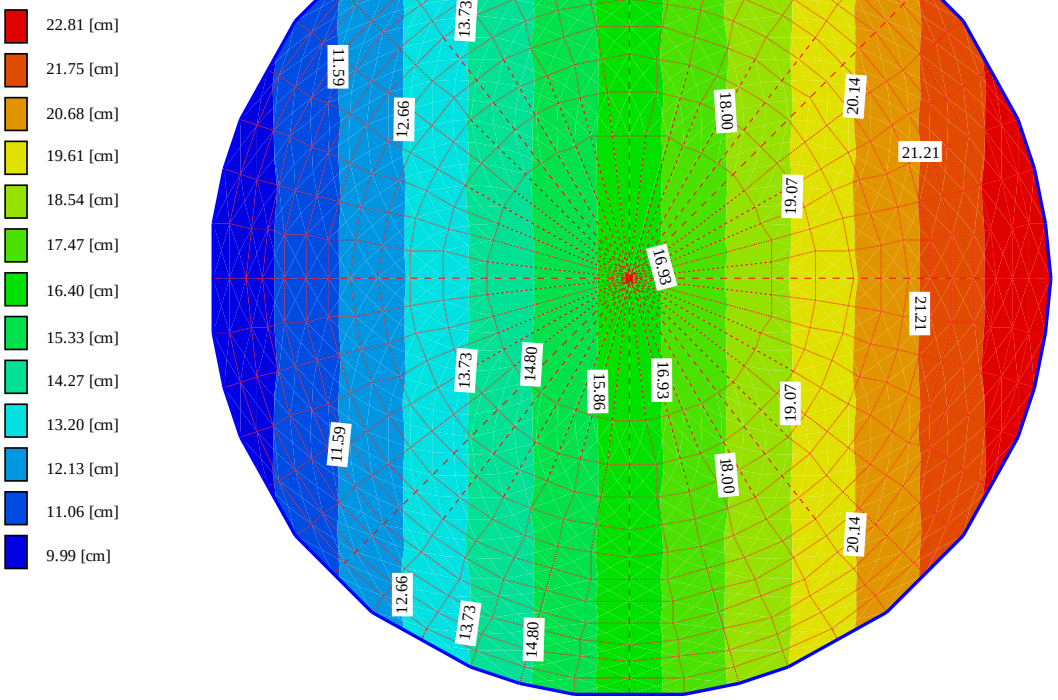

Settlements s [cm]

Max. s = 23.35 at node 13, Min. s = 9.45 at node 301

GEOTEC Software Inc., Calgary AB, Canada T3E 7Y7	
PO Box 14001 Richmond Road PO, Tele.: +1 (587) 332-3323	
Scale: 64	**Project: User's Manual**
File: Ex3-Num	**Date: 10-10-2017**
Page No.:	**Title: Comparison between settlements obtained by analytical and numerical analyses**

Method (8) (Layered soil model)

Modulus of Compressibility for Rigid Raft

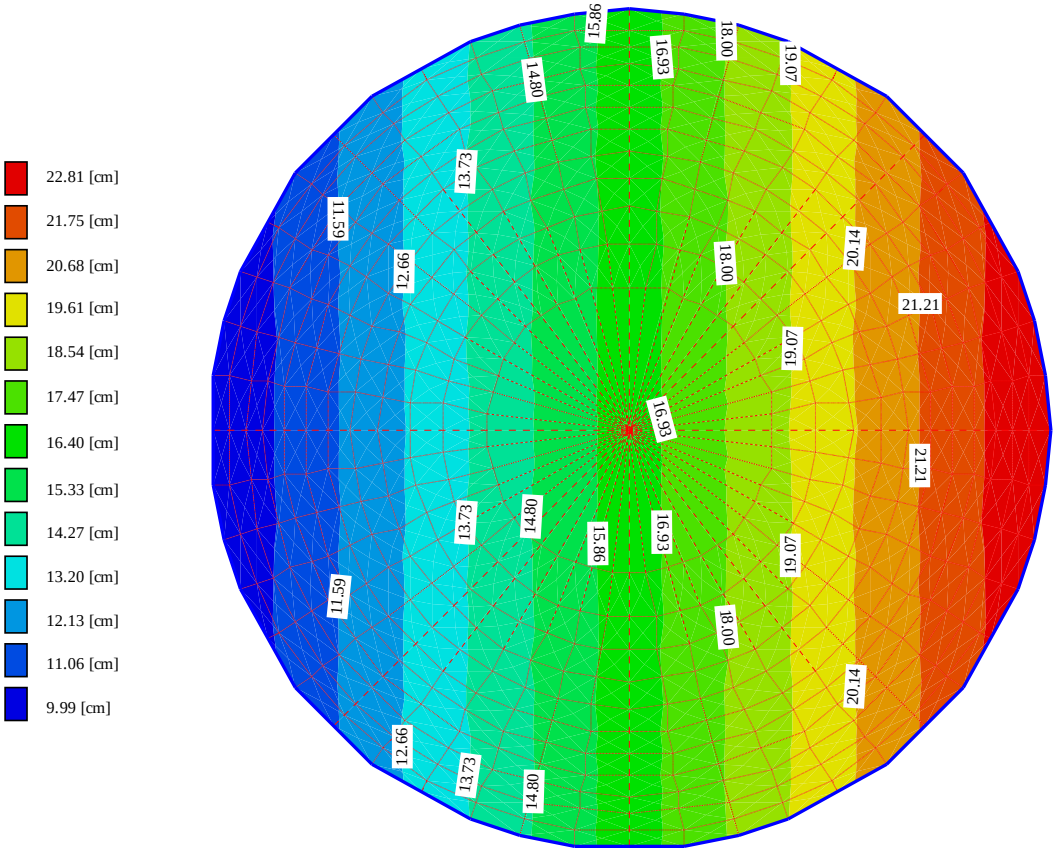

Settlements s [cm]

Max. s = 23.35 at node 13, Min. s = 9.45 at node 301

GEOTEC Software Inc., Calgary AB, Canada T3E 7Y7	
PO Box 14001 Richmond Road PO, Tele.: +1 (587) 332-3323	
Scale: 64	**Project: User's Manual**
File: Ex3-Num	**Date: 10-10-2017**
Page No.:	**Title: Comparison between settlements obtained by analytical and numerical analyses**

8.8.5 Example 4: Limit depth of the clay layer under the rigid raft

8.8.5.1 Description of the problem

The consolidation settlement calculated from Eq. (8.50) is only realistic if the diameter of the raft is great enough in relation to the depth of the clay layer. Therefore, several computations were carried out to determine the limit depth of the clay layer, which is valid for the proposed direct method. To achieve this work, a circular rigid raft on a clay layer was studied at different radii a with different applied load intensities p. Then, the consolidation settlement s was determined in clay layers of different thicknesses H as shown in Figure 8.28.

8.8.5.2 Analysis of the raft

For the purpose of comparison the terms C_c and e_o in Eq. (8.50) were chosen to make the maximum consolidation settlement due to the applied load intensity of p = 200 [kN/m^2] equal to 10.0 [cm]. The dry unit weight of the clay is chosen to be γ = 18.5 [kN/m^3] as in most clay soils. In the analysis, each clay layer is subdivided into several strips, each of thickness D_z = 0.25 [m], while the raft is divided into 576 elements.

Obviously, the physical results of any compressible soil layer indicate that the total settlement increases as the thickness of the soil layer increases because a deeper layer should settle more. This phenomenon is used here to determine the limit depth of the clay layer. In which the settlement of a layer H must be increased when adding to it the settlement of the next strip of the thickness Δh. Theoretically, the increasing in settlement cannot stop in an extended clay layer. Although this settlement phenomenon continues up to very large depths under the raft but the major part of the settlement occurs within a shallow depth.

It can be noticed from Figure 8.28 that the limit depth of a layer of thickness $H_1 = H$ is considered to be realistic when the settlement of this clay layer is less than that of the next clay layer of thickness $H_2 = H_1 + \Delta h$. This condition may be written in the following relation:

$$\frac{C_c}{1+e_o}\log\left(\frac{\sigma_o+\Delta\sigma_o}{\sigma_o}\right)_2 H_2 > \frac{C_c}{1+e_o}\log\left(\frac{\sigma_o+\Delta\sigma_o}{\sigma_o}\right)_1 H_1 \tag{8.90}$$

This relation may be simplified to:

$$(\Delta\sigma_o)_2 - \gamma H_2\left[\left(\frac{\gamma H_1 + (\Delta\sigma_o)_1}{\gamma H_1}\right)^{\frac{H_1}{H_2}} - 1\right] > 0 \tag{8.91}$$

8.8.5.3 Results and discussions

Table 8.10 shows the limit depths under the raft for different radii a and applied load intensities p. It can be noticed from this table that the limit depth depends on the raft dimension and load intensity. Where the raft of the greatest radius has the smallest limit depth and vice verse also the limit depth exceeds by increasing of the applied load. Table 8.10 can

be considered as guidelines to determine the limit depth when analyzing raft on consolidated clay deposit by the proposed numerical modeling.

Table 8.10 Limit depths under the raft for different radii *a* and applied load intensities *p*

Load intensities *p* [kN/m^2]	50				100			
Raft radius *a* [m]	2.5	5.0	7.5	10.0	2.5	5.0	7.5	10.0
Limit depth z_g [m]	8	8	6	6	10	8	8	8
Load intensities *p* [kN/m^2]	150				200			
Raft radius *a* [m]	2.5	5.0	7.5	10.0	2.5	5.0	7.5	10.0
Limit depth z_g [m]	12	10	10	8	14	12	10	10

The results of computations showed that the limit depth depends on the raft dimension and load intensity, where the raft of the greatest radius has the smallest limit depth and vice verse also the limit depth exceeds by increasing of the applied load. The results had been shown that the proposed method can be used to analyze rigid rafts on a clay layer of about 10 [m] thickness.

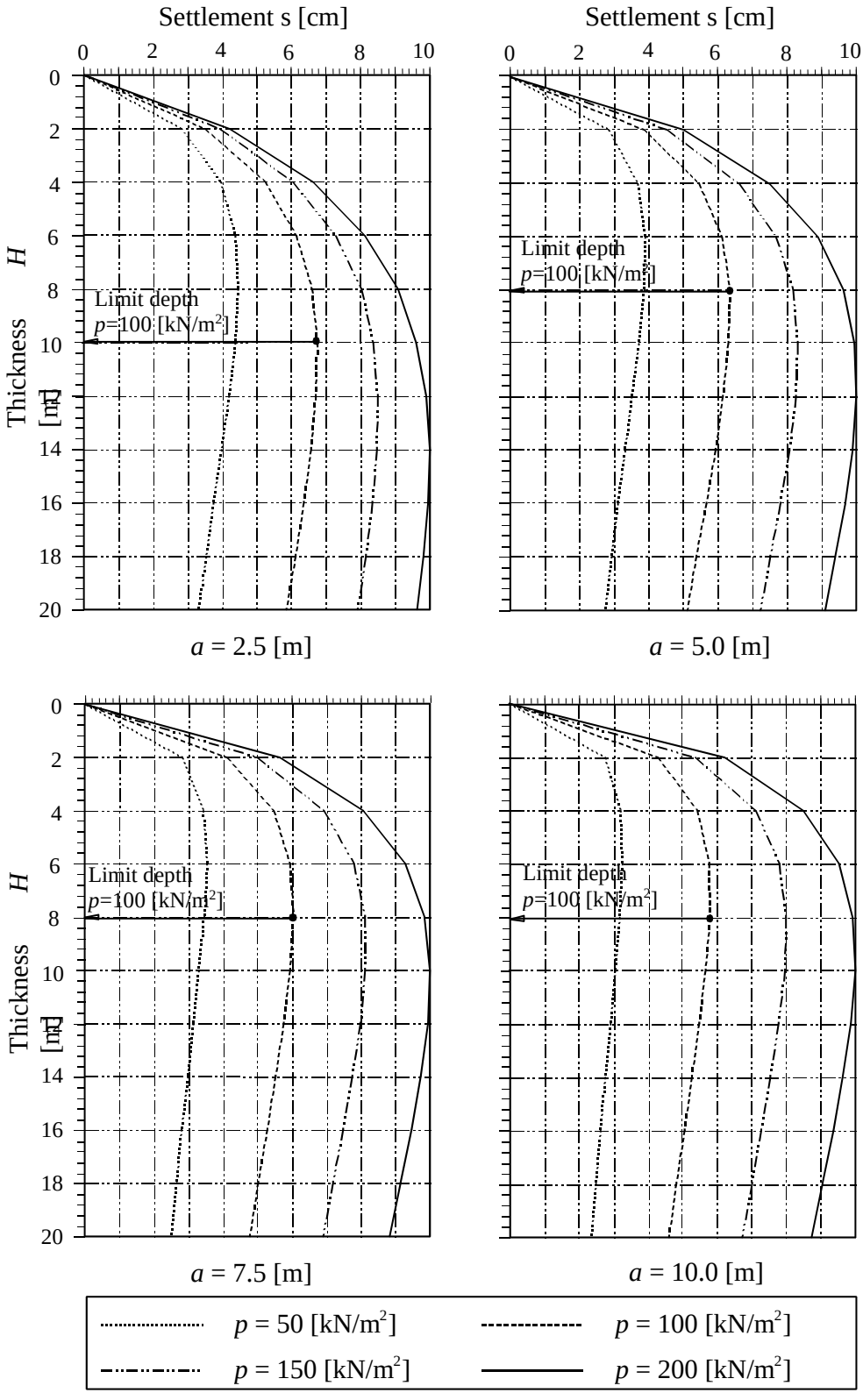

Figure 8.28 Settlement in clay layers at different load intensities *p* and raft radii *a*

8.9 References

[1] *Absi, E*. (1970): Étude de problèmes particuliers
Annls Inst. Tech. Bâtim., No. 265, 173-188

[2] *Akoz, A. & Kadioglu, F.* 1996. The Mixed Finite Element Solution of Circular Beam on Elastic Foundation. *Computers & Structures* 60: 643- 651.

[3] *Borowicka, H*. (1939): Druckverteilung unter elastischen Platten
Ingenieur-Archiv, Band 10, S. 113-125

[4] *Bose, S. & Das, S.* 1997. Nonlinear Finite Element Analysis of Stresses and Deformations Beneath Rigid Footings. *Computers & Structures* 62: 487-492.

[5] *Celep, Z.* 1988. Circular Plate on a Tensionless Winkler Foundation. Engineering Mechanics 114: 1720-1736.

[6] *Chow, Y*. (1987): Vertical Deformation of Rigid Foundations of Arbitrary Shape on Layered Soil Media
International Journal for Numerical and Analytical Methods in Geomechanics, Vol. 11, 1-15, John Wiley & Sons, Ltd.

[7] *Chakravorty, A. & Ghosh, A.* 1975. Finite Difference Solution for Circular Plates on Elastic Foundations. *Numerical Methods in Engineering* 9: 73-84.

[8] DIN 4018. Baugrund. Berechnung der Sohldruckverteilung unter Flächengründungen. Deutsche Institut für Normung, Berlin: Beuth Verlag, 1974.

[9] *El Gendy, M.* Numerical Modeling of Rigid Circular Rafts on Consolidated Clay Deposits. Int. Workshop on Geotechnics of Soft Soils-Theory and Practice. Vermeer, Schweiger, Karstunen & Cudny (eds.), 2003.

[10] *El Gendy, M.* Developing stress coefficients for raft-deformation on a thick clay layer. 2006.

[11] *Fraser, R./ Wardle, L*. (1976): Numerical Analysis of Rectangular Rafts on Layered Foundations
Géotechnique 26, No. 4, 613-630

[12] *Gazetas, G.* 1982. Progressive Collapse of Rigid-Plastic Circular Foundations. *Engineering Mechanics Division* 108: 493-508.

[13] *Griffiths, D.* A chart for estimating the average vertical stress increase in an elastic foundation below a uniformaly loaded rectangular area.
Can. Geotech. J. 21, 1984, 710-713.

[14] *Graßhoff H, Kany, M.* Berechnung von Flächengründungen. In: Grundbautaschen-

buch Teil 3, 5.Auflage, Verlag Ernst & Sohn Berlin, 1997.

[15] *Graßhoff H.* Setzungsberechnungen starrer Fundamente mit Hilfe des kennzeichnenden Punktes. Bauingenieur 1955; 53-54.

[16] *Gorbunov-Possadov, M./ Serebrjanyi, R.* (1961): Design of Structures on Elastic Foundations
Proceedings of the Fifth International Conference on Soil Mechanics and Foundation Engineering, Vol. 1, 643-648, Paris

[17] *Kany, M.* (1974): Berechnung von Flächengründungen, 2. Auflage
Ernst & Sohn, Berlin

[18] *Kamal, K.* 1983. Bending of Circular Plate on Elastic Foundation. Engineering Mechanics 109: 1293-1298.

[19] *Kocatürk, T.* 1997. Elastoplastic Analysis of Circular Plates on Elastoplastic Foundation. *Structural Engineering* 123: 808-815.

[20] *Krajcinovic, D.* 1976. Rigid-Plastic Circular Plates on Elastic Foundation. *Engineering Mechanics Division* 102: 213-224.

[21] *Lang H, Huder J, Amann P.* Bodenmechanik und Grundbau. 6. Aufl. Berlin Heidelberg: Springer-Verlag 1996.

[22] *Li, H./ Dempsey, J.* (1988): Unbounded Contact of a Square Plate on an Elastic Half-Space or a Winkler Foundation
Journal of Applied Mechanics, 55, 430-436

[23] *Melerski, E.* 1997. Numerical Modelling of Elastic Interaction between Circular Rafts and Cross-Anisotropic Media. *Computers & Structures* 64: 567-578.

[24] *Milovic, D. & Djogo, M.* 1991. Settlement of Circular Foundation of Any Rigidity. *Proc. 10th European Conference on Soil Mechanics and Foundation Engineering*, Florance.

[25] *Poulos H, Davis E.* Elastic Solution for Soil and Rock Mechanics. New York: John Wiley & Sons, Inc. 1974.

[16] *Selvaduri A.* Elastic Analysis of Soil-Foundation Interaction. Oxford: Elsevier Scientific Publishing Company, 1979.

[27] *Stark, R.* (1990): Beitrag zur Numerischen Behandlung des Kontaktproblems beliebig

Orthogonal berandeter Fundamentplatten unter Einbeziehung von Grenzzuständen in Boden
Dissertation Uni Innsbruck

[28] *Vallabhan, C.* 1991. Analysis of Circular Tank Foundations. *Engineering Mechanics* 117: 789-797.

[29] *Xiao-jing, Z.* 1988. Exact Solution of Nonlinear Circular Plate on Elastic Foundation. *Engineering Mechanics* 114: 1303-1316.

[30] *Zaman, M. & Faruque, M. & Mahmood, A.* 1990. Analysis of Moderately Thick Restrained Circular Plates Resting on an Isotropic Elastic Half Space. *Applied Mathematical Modelling* 14: 352-361.

[31] *Bowles, J.* (1977): Foundation analysis and design
McGraw-Hill, New York

[32] *Ellner, A./ Kany, M.* (1976): Berücksichtigung der aussteifenden Wirkung von Kellermauern und Decken bei der Berechnung von Sohlplatten mit der FE-Methode
Forschungsbericht Ka 282/6 an die DFG, Nürnberg

[33] EAU (1990): Empfehlungen des Arbeitsausschusses Ufereinfassungen, Seite 10
Berlin/ München/ Düsseldorf

[34] *Terzaghi, K./ Peck, R.* (1967): Soil Mechanics in Engineering Practice, 2nd Edition
Wiley, New York

[35] *Azzouz, A./ Krizek, R./ Corotis, R.* (1976): Regression Analysis of Soil Compressibility
Soil and foundations, Tokyo, vol. 16, no. 2, pp. 19-29

[36] *Gudehus, G.* (1981): Bodenmechanik
Verlag Ferdinand Enke, Stuttgart

[37] *Kullhawy, H., Mayne, P.*: Manual on Estimating Soil Properties for Foundation Design, Electric Power Research Institute, EPRI, 1990.

[38] *Kany, M.* (1976): Setzungsberechnung mit Verwendung Druckabhängiger SteifemodulnVeröffentlichungen des Grundbauinstitutes der Landesgewerbeanstalt Bayern, Heft 24, Einzelbeiträge, Nürnberg